HEPATITIS *DELTA* VIRUS: IDENTIFICATION OF HOST FACTORS INVOLVED IN THE VIRAL LIFE CYCLE, AND THE INVESTIGATION OF THE EVOLUTIONARY RELATIONSHIP BETWEEN HDV AND PLANT VIROIDS

Dorota Sikora

Thesis submitted to the

Faculty of Graduate and Postdoctoral Studies

In partial fulfillment of the requirements

For the PhD degree in Biochemistry

Thesis supervisor: Dr. Martin Pelchat

Department of Biochemistry, Microbiology and Immunology

Faculty of Medicine

University of Ottawa

ABSTRACT

Hepatitis *delta* virus (HDV) is the smallest known human RNA pathogen. It requires the human hepatitis B virus (HBV) for virion production and transmission, and is hence closely associated with HBV in natural infections. HDV RNA encodes only two viral proteins - the small and the large *delta* antigens. Due to its limited coding capacity, HDV needs to exploit host factors to ensure its propagation. However, few human proteins are known to interact with the HDV RNA genome. The current study has identified several host proteins interacting with an HDV-derived RNA promoter by multiple approaches: mass spectrometry of a UV-crosslinked ribonucleoprotein complex, RNA affinity chromatography, and screening of a library of purified RNA-binding proteins. Co-immunoprecipitation, both *in vitro* and *ex vivo*, confirmed the interactions of eEF1A1, $p54^{nrb}$, PSF, hnRNP-L, GAPDH and ASF/SF2 with both polarities of the HDV RNA genome. *In vitro* transcription assays suggested a possible involvement of eEF1A1, GAPDH and PSF in HDV replication. At least three of these proteins, eEF1A1, GAPDH and ASF/SF2, have also been shown to associate with potato spindle tuber viroid (PSTVd) RNA. Because HDV's structure and mechanism of replication share many similarities with viroids, subviral helper-independent plant pathogens, I transfected human hepatocytes with RNA derived from PSTVd. Here, I show that PSTVd RNA can replicate in human hepatocytes. I further demonstrate that a mutant of HDV, lacking the *delta* antigen coding region (miniHDV), can also replicate in human cells. However, both PSTVd and miniHDV require the function of the small *delta* antigen for successful replication. Our discovery that HDV and PSTVd RNAs associate with similar RNA-processing pathways and translation machineries during their replication provides new insight into HDV biology and its evolution.

ACKNOWLEDGEMENTS

I would like to extend a sincere thank you to my advisor, Dr. Martin Pelchat, for all his invaluable assistance, support and guidance during my doctoral study. He has always been accessible and willing to help, and his enthusiasm for research has been inspiring. I would also like to thank my thesis advisory committee members, Dr. Jocelyn Côté, Dr. Daniel Figeys, Dr. Martin Holcik and Dr. Ken Dimock. Their knowledge, advice and encouragement were greatly appreciated.

I am grateful to all the members of the Pelchat lab, past and present, for all their help and advice, and for making it such a great environment to work in. In particular, I would like to thank all the people who have contributed their results to this research thesis: Valerie Greco-Stewart, Paul Miron, Emilie Lemay, Ji Yin and Ali Tanara.

To my friends from the Department of Biochemistry, Microbiology and Immunology, thanks for making grad school so much fun. A special thank you to Natalie Bunimov, for her help and advice on my work, and for all her moral encouragement; Evelin Loit, for her positive attitude; and Teodora Bojić, for brightening up the lab.

My deepest gratitude goes to my family. To my husband Radek Sikora for always believing in me, and to my beautiful daughter Gabriela for making it all worthwhile, I love you. To my mom, Anna Rembisz, for all her support and patience. I could not have done it without their love and support.

Table of Contents

List of Abbreviations

aa	amino acid
ADAR1	adenosine deaminase that acts on RNA 1
ARM	arginine-rich motif
ASF/SF2	alternative splicing factor
ASBVd	avocado sunblotch viroid
ATP	adenosine triphosphate
bp	base pair
cDNA	complementary deoxyribonucleic acid
CHC	clathrin heavy chain
CKII	casein kinase II
CTD	carboxy-terminal domain
DIPA	*delta*-interacting protein A
DRB	5,6-dichloro-1-ß-D-ribofuranosylbenzimidazole
ds	double-stranded
DSIF	DRB sensitivity inducing factor
eEF1A1	eukaryotic elongation factor 1A1
EMSA	electrophoretic mobility shift assay
ERK1/2	extracellular signal-related kinase 1/2
ESE	exonic splicing enhancer
Ftase	farnesyltransferase
GAPDH	glyceraldehyde 3-phosphate dehydrogenase
GFP	green fluorescent protein

GST	glutathione S-transferase
GTP	guanosine triphosphate
HBsAg	hepatitis B surface antigen
HBV	hepatitis B virus
HDV	hepatitis *delta* virus
HDAg-S	small hepatitis *delta* antigen
HDAg-L	large hepatitis *delta* antigen
His-ASF/SF2	6X histidine-tagged ASF/SF2
hnRNP-L	heterogeneous nuclear ribonucleoprotein L
HSF1	heat shock transcription factor 1
Hsp	heat shock protein
IPTG	isopropyl *β*-D-1-thiogalactopyranoside
K_D	dissociation constant
kDa	kilodalton
LC-MS/MS	liquid chromatography-tandem mass spectrometry
mRNA	messenger ribonucleic acid
NE	nuclear extract
NELF	negative elongation factor
NEP	nuclear-encoded polymerase
NES	nuclear export signal
NESI	nuclear export signal-interacting protein
NF-κB	nuclear factor kappa B
NLS	nuclear localization signal

NoLS	nucleolar localization sequence
nt	nucleotide
NTP	nucleoside triphosphate
ORF	open reading frame
$p54^{nrb}$	54 kDa nuclear RNA-binding protein
PAGE	polyacrylamide gel electrophoresis
PCR	polymerase chain reaction
PIC	pre-initiation complex
PLMVd	peach latent mosaic viroid
PKC	protein kinase C
PKR	double-stranded RNA-activated protein kinase R
PPE	pre-mRNA processing enhancer
PRMT1	protein arginine methyltransferase 1
PSF	polypyrimidine tract-binding protein-associated splicing factor
PSTVd	potato spindle tuber viroid
PTB	polypyrimidine tract-binding protein
P-TEFb	positive transcription elongation factor b
Q-PCR	quantitative polymerase chain reaction
RBD	RNA binding domain
RIPA	ribonucleoprotein immunoprecipitation assay
RNAP	DNA-dependent RNA polymerase
RNP	ribonucleoprotein
RRM	RNA recognition motif

RT-PCR	reverse transcription-polymerase chain reaction
Ser	serine
SFPQ	splicing factor proline/glutamine-rich
shRNA	small hairpin RNA
snRNP	small nuclear ribonucleoprotein
SR protein	serine/arginine-rich protein
ss	single-stranded
SUMO1	small ubiquitin-like modifier 1
TBP	TATA-binding protein
TET	tetracycline
TFIIS	general transcription factor IIS
TGF	transforming growth factor
Thr	threonine
TNF	tumour necrosis factor
TRAF2	TNF-activated factor 2
tRNA	transfer RNA
UTR	untranslated region
WHO	World Health Organization
WHV	woodchuck hepatitis virus
YY1	Yin Yang 1

List of Figures

List of Tables

Chapter 1: INTRODUCTION – Hepatitis *delta* virus

1.1 History and classification

The hepatitis *delta* virus (HDV) is the smallest known human RNA virus. It was discovered by Rizzetto *et al*. (1977), who showed the presence of a novel antigen in chronic hepatitis B patients. This antigen, termed *delta*, was subsequently shown to be associated with a defective transmissible agent, which requires the helper function of hepatitis B virus (HBV) infection for transmission and propagation, and exacerbates the liver disease of HBAg-positive patients (Rizzetto *et al*., 1980).

HDV is unique among human pathogens. Although considered a satellite of HBV, HDV does not share any sequence similarity with its helper virus, and replicates independently of HBV. While HDV displays resemblance to viroids and virusoids of plants in terms of genome structure and replication mechanisms, it has been classified into a separate floating genus, *Deltaviridae*.

1.2 Epidemiology

HDV is present worldwide; its distribution parallels that of HBV, although prevalence rates differ between the two viruses (Rizzetto *et al*., 1992). HDV is highly endemic in Mediterranean countries, the Middle East, Central Africa, and northern parts of South America. The World Health Organization (WHO; 2008) estimates that about 350 million people worldwide live with chronic HBV infection. Approximately 20 million are also infected with HDV (Radjet *et al*., 2004).

HDV is transmitted percutaneously or sexually through contact with infected blood. A person may become infected with HDV and HBV simultaneously; this is referred to as a coinfection. A superinfection occurs when an HBV carrier becomes infected with HDV (Farci, 2003). Typically, coinfection leads to development of acute self-limiting hepatitis, which may progress to chronic hepatitis in 2% of cases. Conversely, a superinfection causes severe acute disease, which exacerbates the pre-existing hepatitis B. The established HBV infection allows for a steady accumulation of HDV, leading to rapidly progressive hepatitis in over 90% of patients (Smedile *et al*., 2002). Chronic active hepatitis caused by HDV often progresses to liver cirrhosis (Rizzetto *et al*., 1983), which increases the risk for hepatocellular carcinoma threefold and for mortality twofold (Fattovich *et al*., 2000). Currently, liver transplantation remains the only viable option for treatment of end-stage HDV liver disease (Farci, 2003). Long-term treatment with high doses of interferon *alpha* has also shown improvement in survival of chronic hepatitis D patients (Lau *et al*., 1999; Farci *et al*., 2004). Although there are currently no vaccines against HDV, hepatitis B vaccination will protect against HDV infection.

1.3 Virion structure

HDV requires the presence of HBV for virion production and transmission. The HDV particle is made up of an envelope of HBV origin and a ribonucleoprotein (RNP) complex consisting of an RNA genome and the HDV-encoded hepatitis *delta* antigen (HDAg) (Ryu *et al*., 1993). The HBV-derived envelope is composed of three viral proteins present in both glycosylated and unglycosylated forms. These proteins are referred to as small (S), middle

(M), and large (L), and are translated from three in-phase initiation codons to a common stop codon (Ganem and Varmus, 1987). The contiguous open reading frame (ORF) is comprised of three regions: pre-S1, pre-S2 and S (Figure 1.1). The S region encodes the S protein, and contains the hepatitis B surface antigen (HBsAg). The M protein is encoded by the pre-S2 and S regions, and the L protein is encoded by all three regions. The serum of an HBV-infected person contains mature HBV particles composed of approximately equimolar amounts of all three proteins, and 22-nm-diameter subviral particles present in an excess of 1,000 to 1,000,000-fold over the virions (Ghanem and Varmus, 1987). These subviral particles are comprised almost exclusively of the S protein, and are non-infectious as they lack viral nucleic acid. HDV takes advantage of the excess HBV particles to encapsidate its own genome. The envelope of an HDV particle consists mainly of the S protein, with 5% M and 1% L proteins (Bonino *et al*., 1986). Although the S protein is sufficient for HDV particle assembly, particles containing only S, or S and M proteins, are non-infectious (Sureau *et al*., 1993). Sureau *et al.* (1993) showed that the L protein is necessary for infectivity, since only particles coated with all three proteins (SML) were infectious in an *in vitro* culture system susceptible to HDV infection. Based on their findings, the authors suggested that the L protein is required for receptor binding. A later study by Engelke *et al.* (2006) demonstrated that both HBV and HDV virions require a highly conserved preS1-sequence within the L-protein for infection of cultured HepaRG cells. While these findings suggest that HDV and HBV use a common cell entry strategy, the receptors involved in the cell entry of either virus are yet to be identified.

The RNP complex within the virion was found, using UV crosslinking, equilibrium density centrifugation, and immunoprecipitation approaches, to be comprised of the *delta*

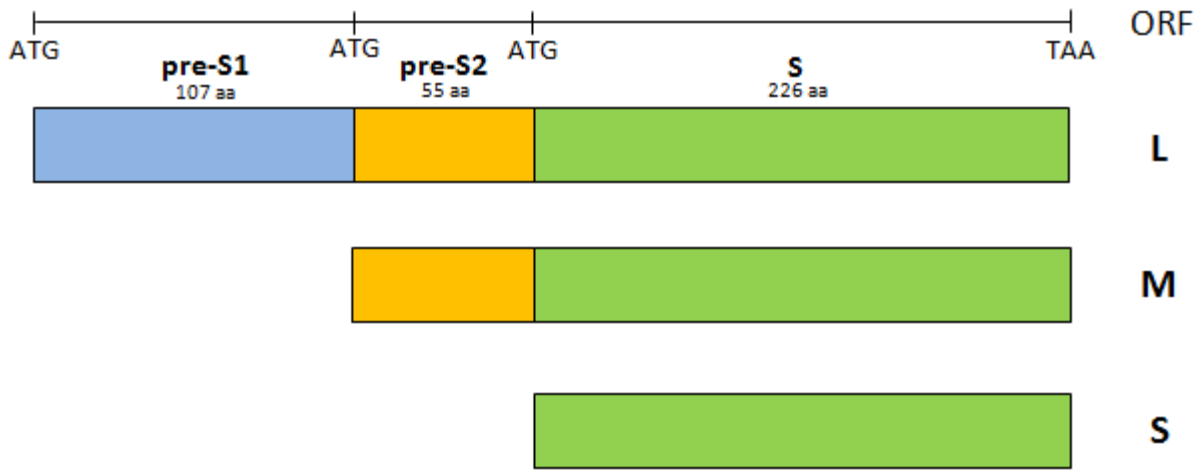
ATG
ATG
ATG
TAA
ORF
pre-S1
107 aa
pre-S2
55 aa
S
226 aa
L
M
S

Figure 1.1: Schematic representation of the HBV surface proteins and the organization of the pre-S1/pre-S2/S open reading frame.

S, M, and L proteins are translated from three in-phase initiation codons to a common stop codon. The L protein contains all three regions (pre-S1 + pre-S2 + S), the M protein contains the pre-S2 and S regions, and the S protein is comprised solely of the S region.

antigen and genomic RNA, in an approximate ratio of 70 HDAgs for every molecule of the HDV genome (Ryu *et al*., 1993). Subsequently, quantitative assays suggested that the molar ratio of HDAg to genomic HDV RNA in assembled HDV particles is closer to 200 (Gudima *et al*., 2002). Electron microscopy revealed a spherical core-like structure 18.7 ± 2.5 nm in diameter (Ryu *et al*., 1993). To date, the antigenomic strand of HDV RNA has not been found in the viral particle (Sureau, 2006). HDV particle assembly is mediated by the direct interaction of the large form of HDAg (HDAg-L) and HBsAg (Hwang and Lai, 1993). These two proteins are both necessary and sufficient to form particles; when hepatocytes were cotransfected with plasmids encoding each protein, HBsAg particles containing HDAg-L were recovered. No other HDV components were required for particle formation (Chen *et al*., 1992), although these particles were non-infectious since they lacked viral nucleic acid. Although the small form of HDAg (HDAg-S) is not required for particle assembly, it has been shown to increase packaging efficiency (Chen *et al*., 1992; Wang *et al*., 1994).

1.4 Genome structure

The HDV genome consists of a small (~1700 nucleotides), negative strand, circular RNA molecule (Figure 1.2). Its only known gene product is the *delta* antigen (HDAg); two essential forms of HDAg are produced owing to specific RNA editing of the antigenomic strand (Casey and Gerin, 1995). A polyadenylation signal is located downstream of the open reading frame (Hsieh *et al*., 1990). The RNA genome is about 70 % self-complementary, a feature which allows it to adopt an unbranched, rod-like structure (Wang *et al*., 1986); the

A)

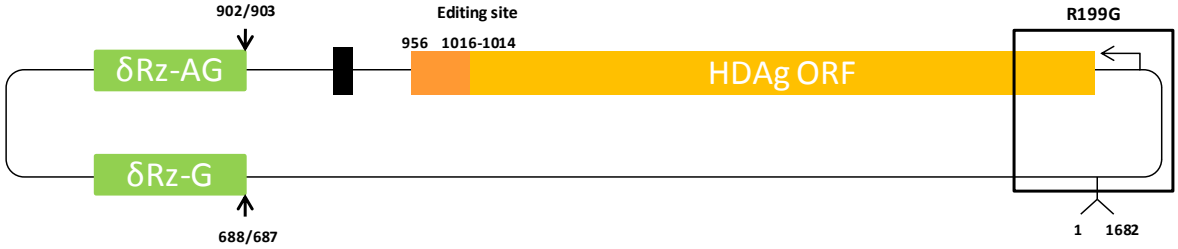
902/903
Editing site
956 1016-1014
R199G
δRz-AG
HDAg ORF
δRz-G
688/687
1 1682

B)

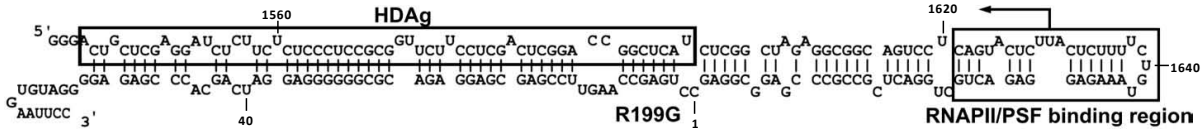
HDAg
1560
1620
1640
R199G
RNAPII/PSF binding region

Figure 1.2: Organization of the hepatitis *delta* virus RNA genome.

(A) Genomic and antigenomic polarities of HDV RNA are superimposed; locations of genomic (G) and antigenomic (AG) *delta* ribozymes are shown, and cleavage sites are indicated by arrows. HDAg coding region is present on the antigenome; predicted transcription start site is depicted by an arrow, and the black box depicts the polyadenylation site. The boxed region indicates the location of the genomic right terminal stem-loop domain (referred to herein as R199G), containing the putative promoter for the transcription of HDAg mRNA. (B) Secondary structure of R199G. RNAP II/PSF binding region is indicated. The location of the 5' end of the HDAg coding region is boxed.

two stem-loop domains formed by this structure are believed to contain RNA promoter elements (Abrahem and Pelchat, 2008; Beard *et al*., 1996; Filipovska and Konarska, 2000). Interestingly, the HDV genome is structurally more similar to plant viroids and virusoids than to animal viruses.

The HDV RNA possesses focal structural and functional aspects that are essential for replication. The genome and the antigenome each contain a functional ribozyme domain, called the *delta* ribozyme (Figure 1.3), which adopts a complex, nested, double pseudoknot structure (Wadkins *et al*., 1999) that supports self-cleavage at specific sites (Kuo *et al*., 1988; Sharmeen *et al*., 1988; Wu and Lai, 1989; Wu *et al*., 1992). Although the *delta* ribozymes have been demonstrated to undergo self-ligation *in vitro* (Sharmeen *et al*., 1989), the reaction was inefficient and required the presence of a splint RNA that was partially complementary to the ends of two precleaved RNAs. A subsequent study by Reid and Lazinski (2000) suggested the involvement of a host ligase *in vivo*; by testing identical substrates *in vivo*, *in vitro* and in *Escherichia coli*, the authors found that ligation occurred exclusively in host cells. Until recently, these self cleaving motifs were thought to be unique to HDV; however, a number of HDV-like ribozymes have been identified in a broad range of organisms, including viruses, bacteria, plants and mammals (Salehi-Ashtiani *et al*., 2006; Webb *et al*., 2009; Webb and Lupták, 2011), indicating a widespread occurrence of these motifs in nature, and suggesting that self-cleaving RNAs may serve important biological functions.

1.5 Pathogenicity

The pathogenicity of HDV is still poorly understood. The expression of HDAg in HeLa and HepG2 cells has been reported to result in extensive cell death, suggesting that HDAg may be cytotoxic (Macnaughton *et al*., 1990); in another study, HDAg was associated with a significant reduction in the rate of RNA, but not DNA, synthesis (Cole *et al*., 1991). When overexpressed in recombinant baculovirus-infected insect cells, HDAg mediated cell cycle arrest (Hwang and Park, 1999). In a more recent study using transgenic *C. elegans*, growth retardation and brood size reduction was observed in worms expressing HDAg (Lee *et al*., 2011); this study suggested that the nuclear localization signal of HDAg is required for the observed effect. In contrast, other studies have observed no cytopathic effects associated with HDAg expression in cultured cells (Chang *et al*., 2005) and in transgenic mice (Guilhot *et al*., 1994). A study by Wang *et al*. (2001) has suggested that HDV RNA replication, rather than expression of the *delta* antigen alone, is responsible for cytopathic effects. While HDV RNA replication resulted in limited cellular injury in transgenic mice (Polo *et al*., 1995), Wang *et al*. (2001) and others (Chang *et al*., 2005) observed that HDV replication reduced cell growth and viability in cultured cells, albeit not by direct induction of apoptosis; in transient transfection assays, HDV-replicating HeLa cells did not display an enhanced staining with annexin 5, a specific and sensitive marker of apoptosis (Martin *et al*., 1995), nor did HDV replication render the host cells more sensitive to inducers of apoptosis (Wang *et al*., 2001). The precise mechanisms underlying the observed cellular growth impairment following HDV RNA replication are unknown; Wang *et al*. (2001) suggested that while the observed growth disadvantage alone is unlikely to cause hepatitis *in vivo*, it may contribute to

liver disease by compromising the ability of the HDV-infected cell to participate in liver regeneration.

1.6 Experimental Models

Successful experimental infection and replication of HDV in animal models is limited to species that can support the replication of a hepadnavirus able to supply the helper function. These include the HBV-infected chimpanzee (Rizzetto *et al*., 1980), and the eastern woodchuck infected with the woodchuck hepatitis virus (WHV; Ponzetto *et al*., 1984). Experimental transmission of HDV to mice by intravenous or intraperitoneal injection has lead to infection in hepatocytes (Netter *et al*., 1993), although the infection was limited to a single replication cycle due to the absence of the helper virus. Transgenic mice that express replication-competent genomic dimers of HDV RNA have been successfully developed, with efficient RNA replication observed in the liver as well as other tissues (Polo *et al*., 1995). Hydrodynamic transfection of HBV transgenic mice with a plasmid capable of initiating HDV replication has resulted in virus replication and virion assembly; however, the virus was cleared within 21 days post-transfection (Bordier *et al*., 2003). HDV infection has also been achieved in mice transplanted with primary human hepatocytes (Ohashi *et al*., 2000); in this model system, the transplanted hepatocytes were susceptible to HBV and HDV infection, and supported the replication and virus release into the serum. Recently, a new chimeric mouse model of HDV infection was developed (Lütgehetmann *et al*., 2012). In this study, humanized chimeric uPA/SCID mice were successfully employed to study the HBV/HDV co- and superinfection.

While an *in vitro* model system for the propagation of HDV does not exist, primary woodchuck and chimpanzee hepatocytes have successfully been infected with HDV (Sureau *et al*., 1991; Taylor *et al*., 1987). Infection is limited to primary hepatocytes, while formation and release of virions is restricted to primary hepatocytes that are co-infected with a hepadnavirus, or to cultured cells co-transfected with HDV and hepadnavirus cDNAs (Gudima *et al*., 2007; Ryu *et al*., 1992; Sureau *et al*., 1993; Wu *et al*., 1991). Because HDV can replicate independently of HBV, HDV RNA replication has been achieved in a number of mammalian cell types following cDNA or RNA transfection. Transfection with HDV cDNA was shown to lead to RNA-directed RNA synthesis, as long as functional HDAg-S could be produced from the transfected cDNA (Kuo *et al*., 1989). However, obvious drawbacks are associated with using a cDNA transfection system, as it involves a DNA-dependent transcription step to generate a precursor HDV RNA. Transfection with HDV RNA eliminates the need for a cDNA step; this approach has been used successfully to study HDV RNA replication (Chang *et al*., 2005; Dingle *et al*., 1998; Glenn *et al*., 1990; Modahl and Lai, 1998). Since HDAg-S is necessary for the initiation of HDV RNA-directed RNA synthesis, this method requires that HDAg-S be supplied *in trans*.

1.7 *Delta* antigens

The HDV genome contains a single open reading frame encoding two viral proteins (HDAgs). These two proteins are mostly identical in sequence except that the large HDAg (HDAg-L) contains 19 additional amino acids at its C-terminus resulting from RNA editing

A)

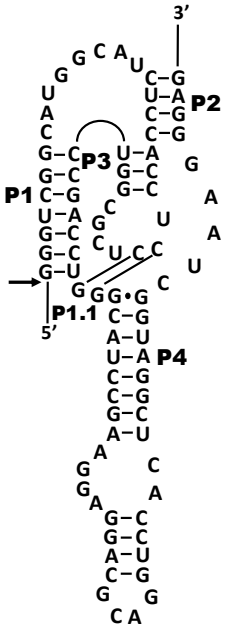

B)

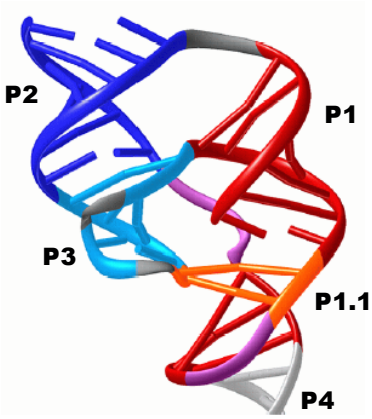

Figure 1.3: The *delta* ribozyme.

(A) Secondary structure of the antigenomic *delta* ribozyme. Ribozyme cleavage site is indicated by an arrow. B) 3-dimensional structure of the genomic *delta* ribozyme (PDB#: 1drz), solved by Ferré-D'Amaré *et al*. (1998). Reprinted by permission from Macmillan Publishers Ltd: Nature 395:567, copyright 1998.

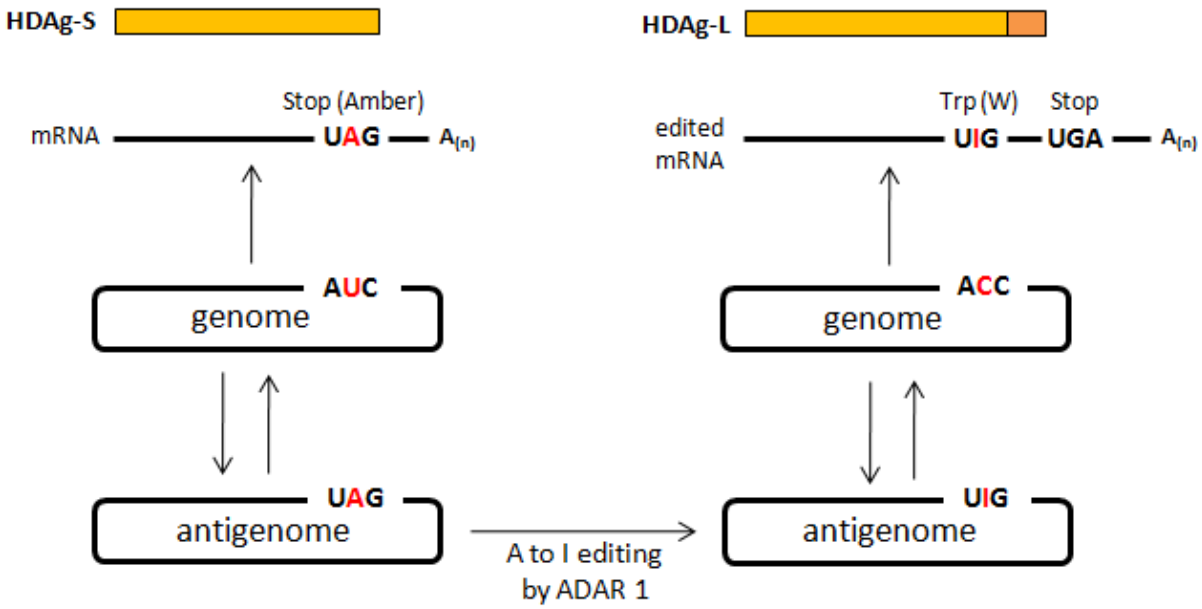
HDAg-S
HDAg-L
Stop (Amber)
mRNA
UAG
A(n)
Trp (W)
Stop
edited
mRNA
UIG
UGA
A(n)
AUC
genome
ACC
genome
UAG
antigenome
UIG
antigenome
A to I editing
by ADAR 1

Figure 1.4: Editing of antigenomic HDV RNA.

The amber stop codon (UAG; position 1014) is used during HDAg mRNA translation to produce HDAg-S. When the A (adenosine) of the amber stop codon is deaminated to I (inosine) on the antigenomic RNA, the modified residue forms a Watson-Crick base pair with C rather than U during the next round of replication, effectively changing the original UAG stop codon to a UGG tryptophan codon in the HDAg mRNA; this results in usage of a downstream stop codon (UGA), and leads to the production of an extended protein – HDAg-L. Figure adapted from Molecular Diversity Preservation International: Viruses 2:131,

of the termination codon of the small HDAg (HDAg-S) gene to a tryptophan codon (Figure 1.4). This editing site is referred to as the amber/W site to indicate the codon change produced (Polson *et al*., 1996). HDAg-L is produced later in infection; this is likely because the amber/W site is located in a structural context that is suboptimal for editing, hence efficient editing occurs only after a substantial amount of antigenomic HDV RNA has accumulated in the cell (Jayan and Casey, 2005; Sato *et al*., 2004).

Several structural domains have been identified in HDAg (Figure 1.5). A coiled coil domain is found in the N-terminus (amino acids 12-60) and enables HDAg oligomerization (Xia and Lai, 1992; Zuccola *et al*., 1998). Point-directed mutagenesis of this region reduced the ability of HDAgs to form dimers, and the extent of oligomerization was correlated to their biological activities (Xia and Lai, 1992). A nuclear localization signal (NLS), required for nuclear entry of HDV RNP complexes, is located between amino acids 66-75 (Alves *et al*., 2008), and was first identified by expressing fusion proteins consisting of different functional domains of HDAg fused with the human *α*-globin, a cytoplasmic protein (Xia *et al*., 1992).

HDAg contains an RNA-binding domain (RBD) consisting of two arginine-rich motifs (ARMs; amino acids 97-107 and 136-146), and a cryptic RNA-binding domain found in its N-terminus (amino acids 2-29); these motifs were shown to bind specifically to HDV RNA *in vitro* (Lee *et al*., 1993; Lin *et al*., 1990; Poisson *et al*., 1993). Using site-directed and truncation mutagenesis of the HDAg RBDs, Chou *et al*. (1998) demonstrated that the HDAg –HDV RNA interaction is essential for nuclear import of HDV RNA; interestingly, either one of the three RBDs was sufficient to confer this activity, even though both ARMs had been shown to be required for RNA binding *in vitro* (Lee *et al*., 1993). Mutational analysis

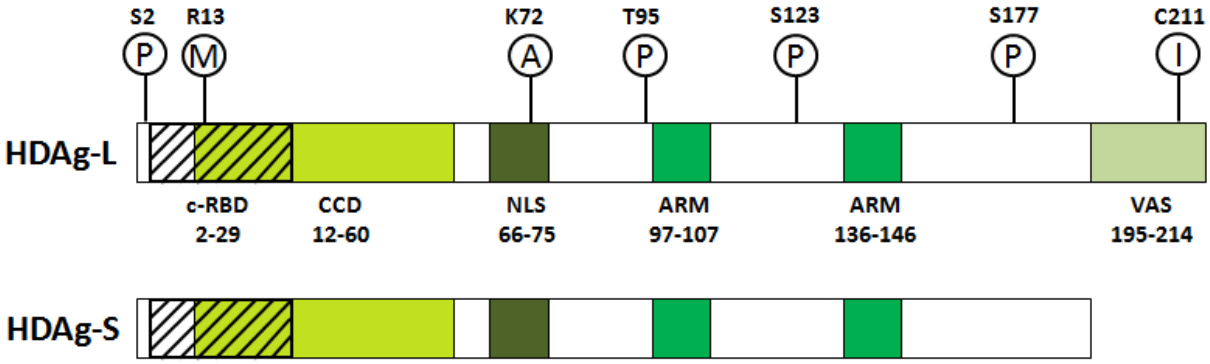
S2
R13
K72
T95
S123
S177
C211
P
M
A
P
P
P
I
HDAg-L
c-RBD
2-29
CCD
12-60
NLS
66-75
ARM
97-107
ARM
136-146
VAS
195-214
HDAg-S

Figure 1.5: Structural organization of the hepatitis *delta* antigens.

The indicated structural motifs are the cryptic RNA binding domain (c-RBD); the coiled-coil domain (CCD); the nuclear localization signal (NLS); two arginine-rich motifs (ARMs), comprising the main RBD; and the viral assembly signal (VAS), unique to HDAg-L. The following post-translational modifications are indicated: phosphorylation (P), methylation (M), acetylation (A), and isoprenylation (I).

also demonstrated that the RNA binding ability of HDAg is essential for viral RNA packaging, and at least the first ARM was required for this activity, as mutations introduced in this motif resulted in ineffective RNA packaging (Wang *et al*., 1994). The cryptic RNA-binding domain of HDAg was also demonstrated to act as a nucleic acid chaperone *in vitro*, and modulate the activity of the *delta* ribozyme. This activity of HDAg did not require the major RBD (Huang and Wu, 1998; Wang *et al*., 2003).

The carboxy-terminal 19 amino acids of HDAg are unique to the large isoform, and contain the viral assembly signal (VAS; amino acids 195-214), comprised of an isoprenylation site (Glenn *et al*., 1992; Lee *et al*., 1994; Otto and Casey, 1996) and a nuclear export signal (NES) (Lee *et al*., 2001). In cotransfection experiments, the 19 C-terminal amino acids of HDAg-L were shown to be required for viral particle assembly with HBsAg (Chang *et al*., 1994). Mutational analyses have found that other regions of HDAg-L are dispensable for packaging (Chang *et al*., 1994; Lee *et al*., 1995); indeed, when this 19 amino acid sequence was fused to a foreign protein, it directed the packaging of the fusion protein by HBsAg (Lee *et al*., 1995). The isoprenylation motif, comprised of the C-terminal last 4 amino acids of HDAg-L (Cys-Arg-Pro-Gln), is also essential for packaging; isoprenylation-defective mutants were found to be defective in co-packaging with HBsAg into virions (Lee *et al*., 1994).

1.7.1 Function of HDAg-S

Although HDAg-S and –L share common functional domains, each protein has distinct functions in the HDV life cycle. HDAg-S was shown to be essential for HDV

accumulation in cell culture; an HDV genome harbouring a mutation in the HDAg-S coding region was unable to initiate HDV replication (Kuo *et al*., 1989). Furthermore, a direct interaction between HDAg-S and HDV RNA via the RNA-binding domain was found to be necessary to activate viral replication (Lin *et al*., 1990; Lee *et al*., 1993). However, it is not clear whether HDAg-S participates directly in the RNA-templated transcription process. HDAg may be contributing to HDV replication by acting as an RNA chaperone; its N-terminus, including the cryptic RNA-binding domain and the coiled-coil domain (amino acids 1-59), was shown to facilitate *delta* ribozyme cleavage by accelerating the unfolding and refolding of RNA molecules, and by promoting strand annealing and dissociation (Huang and Wu, 1998; Wang *et al*., 2003). HDAg-S has also been reported to bind to HDV RNA and mediate its transport to the nucleus, where HDV transcription occurs (Chou *et al*., 1998). Although *in vitro* HDV RNA transcription has been achieved in the absence of HDAg-S (Abrahem and Pelchat, 2008; Beard *et al*., 1996; Filipovska and Konarska, 2000), addition of HDAg-S to the reaction was shown to increase the length of transcripts, suggesting a role for HDAg-S in transcription elongation by the DNA-dependent RNA polymerase II (RNAP II; Yamaguchi *et al*., 2001), the enzyme believed to be responsible for at least some HDV RNA-templated transcription (Abrahem and Pelchat, 2008; Gudima *et al*., 1999; Chang *et al*., 2006).

The elongation activity of RNAP II is repressed by the cooperative action of DRB-sensitivity inducing factor (DSIF) and the negative elongation factor (NELF; Yamaguchi *et al*., 1999). This repression is reversed by the positive elongation factor b (P-TEFb), which phosphorylates the C-terminal domain (CTD) of RNAP II (Wada *et al*., 1998) and a subunit of DSIF (Kim and Sharp, 2001). HDAg has a weak sequence homology (27%) to NELF-A,

the subunit of NELF implicated in direct RNAP II binding (Narita *et al*., 2003). Based on observations that HDAg binds RNAP II directly and inhibits NELF-RNAPII association without considerably affecting the DSIF-RNAP II interaction, Yamaguchi *et al*. (2001) proposed that HDAg-S competes with NELF-A for a common RNAP II site, thereby reversing the negative effects of DSIF/NELF. Interestingly, in the same study HDAg-S was also shown to stimulate RNAP II elongation in a DSIF/NELF-independent manner. It was subsequently shown by Yamaguchi *et al*. (2007) that HDAg-S affects transcriptional fidelity. The authors postulated that by interacting with RNAP II, HDAg-S loosens the clamp of the polymerase, a mobile structure that holds the template and product together, thereby accelerating elongation; and that the resulting decreased transcriptional fidelity may facilitate RNAP II-mediated transcription from an RNA template.

1.7.2 Function of HDAg-L

HDAg-L is reported to be an inhibitor of replication; when HDAg-L is expressed from a plasmid at the onset of replication, it inhibits the *trans*-activation activity of HDAg-S in a dominant manner (Chao *et al*., 1990; Lee *et al*., 1995). Mutations in the coiled-coil domain of HDAg-L were shown to interfere with its inhibitory function (Chang *et al*., 1994; Chen *et al*., 1992), and a truncation mutant of HDAg containing only amino acids 1 to 88 was able to suppress HDV replication (Lazinski and Taylor, 1993). It has been suggested that HDAg-L inhibits HDV replication by directly binding to HDAg-S via the coiled-coil domain (Lazinski and Taylor, 1993; Xia *et al*., 1992). Furthermore, HDAg-L's ability to suppress HDV replication was shown to be dependent on isoprenylation of its C terminus by the

cellular protein farnesyltransferase (FTase), which masks a conformation normally present in HDAg-S; this conformation has been mapped to amino acids 164 to 195, and is required for HDAg-S's *trans*-activation activity (Hwang and Lai, 1993, 1994; Otto and Casey, 1996), presumably because it contains the RNAP II binding site (Yamaguchi *et al*., 2001, 2007). These conformational differences between HDAg-S and -L may explain their opposing roles in HDV RNA replication.

HDAg-L also plays an essential role in HDV particle assembly (Chang *et al*., 1991). In the presence of the cytoplasm-localized HBsAg (Ou and Rutter, 1987), HDAg-L redistributes from the nucleus to the cytoplasm (Hwang and Lai, 1993). The two proteins were shown to interact directly, and this interaction was dependent on isoprenylation of the C-terminal domain of HDAg-L (Hwang and Lai, 1993). Isoprenylation was subsequently shown to be required for viral assembly (Lee *et al*., 1994; Bordier *et al*., 2002). An intact NES is also necessary for HDAg-L's ability to support HDV packaging into virions; an HDAg-L with a mutated NES was confined to the nucleus, and was unable to support assembly of HDV-like particles (Lee *et al*., 2001).

1.7.3 Posttranslational modifications of HDAgs

Several post-translational modifications of both HDAgs have been described in addition to isoprenylation of HDAg-L (Figure 1.5). These include phosphorylation (Chang *et al*., 1988; Mu *et al*., 1999), acetylation (Mu *et al*., 2004), methylation (Li *et al*., 2004) and sumoylation (Tseng *et al*., 2010). A study by Mu *et al*. (1999) used a nonequilibrium pH gradient electrophoresis technique to discover two major phosphorylated forms of HDAg-S;

in contrast, only one phospho isoform of HDAg-L could be isolated. It was determined that HDAg-S is phosphorylated at both serine and threonine residues, whereas HDAg-L is only phosphorylated at serine residues. Although the exact phosphorylation sites on HDAg are not known, Mu *et al*. (1999) found that Ser-2, -123, and -177, and Ser/Thr-95 of HDAg are conserved among all HDV strains. Of these, Ser-177 was shown to be important for genomic HDV RNA synthesis (Mu *et al*., 2001); a mutant HDAg-S, whose Ser-177 was replaced by alanine, could not support HDV replication. Furthermore, Ser-177-phosphorylated HDAg-S was found to interact specifically with the hypophosphorylated isoform of RNAP II, which is normally involved in transcription initiation, while HDAg-S dephosphorylated at Ser-177 preferentially bound the hyperphosphorylated, or transcription elongation, isoform of RNAP II (Hong and Chen, 2010), suggesting that the Ser-177 phosporylation status acts as a switch between transcription initiation and elongation. The extracellular signal-related kinases 1 and 2 (ERK1/2) have been implicated in Ser-177 phosphorylation and the associated regulation of HDV replication (Chen *et al*., 2008), although the involvement of other kinases in HDAg phosphorylation has been suggested, including casein kinase II (CKII), protein kinase C (PKC), and the double-stranded RNA-activated protein kinase R (PKR; Chen *et al*., 2002; Mu *et al*., 1999; Yeh *et al*., 1996). The function of HDAg-L phosphorylation is largely unknown; although site-directed mutagenesis of conserved serine residues had no effect on virion assembly or the inhibitory function of HDAg-L in RNA replication (Bichko *et al*., 1997; Yeh *et al*., 1996; Yeh *et al*., 1998), Tan *et al*. (2004) showed that mutagenesis of serine-123 resulted in HDAg-L translocation from the nucleolus to nuclear speckles. The same study found that serine-123 mutants as well as cysteine-211 (isoprenylation site) mutants were less efficiently transported to the cytoplasm; this finding is in line with an

earlier observation where mutagenesis of the isoprenylation site completely inhibited phosphorylation of HDAg-L (Bichko *et al*., 1997).

Acetylation of both HDAg-S and -L in cell culture has also been reported (Mu *et al*., 2004). *In vitro* assays identified the cellular acetyltransferase p300 to be able to acetylate HDAg-S. The acetylation of lysine-72 was shown to be necessary for the nuclear transport of HDAg-S; a lysine to arginine substitution caused a redistribution of HDAg-S from the nucleus to the cytoplasm. In addition, the mutation resulted in reduced accumulation of viral RNA, specifically genomic RNA, and lead to the earlier appearance of HDAg-L.

Similarly, methylation of HDAg-S has been shown to affect its cellular localization, and to modulate viral RNA accumulation (Li *et al*., 2004). HDAg-S was found to be methylated by protein arginine methyltransferase (PRMT1) at arginine-13, located in the RNA binding domain; methylation was essential for accumulation of genomic HDV RNA, and a methylation-defective mutant of HDAg-S localized to the cytoplasm.

Recently, Tseng *et al*. (2010) reported that HDAg-S is posttranslationally modified by the small ubiquitin-like modifier 1 (SUMO1). Sumoylation can affect intracellular localization, protein-protein interaction, protein-DNA interaction, and stability and activity of modified proteins (reviewed in Boggio and Chiocca, 2006). HDAg-S was shown to interact directly with SUMO1 and Ubc9, a SUMO E2 conjugating enzyme, and to be sumoylated at multiple lysine residues; this modification enhanced synthesis of genomic HDV RNA as well as HDAg mRNA, but had no effect on the synthesis of antigenomic RNA (Tseng *et al*., 2010).

Posttranslational modifications play a major role in the biology of HDV by modulating the activities of the two *delta* antigens; extensive modification allows HDV to expand its functional capacity. Clearly, more research is necessary to uncover the significance of these modifications in HDV's life cycle.

1.8 Viral Replication

1.8.1 Rolling circle model of replication

HDV RNA replication takes place in the nucleus of infected cells, and is proposed to occur via a symmetrical double rolling circle mechanism (Figure 1.6) analogous to that first observed in plant viroids (Branch and Robertson, 1984). According to this model, the HDV genome is used to produce linear antigenomic transcripts, which are either processed by polyadenylation to become HDAg mRNA, or are cleaved to unit-length RNAs by intrinsic *delta* ribozymes, and ligated to produce circular molecules; both RNA species are transcribed by the same RNA polymerase from a common RNA template (Nie *et al*., 2004; Taylor, 2009). Likewise, transcription of these circular antigenomes produces linear genomic multimers, which are processed into unit-length circular genomes. A somewhat modified model (Modahl and Lai, 1998) suggests that the transcription of the mRNA and the replication of the HDV genome are independent processes even though the mRNA and the antigenomic RNA are both made from the same RNA template. This is because synthesis of each RNA transcript is proposed to be carried out by a different RNA polymerase (see below). During infection, as many as 300,000 copies of genomic strand RNA accumulate per cell, while the abundance of the antigenome is about $1/10^{th}$ that of the genome (Chen *et al*.,

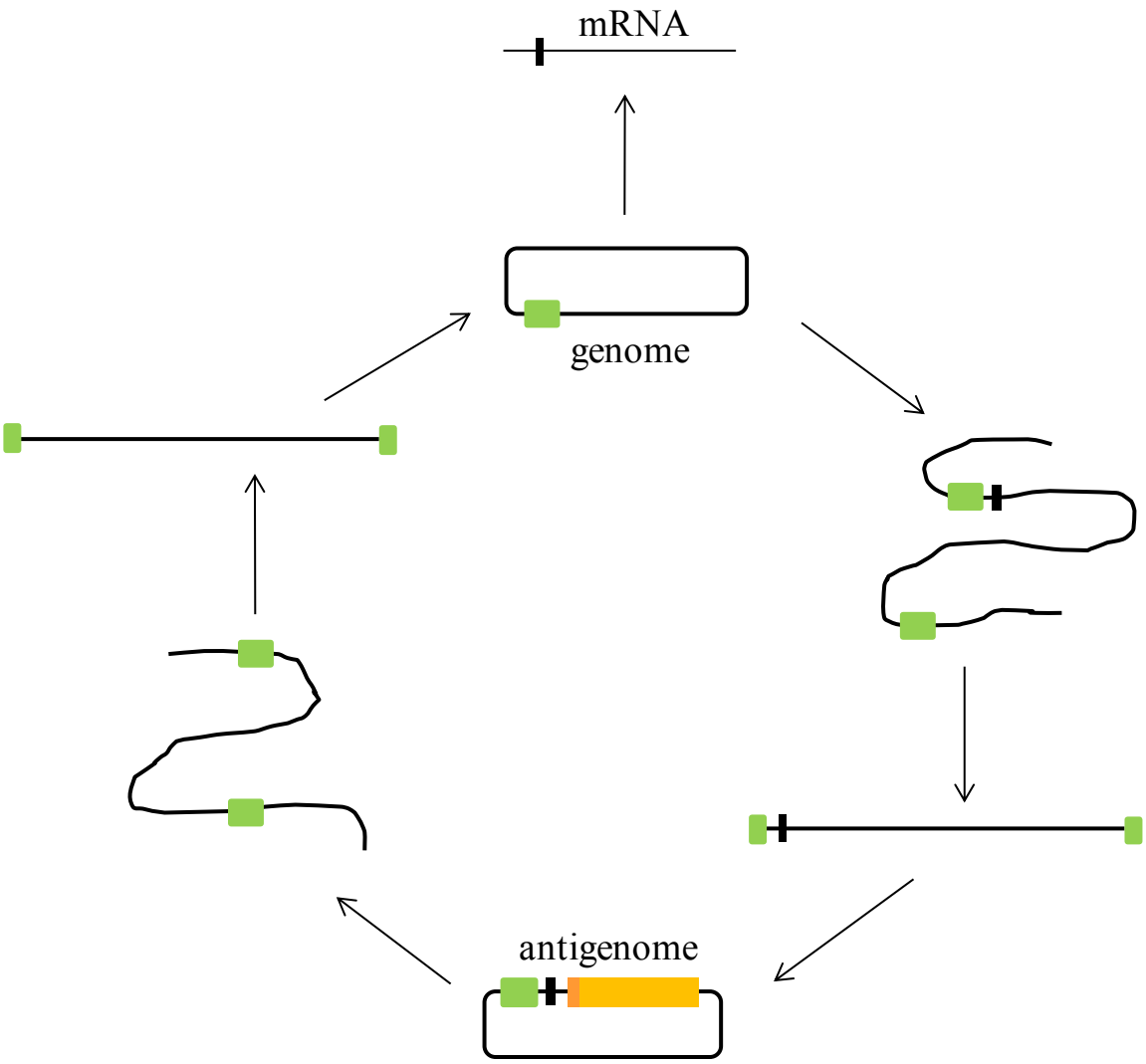
mRNA
genome
antigenome

Figure 1.6: Symmetrical rolling circle model of HDV replication.

The genomic circular RNA is used as a template for synthesis of HDAg mRNA, or antigenomic multi-length RNA. This RNA is processed by *delta* ribozyme (green boxes) cleavage, followed by ligation to produce circular unit-length RNAs. These act as templates for the transcription and processing of new genomic circular RNAs. The ORF (orange box) and the polyadenylation signal (black box) are indicated. Figure adapted by permission from Macmillan Publishers Ltd: Virology 344:71, copyright 2006.

1986). A linear mRNA species of about 800 nucleotides also accumulates, and is about 500 times less abundant than full-length genomic RNA (Hsieh *et al*., 1990).

HDV replication is RNA-templated, lacking DNA intermediates, and is entirely independent of the helper virus, HBV. As the virus does not encode its own replicase, it uses host-encoded RNA polymerase(s) (RNAPs) to replicate its genome. Although human RNAPs are traditionally regarded as DNA-dependent enzymes, HDV is able to redirect them to carry out RNA-templated transcription. The following sections will summarize the current body of knowledge on the process of HDV genome replication.

1.8.2 Polymerase requirements

One of the most intriguing aspects of HDV biology is the mechanism by which the viral RNA is replicated. Several approaches have been used to identify host polymerase(s) involved in the HDV replication cycle, and many observations implicated RNAP II as a key enzyme. The synthesis of HDAg mRNA is likely mediated by RNAP II, since the mRNA has a 5' cap and a 3' poly(A) tail (Gudima *et al*., 1999; Hsieh *et al*., 1990; Nie *et al*., 2004), features unique to RNAP II transcripts. The association of RNAP II with different fragments of HDV RNA has also been demonstrated (Abrahem and Pelchat, 2008; Greco-Stewart *et al*., 2007), and *in vitro* HDV transcription was inhibited by an antibody directed against the carboxy-terminal domain (CTD) of RNAP II (Abrahem and Pelchat, 2008). Furthermore, HDV RNA accumulation in cells replicating HDV RNA was shown to be sensitive to low doses of α-amanitin (Chang *et al*., 2006; Macnaughton *et al*., 1991; Modahl *et al*., 2000;

Moraleda and Taylor, 2001). This mycotoxin specifically inhibits RNAP II at very low concentrations by direct binding of the polymerase (Bushnell *et al*., 2002), while having only a moderate inhibitory effect on RNAPs I and III (reviewed by Chambon, 1975). A recent study by Chang *et al*. (2008) used nuclear run-on experiments with an endogenous template to show that the synthesis of new genomic and antigenomic RNAs was sensitive to α-amanitin, suggesting the involvement of RNAP II in the replication of both polarities of HDV RNA. However, several other studies have shown that antigenomic HDV RNA synthesis was resistant to α-amanitin (Macnaughton *et al*., 2002; Modahl *et al*., 2000), suggesting that while the mRNA and the genome are produced by RNAP II, another polymerase is involved in the synthesis of antigenomic RNA.

The involvement of RNAP I in HDV antigenome synthesis is supported by several findings. HDV RNA was shown to co-immunoprecipitate with the RNAP I-associated transcription factor SL1 (Greco-Stewart *et al*., 2009; Li *et al*., 2006). Furthermore, genomic and antigenomic HDV RNA was shown to associate with different subnuclear bodies: in metabolic labelling studies, antigenomic RNA localized to the nucleolus, while the genomic RNA localized more diffusely in the nucleoplasm, and colocalized with PML (promyelocytic leukemia protein) nuclear bodies (Li *et al*., 2006). PML bodies are heterogeneous protein complexes associated with different cellular functions (reviewed by Bernardi and Pandolfi, 2007). Some of the constituents of PML bodies have been reported to be involved in gene expression and replication of certain DNA viruses (Kelly *et al*., 1995; Rosa-Calatrava *et al*., 2003; Tang *et al*., 2000). In the study by Li *et al*. (2006), HDAg co-immunoprecipitated with PML as well as with RNAP II and with SL1. In *in vitro* replication assays, pretreatment with an antibody against SL1 reduced synthesis of antigenomic RNA. While neither an anti-

RNAP II nor an anti-PML antibody had an effect on antigenomic RNA synthesis, both inhibited synthesis of genomic RNA. These findings are corroborated by a recent study by Huang *et al*. (2008a), in which a recombinant HDAg-S, fused with a nucleolar localization sequence (NoLS), was used to confine its subcellular localization to nucleoli. The initiation of genomic RNA synthesis was hardly detectable when HDAg-S localized mainly in the nucleoli, while initiation of antigenomic RNA synthesis was not affected, suggesting that antigenomic RNA synthesis occurs in the nucleolus. Furthermore, when confined to the nucleolus, HDAg-S could not be precipitated with RNAP II until it was released into the nucleoplasm following drug treatment. However, contrary to the findings by Li *et al*. (2006), this study was unable to show interaction of RNAP I with HDAg-S.

Additional support for the involvement of at least two different polymerases in HDV replication comes from observations by Tseng *et al*. (2008), who showed that Arg-13 methylation, Lys-72 acetylation, and Ser-177 phosphorylation of HDAg-S are important for HDV mRNA transcription, and confirmed previous findings that these three HDAg-S modifications are required for genomic RNA synthesis but are dispensable for antigenomic RNA synthesis (Li *et al*., 2004; Mu *et al*., 2001; Mu *et al*., 2004). These data suggest the involvement of distinct cellular machineries in the synthesis of the different HDV RNAs, where antigenomic RNA synthesis is mediated by an unmodified HDAg-S, and both HDV mRNA transcription and genomic RNA synthesis involve posttranslational modifications of HDAg-S.

The involvement of yet another polymerase in the replication of HDV cannot be excluded. RNAP III was recently shown to interact specifically with HDV RNA, both *in*

vitro and in cells replicating HDV RNA (Greco-Stewart *et al*., 2009), although the significance of this interaction is unclear.

1.8.3 HDV RNA promoters

Although human RNAP-mediated transcription is traditionally DNA-templated, HDV RNA may be redirecting the polymerase by mimicking double-stranded DNA. The extensive intramolecular complementarity that allows HDV RNA to fold into a rod-like structure may enable the polymerase to recognize it as a suitable template. Indeed, both right and left terminal hairpins of genomic and antigenomic HDV RNAs were shown to bind RNAPs I, II, and III (Greco-Stewart *et al*., 2007, 2009).

Transcription of the HDAg mRNA is believed to be initiated at a unique site located in the top strand of the right terminal stem-loop domain of genomic HDV RNA (Figure 1.2; Gudima *et al*., 1999, 2000), although it is not known whether the initiation site of antigenomic RNA synthesis is identical to that of mRNA transcription. This region of HDV RNA was shown to act as an RNA promoter *in vitro* (Abrahem and Pelchat, 2008; Beard *et al*., 1996), and to co-immunoprecipitate with RNAP II (Greco-Stewart *et al*., 2007). Mutations introduced in this region resulted in decreased HDV accumulation in cell culture (Beard *et al*., 1996; Gudima *et al*., 1999; Wu *et al*., 1997). Notably, the basic hairpin conformation was essential for RNAP II binding and transcription initiation *in vitro* (Beard *et al*., 1996; Greco-Stewart *et al*., 2007). Recently, Abrahem and Pelchat (2008) demonstrated *in vitro* formation of an active RNAP II pre-initiation complex (PIC) on an RNA fragment

containing the putative HDV promoter. This PIC closely resembled one that forms on a canonical DNA promoter.

Synthesis of the genomic strand has been proposed to initiate in the left terminal stem-loop domain of antigenomic HDV RNA. This region was shown to interact with RNAP II (Greco-Stewart *et al*., 2007), and to act as an RNA promoter for RNAP II *in vitro* (Filipovska and Konarska, 2000). As observed for the genomic promoter, the rod-like structure was essential for transcription initiation. However, transcription was reported to occur by an alternate process, in which the template is cleaved and the newly generated 3′ end serves as a primer for RNAP II transcription, producing a hybrid transcript consisting of the newly synthesized genomic RNA joined to the 5' portion of the antigenomic template. These findings were supported by Lehmann *et al*. (2007) who observed that the general transcription factor IIS (TFIIS) can cleave one HDV strand, creating a reactive stem-loop in the hybrid site, allowing RNAP II to extend the new 3′ end to create a chimeric product. Although this cleavage-extension mechanism is not consistent with the rolling circle model of replication, a similar hybrid RNA, derived from the right terminal hairpin, was detected *in vivo* by reverse-transcription PCR (Haussecker *et al*., 2008), suggesting that this mechanism may represent an alternative, rare method of HDV transcription initiation.

The study by Haussecker *et al*. (2008) further suggested a primed mechanism of HDV transcription initiation based on the identification of small, 5′-capped RNAs (18-25 nucleotides) corresponding to the 5′ end of HDAg mRNA, presumably produced by *de novo* transcription initiation followed by polymerase pausing. These small RNAs were also observed in HDV virions, prompting the authors to suggest a replication model in which these RNAs facilitate transcription initiation by acting as primers, thereby increasing the

chances for a successful infection. Further studies are needed to test the validity of this hypothesis.

1.9 Host-virus interactions

HDV has a very limited coding capacity; in effect, it must make use of numerous host proteins to ensure its propagation. Both HDAg and HDV RNA interact with various host factors at different stages of the viral life cycle. While some of these factors have been identified (Greco-Stewart and Pelchat, 2010), the functional relevance of the majority of these interactions is still unknown. Recent proteomic analyses of a human hepatocellular carcinoma cell line (Huh7) transfected with different components of HDV (Mota *et al*., 2008), or stably expressing HDV RNPs (Mota *et al*., 2009) revealed at least 50 differentially expressed proteins. Another proteomic screen identified over 100 HDAg-S-associated proteins (Cao *et al*., 2009); an RNAi analysis revealed 18 factors that influenced HDV accumulation upon siRNA-mediated knockdown. Although the biological significance of these findings remains unclear, it is apparent that extensive interactions of HDV with its host have a great impact on HDV biology and pathogenicity. Identification of host factors interacting with HDV is crucial to the understanding of the host-pathogen relationship.

1.9.1 Interaction of HDV RNA with host proteins

In addition to RNAPs I, II, and III, which interact with genomic and antigenomic HDV RNA (Chang *et al*., 2008; Greco-Stewart *et al*., 2007), likely via the TATA-binding

protein (TBP; Abrahem and Pelchat, 2008; Greco-Stewart *et al*., 2009), a transcription factor common to all three RNAPs, various other host factors have been reported to associate with HDV RNA (Table 1.1). ADAR1 is a host protein that is indispensable for the life cycle of HDV, as it allows for the production of HDAg-L. ADARs catalyze the deamination of adenosine to inosine in perfect and imperfect double stranded RNA (Kim *et al*., 1994; Melcher *et al*., 1996). During HDV RNA replication, a fraction of the antigenome is edited by ADAR1, which converts the adenosine in the UAG (amber stop codon) of the HDAg-S gene to an inosine. During the subsequent antigenome to genome replication, the inosine pairs with a cytosine, effectively changing the UAG codon in the HDAg ORF (Casey and Gerin, 1995). Two forms of ADAR1 exist in mammalian cells: the large, full length form (ADAR1-L), localized mainly to the cytoplasm, and the small form (ADAR1-S), found exclusively in the nucleus (Patterson and Samuel, 1995). Although both forms can edit HDV RNA, editing of the HDV antigenome occurs in the nucleus and is mediated by ADAR1-S (Wong and Lazinski, 2002).

Another host protein involved in the replication of HDV RNA is glyceraldehyde 3-phosphate dehydrogenase (GAPDH). GAPDH was shown to interact with the HDV antigenome and enhance ribozyme activity (Lin *et al*., 2000). In the cell, GAPDH is prominently known for catalyzing the conversion of glyceraldehyde 3-phosphate to $_{D}$-1,3-bisphosphoglycerate during glycolysis; in addition, it is involved in many other cellular processes, including DNA replication (Baxi and Vishwanatha, 1995) and repair (Meyer-Siegler *et al*., 1991), binding and nuclear transport of tRNA (Singh and Green, 1993), binding to AU-rich RNA (Nagy and Rigby, 1995), and apoptosis (Ishitani *et al*., 1996). In the study by Lin *et al*. (2000), GAPDH was detected to relocalize from the cytoplasm to the

Table 1.1: Host factors interacting with HDV RNA.

Host Protein	Proposed Function	Reference
Adenosine deaminase that acts on RNA (ADAR) 1	Posttranscriptional modification of antigenomic HDV RNA	Wong and Lazinski, 2002
Glyceraldehyde 3-phosphate dehydrogenase (GAPDH)	Enhances *delta* ribozyme activity	Lin *et al*., 2000
Double-stranded RNA-dependent protein kinase (PKR)	PKR activation	Circle *et al*., 1997
DNA-dependent RNA polymerase (RNAP) I	Synthesis of antigenomic HDVRNA	Greco-Stewart *et al*., 2009 Li *et al*., 2006
RNAP II	Synthesis of HDAg mRNA and genomic HDV RNA	Abrahem and Pelchat, 2008; Greco-Stewart *et al*., 2007
RNAP III	Unknown/HDV RNA synthesis	Greco-Stewart *et al*., 2009
Polypyrimidine tract-binding protein associated splicing factor (PSF)	Unknown/possibly involved in recruitment of HDV RNA to RNAP II	Greco-Stewart *et al*., 2006

nucleus in the presence of HDV RNA, and to interact directly with a small UC-rich region of the antigenome, found between nucleotides 379 and 414. *In vitro cis*-cleavage of a 741-nt RNA fragment corresponding to the left half of HDV antigenome was enhanced in the presence of GAPDH. The observed specific two-fold enhancement on the *cis*-cleavage activity of the antigenomic RNA suggests that GAPDH acts as a molecular chaperone to unwind the double-stranded RNA structure, thereby allowing the RNA to fold into the double pseudo-knot structure necessary for cleavage.

HDV RNA also interacts with the double-stranded (ds) RNA-activated protein kinase R (PKR), a cellular mediator of interferon-induced antiviral response and a tumor suppressor (Hovanessian, 1993; Matthews, 1993; Muers *et al*., 1993). Activation of PKR by dsRNA results in global protein synthesis inhibition (Hunter *et al*., 1975; Manche *et al*., 1992; Matthews, 1993). PKR was shown to interact directly and specifically with a region of HDV genomic RNA corresponding to the left terminal stem-loop domain (nucleotides 699 – 884) (Circle *et al*., 1997). Furthermore, full-length genome and antigenome, as well as subgenomic fragments of HDV RNA were shown to activate PKR *in vitro* (Robertson *et al*., 1996). Although HDV RNA is single-stranded (ss), and binding of highly-structured ssRNA is known to inhibit PKR (Manche *et al*., 1992), the collapsed-rod structure of HDV might be able to mimic dsRNA. Surprisingly, HDV RNA failed to inhibit protein synthesis in a rabbit reticulocyte lysate translation system, and instead interfered with PKR activation by dsRNA (Robertson *et al*., 1996), although this finding might be caused by differences between the human kinase and the rabbit translation system used. Nonetheless, the authors suggest that HDV RNA's inability to activate PKR in reticulocyte lysates is due to alternate folding of the RNA at the PKR binding site. The region of HDV genomic RNA found to bind PKR (Circle

et al., 1997) was previously shown capable of folding into a cruciform structure that disrupts the rod-like conformation (Branch and Robertson, 1991). This alternate RNA structure reduces the potential of HDV RNA to mimic dsRNA, thus rendering it incapable of activating PKR (Robertson *et al*., 1996). It is probable that *in vivo*, HDV RNA suppresses PKR activation to hinder an anti-viral response. It is also possible that the binding of HDV RNA to PKR mediates the interaction between PKR and HDAg-S, facilitating PKR phosphorylation of HDAg. The exact role of PKR in the life cycle of HDV remains to be elucidated.

The polypyrimidine tract-binding (PTB) protein-associated splicing factor (PSF) is another host protein that interacts specifically and directly with HDV RNA of both polarities (Greco-Stewart *et al*., 2006). PSF is a multifunctional protein involved in many cellular processes, including pre-mRNA splicing, transcriptional regulation, nuclear retention of defective RNAs, DNA unwinding and pairing, and pH homeostasis (reviewed by Shav-Tal and Zipori, 2002). PSF was shown to interact with the CTD of RNAP II during transcription initiation and elongation, and promoted the binding of RNA to immobilized CTD matrices (Emili *et al*., 2002). Since PSF and RNAP II bind the same region(s) of HDV RNA (Greco-Stewart *et al*., 2006; Greco-Stewart *et al*., 2007), it is possible that PSF plays an essential role in HDV transcription by providing a direct physical link between the polymerase and the RNA template. The interaction of HDV RNA and PSF may also contribute to HDV pathogenicity; PSF represses the expression of numerous oncogenes (Song *et al*., 2004), and the binding of HDV RNA might interfere with its tumour suppression function and promote metastasis (Song *et al*., 2002; Song *et al*., 2004; Song *et al*., 2005), thereby contributing to

the development of HDV-associated liver cancer (Fattovich *et al*., 2004; Romeo *et al*., 2009; Su *et al*., 2006).

1.9.2 Interaction of HDAgs with host proteins

Several host proteins have been reported to interact with HDAgs (Table 1.2), in addition to the factors involved in post-translational modifications of HDAg-S and/or HDAg-L. Proteins involved in the transport of HDAgs across the nuclear membrane have already been identified. Karyopterin α2, a transport factor involved in targeting substrates to the nuclear pore complex (Moroianu *et al*., 1995), was shown to interact with HDAg *in vitro* via the NLS, and is thought to be responsible for the import of HDV RNPs into the nucleus (Chou *et al*., 1998). Nuclear export of HDV RNPs is believed to be mediated by the direct interaction between the NES of HDAg-L and the NES-interacting protein (NESI) (Wang *et al*., 2005); inhibition of NESI expression resulted in significant reduction of viral genomic RNA accumulation in the cytoplasm, and prevented packaging of the RNA into virus-like particles. The extended C-terminus of HDAg-L also contains a putative clathrin box, which was shown to directly interact with the clathrin heavy chain at the *trans*-Golgi network (CHC; Huang *et al*., 2007; Wang *et al*., 2009). Clathrin is involved in the endocytosis and exocytosis of cellular proteins and the process of virus infection. The clathrin-mediated endocytic route is commonly used for viral entry (Ehrlich *et al*., 2004; Rust *et al*., 2004), and clathrin-mediated exocytosis has been shown to promote viral release at the plasma membrane (Alconada *et al*., 1996; Van Damme and Guatelli, 2007). It was recently shown that CHC is essential for the formation of HDV virus-like particles by HDAg-L (Huang *et*

Table 1.2: Host factors interacting with HDAg.

Host Protein	Proposed Function	Reference
Casein kinase II (CKII)	Posttranslational modification	Yeh *et al*, 1996
Protein kinase C (PKC)	Posttranslational modification	Lin *et al*., 2000
Double-stranded RNA-dependent protein kinase (PKR)	Posttranslational modification	Chen *et al*., 2002
Extracellular signal-related kinases 1and 2 (ERK1/2)	Posttranslational modification	Chen *et al*., 2008
Protein farnesyltransferase (FTase)	Posttranslational modification	Glenn *et al*., 1992; Otto and Casey, 1996
Protein arginine methyltransferase 1 (PRMT1)	Posttranslational modification	Li *et al*., 2004
p300 cellular acetyltransferase	Posttranslational modification	Huang *et al*., 2008; Mu *et al*., 2004
Small ubiquitin-related modifier isoform 1 (SUMO1)	Posttranslational modification	Tseng *et al*., 2008
Ubc9 (SUMO E2 conjugating enzyme)	Posttranslational modification	Tseng *et al*., 2008
Karyopherin (importin) 2α	Nuclear import	Moroianu *et al*., 1995
Nuclear export signal-interacting protein (NESI)	Nuclear export	Wang *et al*., 2005
Clathrin heavy chain (CHC)	Exocytosis	Huang *et al*., 2007; Wang *et al*., 2009
Nucleolin (C23)	Nucleolar targeting	Lee *et al*., 1998
Nucleophosmin (B23)	Nucleolar targeting	Huang *et al*., 2001
RNAP II (Rpb1/2 mobile clamp element)	HDV RNA synthesis	Yamaguchi *et al*., 2007; Cao *et al*., 2009
Delta-interacting protein A	Unknown	Brazas and Ganem, 1996
Histone H1e	Unknown	Lee and Sheu, 2008
Yin Yang 1 (YY1)	Unknown	Huang *et al*., 2008
MOV10	Unknown	Haussecker *et al*., 2008
Smad3	Alters host gene expression	Choi *et al*., 2007
c-Jun	Alters host gene expression	Choi *et al*., 2007
TRAF2	Alters host gene expression	Park *et al*., 2009

al., 2009), suggesting that HDV particles are released by clathrin-mediated exocytosis. The HDAg-L-CHC interaction might also contribute to viral pathogenesis, as cytoplasm-localized HDAg-L was shown to interfere with the clathrin-mediated endocytosis and exocytosis of cellular proteins (Huang *et al*., 2007).

Although numerous additional proteins have been shown to bind HDAg, the biological significance of these interactions has not been elucidated. Two nucleolar phosphoproteins, nucleolin and nucleophosmin, were shown to interact with HDAg-S and -L (Huang *et al*., 2001; Lee *et al*., 1998). Nucleophosmin binds directly to the nucleolar localization signal of nucleolin and this interaction may be required for the nucleolar targeting of nucleolin (Li *et al*., 1996). Both proteins perform similar cellular functions, including cellular proliferation, nuclear shuttling and ribosome synthesis (reviewed in Okuwaki, 2008; Tuteja and Tuteja, 1998), and were both found in association with HDAg as part of a large nuclear complex (Huang *et al*., 2001). While the nucleolin-HDAg interaction involves a region within the coiled-coil domain of HDAg, nucleophosmin binding occurs via the NLS of HDAg. Nucleophosmin might be involved in the nuclear transport of HDV RNPs, as it has been shown to mediate nuclear import of NLS-containing proteins (Szebeni *et al*., 1995, 1997). Both proteins were shown to have a positive effect on the accumulation of HDV RNA (Huang *et al*., 2001; Lee *et al*., 1998), possibly by modulating HDV RNA replication through nucleolar targeting of HDAgs.

Another protein that interacts with both isoforms of HDAg is the multifunctional transcription factor Ying Yang 1 (YY1) (Huang *et al*., 2008b). YY1 is involved in activation or repression of many cellular and viral promoters, and interacts with many transcriptional regulators (reviewed by Gordon *et al*., 2006). Interestingly, YY1 also interacts with

nucleolin, nucleophosmin and RNAP II (Inouye and Seto, 1994; Lee and Lee, 1994; Usheva and Shenk, 1996), and all four proteins have been shown to enhance HDV RNA accumulation (Chang *et al*., 2006; Huang *et al*., 2001, 2008b; Lee *et al*., 1998; Macnaughton *et al*., 1991). The findings of Huang *et al*. (2008b) suggested that HDAg and YY1, along with its associated acetyltransferases CBP and p300, form large nuclear complexes which also contain nucleolin and nucleophosmin. It is possible that these high-molecular-weight nuclear complexes function as activating complexes to enhance the replication of HDV RNA. Furthermore, backed by previous findings that HDAg-S interacts with and is acetylated by p300 (Mu *et al*., 2004), Huang and colleagues showed that overexpression of p300, but not an acetylation-defective mutant, enhanced HDV RNA replication, thus suggesting that YY1 may be recruiting the acetyltransferase to the complex to modulate HDV replication through acetylation of HDAg-S.

A further host factor found to interact with HDAg-S and affect HDV replication is the linker histone H1e (Lee and Sheu, 2008). H1 histones interact with linker DNA that extends between nucleosome core particles, thereby stabilizing the structure of the nucloesome. They are involved in the formation of higher order chromatin structures and are implicated in regulation of gene expression by modulating the accessibility of regulatory proteins to their target sites (reviewed by Happel and Doenecke, 2009). H1e bound to the N-terminus of HDAg-S, but failed to interact with HDAg-L due to an isoprenylation-induced conformational change that masked the H1e binding site (Lee and Sheu, 2008). This binding was required for HDV RNA accumulation: when the H1e-HDAg-S interaction was challenged by overexpression of an H1e mutant capable of binding HDAg-S, HDV

replication was inhibited but could be rescued by wild type H1e. These findings suggested a significant role of H1e in HDV replication.

MOV10, a host protein identified as a constituent of an HDAg-containing complex, may also be involved in HDV replication (Haussecker *et al*., 2008). MOV10 is a human homologue of a putative RNA helicase from *Arabidopsis thaliana* required for the amplification step of ssRNA-induced RNAi in plants (Dalmay *et al*., 2001). The human MOV10 is associated with Argonaute (AGO) proteins, yet it is unclear what role it plays in RNAi (Meister *et al*., 2005). In the study by Haussecker *et al*. (2008), *MOV10* knockdown inhibited HDV replication, supporting a role for MOV10 in HDV RNA transcription. *AGO4* knockdown also inhibited HDV replication, although the knockdown of other microRNA-processing factors showed no appreciable effect. While the MOV10-HDAg-S interaction is likely not related to the RNAi pathway, it is possible that MOV10 and AGO4 cooperatively influence transcription initiation competency by remodelling HDV RNA.

HDAg also interacts with its putative cellular homologue, first identified in a yeast-two-hybrid screen, and termed the *delta*-interacting protein A (DIPA; Brazas and Ganem, 1996). According to Brazas and Ganem (1996), DIPA shares 24% sequence identity and 56% sequence similarity with HDAg, which extends over the entire length of both proteins, and includes the C-terminus of HDAg-L; however, the validity of the homology has been disputed by other bioinformatics analyses (Veretnik and Gribskov, 1999). The coiled-coil motifs present in each protein were found to be involved in the binding. Furthermore, the overexpression of DIPA in cells replicating HDV RNA led to apparent inhibition of HDV RNA synthesis (Brazas and Ganem, 1996). Since DIPA has been shown to act as a repressor

of cellular gene transcription (Bezy *et al*., 2005; Du *et al*., 2006), it is possible that it is also a negative regulator of HDV transcription *in vivo.*

HDAg has also been shown to interact with other cellular transcription factors. A recent study demonstrated the direct association of both HDAg-S and –L with Smad3 and c-Jun (Choi *et al*., 2007). Smad3 functions in a complex with other Smads and controls gene expression through direct DNA binding. It belongs to a family of intracellular signalling effectors for transforming growth factor-β (TGF-β) –induced transcriptional responses (Derynck *et al*., 1998); TGF-β regulates cell growth and differentiation (Derynck *et al*., 2001), and is also a potent fibrogenic cytokine that plays a major role in liver fibrosis and cirrhosis (Castilla *et al*., 1991; Nagy *et al*., 1991). Inagaki *et al*. (2001) showed Smad3 to be activated in fibrotic liver disease. It is possible that the interaction between HDAg and Smad3 modulates the activity of the latter, contributing to liver pathology. Interestingly, while both HDAg isoforms interacted with Smad3, only HDAg-L activated the TGF-β signalling pathway, and this activation was dependent on HDAg-L isoprenylation (Choi *et al*., 2007).

C-Jun is a component of the activator protein-1 (AP-1) transcription factor complex. Through direct binding to promoter elements, AP-1 controls a vast amount of biological processes, including cell proliferation, inflammation, differentiation and apoptosis (Karin *et al*., 1997). C-Jun is activated by c-Jun N-terminal kinase (JNK) –mediated phosphorylation, while JNK expression is regulated by many stimuli, including cytokines such as TGF-β (Karin and Gallagher, 2005). C-Jun has paradoxical roles in the cell, which are highly dependent on the cellular context. Numerous studies have identified c-Jun as an oncoprotein, while others have shown it to be involved in the prevention of tumorigenesis (reviewed by

Shaulian, 2010). In the study by Choi *et al*. (2007), c-Jun-mediated activation of an AP-1 reporter gene was specifically enhanced by isoprenylated HDAg-L. Based on an earlier finding that c-Jun interacts with Smad3 to inhibit the TGF-β signalling pathway (Dennler *et al*., 2000), Choi *et al*. investigated whether the interaction of HDAg with c-Jun would interfere with the inhibitory effect of c-Jun on TGF-β-mediated signal transduction. While both HDAg-S and –L prevented the c-Jun-Smad3 complex formation in a GST pull-down experiment, only HDAg-L was able to reverse the inhibitory effect of c-Jun on Smad3-mediated transcriptional activation in cell culture, in a dose-dependent manner.

Both HDAg isoforms have also been shown to interact with tumour necrosis factor (TNF) receptor-associated factor 2 (TRAF2), a signal transducing protein involved in the TNF-α-mediated activation of nuclear factor kappa B (NF-κB; Park *et al*., 2009). NF-κB is a dimeric transcription factor that plays important regulatory roles in inflammation, immunity, cell proliferation and apoptosis (Aggarwal, 2004; Ghosh and Karin, 2002; Silverman and Maniatis, 2001). Only HDAg-L was shown to enhance TNF-α-induced NF-κB transcriptional activation in an isoprenylation-independent manner.

The interaction of HDV with cellular transcription regulators likely plays a considerable role in HDV pathogenesis. By modulating the functions of transcription factors involved in regulation of fibrogenesis, cell proliferation and tumorigenesis, HDV may be contributing to the progression of liver disease. HDV likely interacts with many other transcription factors, which are yet to be identified. Altered gene expression patterns have been observed in cells expressing HDAgs (Mota *et al*., 2009). Particularly, HDAg-L has been shown to stimulate transcription of reporter genes by diverse eukaryotic promoters (Wei and Ganem, 1998). In subsequent studies, HDAg-L was found to activate the serum response

element (SRE)-dependent pathway (Goto *et al*., 2000, 2003) and the α interferon-inducible MxA gene (Williams *et al*., 2009). Furthermore, a recent study by Liao *et al*. (2009) showed enhanced expression of clusterin, a regulator of apoptosis (reviewed by Trougakos and Gonos, 2006), in HDAg-expressing cells. HDV was shown to epigenetically control clusterin expression, via histone acetylation within the clusterin promoter; the HDV-induced clusterin expression was correlated to increased cell survival potential. Although it is clear that HDV interferes with numerous transcription regulatory mechanisms, the HDV-host interactions responsible for these observations need to be identified to better understand HDV biology and pathogenicity.

1.10 Origin of HDV

The hepatitis *delta* virus is unlike any known human pathogen. Although its evolutionary origin is not clearly understood, numerous hypotheses attempt to explain how HDV might have arisen (Taylor and Pelchat, 2010). As a subviral satellite of HBV, HDV relies on its helper virus for its virion assembly and propagation; in all other aspects of viral biology, the two pathogens are very distinct. Interestingly, HDV bears a striking resemblance to plant viroids, helper-independent subviral agents, suggesting an evolutionary relationship between the two (Taylor and Pelchat, 2010). However, other possible origins of HDV cannot be ignored: structural and functional similarities have been observed between HDV and plant virusoids, circular, viroid-like satellite RNAs associated with certain plant viruses; it is also possible that an HDV-like species arose from a host precursor mRNA, based on the recent

identification of many HDV-like ribozymes in animal cells (Taylor and Pelchat, 2010; Webb *et al*., 2009).

1.10.1 Parallels between HDV and plant viroids

Viroids exhibit several structural and functional parallels to HDV. Their small, single-stranded RNA genomes range in size between 250-400 nucleotides (Tabler and Tsagris, 2004). Unlike HDV, viroid genomes are non-coding, which may account for the difference in size between the two. Their discovery came about in 1971, as the potato spindle tuber viroid (PSTVd) was identified as the causative agent of a potato disease (Diener, 1971). Since then, 31 different species have been identified, which are classified into two families: *Pospiviroidae* (27 members) and *Avsunviroidae* (4 members). The two families are distinguished by several characteristics (Table 1.3). Most RNA genomes of pospiviroids adopt unbranched, rod-like structures, resembling the structure of HDV RNA (Figure 1.7); while most avsunviroids fold into complex, branched secondary structures, with many stem-loop regions, they can also adopt quasi-rod-like structures (Navarro and Flores, 2000). Avsunviroids replicate in the chloroplast by a symmetrical rolling circle mechanism, similar to that believed to occur in HDV, in which linear multimers are processed by intrinsic hammerhead ribozymes. In contrast, pospiviroids have no apparent self-cleaving motifs, and they replicate in the nucleus via an asymmetrical rolling circle mechanism. In this alternative replication system, the (-) polarity multimers, generated from the infective (+) polarity circular RNAs, are not processed into monomers; instead they serve directly as templates for

Table 1.3: Key differences between the *Pospiviroidae* and *Avsunviroidae* families.

Feature	*Pospiviroidae*	*Avsunviroidae*
Secondary genome structure	rod-shaped	branched
Site of replication	nucleus	chloroplast
Rolling circle replication	asymmetrical	symmetrical
Polymerase involved	RNA polymerase II	chloroplastic single-unit nuclear-encoded polymerase
RNA cleavage	likely mediated by host factor(s)	self-cleaved by the hammerhead ribozyme
RNA ligation	likely mediated by host factor(s)	likely self-ligated
Number of known members	27	4

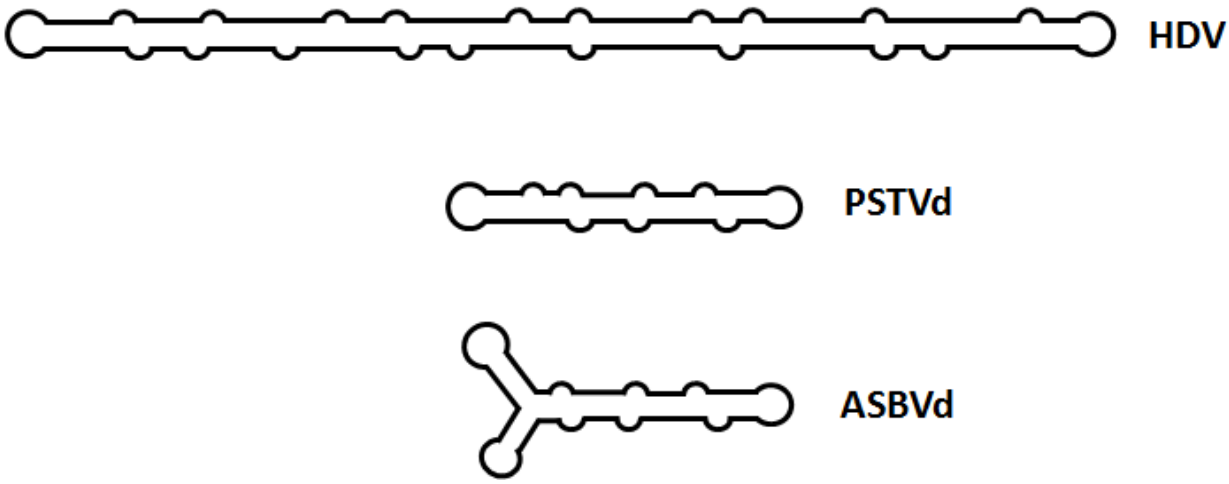
HDV
PSTVd
ASBVd

Figure 1.7: Structural comparison of HDV and viroid RNAs.

Schematic depictions of the RNA genomes of HDV, potato spindle tuber viroid (PSTVd), the type species of *Pospiviroidae*, and avocado sunblotch viroid (ASBVd), the type species of *Avsunviroidae*.

the production of (+) multimers, which are then cleaved and ligated into circular (+) monomers (Ding and Itaya, 2007; Flores *et al*., 2005).

Both HDV and viroids rely on redirection of host-encoded RNAPs for transcription of their RNA genomes. While avsunviroids are believed to be transcribed by the chloroplastic single-unit nuclear-encoded polymerase (NEP) (Navarro *et al*., 2000; Rodio *et al*., 2007), pospiviroids have been shown to use RNAP II (Kolonko *et al*., 2006; Schindler and Mühlbach, 1992; Warrilow and Symons, 1999), the key polymerase involved in HDV transcription. Moreover, PSTVd, the type-species of the *Pospiviroidae* family, has recently been reported to interact with transcription factor IIIA (Eiras *et al*., 2011), suggesting involvement of RNAP III in PSTVd replication; RNAP III was also shown to associate with HDV RNA (Greco-Stewart *et al*., 2009).

The structural and functional similarities that exist between these RNA pathogens support the likelihood of an evolutionary relationship. Although they exist in different hosts, HDV and viroids seem to use common strategies to effect their replication. Additional studies on the mechanisms of RNA-directed transcription occurring in these species are needed to clarify the potential evolutionary link between them.

1.10.2 Origin of HDAg

The evolutionary origin of the *delta* antigen is elusive. While it is believed that HDAg may have evolved from a host gene, the source of the genetic information is under debate. *Delta*-interacting protein A (DIPA) has been proposed to be the cellular homologue of HDAg

(Brazas and Ganem, 1996), a claim that has been contested by additional bioinformatics analyses (Long *et al*., 1997; Veretnik and Gribskov, 1998). Indeed, Veretnik and Gribskov (1998) reported significant sequence similarity between the RNA-binding domain of HDAg and the HMG (High Mobility Group) box of SRY, a DNA-binding protein essential for sex determination (Sinclair *et al*., 1990). They suggested that the HDAg RNA binding domain evolved from the conserved DNA-binding motif present in the HMG box of SRY.

HDAg also displays limited sequence similarity to a 66-kilodalton subunit of the negative elongation factor (NELF-A; Yamaguchi *et al*., 2001). HDAg is believed to stimulate HDV RNA-directed transcription by RNAP II by displacing NELF. NELF orthologues are not found in plants, suggesting the possibility that HDV is the result of an evolutionary adaptation that arose following the capture of a cellular transcript by a primitive viroid-like RNA.

1.11 Hypotheses and Objectives

The hepatitis *delta* virus has a very limited coding capacity. Due to its minimalist nature, HDV needs to manipulate its host at different stages of its life cycle. Based on the limited knowledge on the host's involvement in HDV replication and propagation, **the main hypothesis addressed by this project is that HDV RNA interacts with specific RNA binding proteins to ensure successful replication.**

HDV shares many similarities with viroids - subviral, non-coding, helper-independent plant RNA pathogens. HDV and the potato spindle tuber viroid (PSTVd) have common

structural and functional characteristics: both are single-stranded circular RNA molecules that adopt unbranched rod-like structures; they replicate autonomously in their respective hosts via the rolling circle mechanism; and they are reported to interact with components of their hosts' transcriptional machineries (reviewed in Taylor and Pelchat, 2010). These similarities suggest a common evolutionary origin between HDV and viroids. Therefore, **my secondary hypothesis is that HDV and viroids use parallel replication strategies in their respective hosts.**

The objectives of this study are as follows:

- To identify nuclear proteins that associate with the HDV RNA genome
- To explore the potential involvement of these proteins in the synthesis of HDV RNA
- To characterize the interaction of HDV RNA with one of these proteins (i.e. ASF/SF2)
- To explore the evolutionary relationship between HDV and viroids

Chapter 2: Materials and Methods

2.1 Synthesis of RNA fragments

DNA templates used for the synthesis of HDV RNA fragments were generated by PCR off the pHDVd2 plasmid, a derivative of pBluescriptKS$^+$ (Stratagene) harboring a dimer of HDV cDNA (Kuo *et al*., 1988). Similarly, DNA templates for the synthesis of PSTVd monomers were amplified off a pBluescriptKS$^+$ derivative containing a trimer of PSTVd cDNA (pPSTVd3). The forward primer was designed to contain the T7 promoter sequence (5'-GGAATTCTAATACGACTCACTATAGGG-3'). HDV RNA fragments smaller than 100 nucleotides, as well as the P11.60 RNA, were transcribed from DNA templates generated by annealing and extension of two oligonucleotides. Sequences of primers used to generate the DNA templates are listed in Appendix I. Linearized pPSTVd3 and pminiHDV1.4, a pUC57 derivative containing a 1.4-mer insert of miniHDV, were used to synthesize the PSTVd(+) trimer and genomic miniHDV 1.4-mer, respectively.

RNA was synthesized by *in vitro* transcription off a linear DNA template (0.1 – 1 μg), using 200 U of T7 RNA polymerase (New England Biolabs; NEB) in 1X transcription buffer (80 mM Tris-HCl, pH 7.9, 40 mM dithiothreitol, 20 mM $MgCl_2$, 2 mM spermidine), with 5 mM of each NTP. Transcription reactions were carried out at 37°C for 4 h. DNA templates were removed by incubation with 10 U DNase I (Promega) at 37°C for 30 min. Products were resolved on denaturing 5 % polyacrylamide/7 M urea gel in 1X Tris-Borate-EDTA (TBE) buffer (90 mM Tris-HCl, pH 8.3, 90 mM boric acid, 2 mM EDTA). Following electrophoresis, RNA bands were visualized by UV shadowing, excised, and eluted in 500 mM ammonium acetate, 0.1 % SDS, 10 mM EDTA overnight at room temperature. The eluted RNA was then ethanol-precipitated in the presence of 0.3 M NaOAc, pH 5.0, resuspended in 100 μl H_2O, passed through a 1 mL Sephadex G-50 column (GE Healthcare),

and ethanol-precipitated for a second time. RNA was quantified by spectrophotometry at a wavelength of 260 nm.

2.2 Radiolabelling

Radiolabelling of RNA or DNA was carried out as follows. Ten pmoles of nucleic acid was dephosphorylated by 1 unit of calf intestinal phosphatase (NEB) in 50 mM Tris-HCl, pH 7.9, 100 mM NaCl, 10 mM $MgCl_2$, 1 mM dithiothreitol. Following a 30-min incubation at room temperature, the dephosphorylated product was extracted with equal volumes of phenol and chloroform, and ethanol-precipitated. 5'-labelling was carried out using 10 units of T4 polynucleotide kinase (NEB) in 70 mM Tris-HCl, pH 7.6, 10 mM $MgCl_2$, 5 mM dithiothreitol, in the presence of 10 μCi [γ-^{32}P] ATP (GE Healthcare), at 37 ^{o}C for 1 h. Radiolabelled nucleic acid was extracted with equal volumes of phenol and chloroform, passaged through 1 mL Sephadex G-50 (GE Healthcare), ethanol-precipitated, and resuspended in H_2O.

2.3 UV crosslinking

Radiolabelled R199G (100 fmol) was incubated with 10 μg of HeLa nuclear extract (Accurate Chemical and Scientific) in 20 mM HEPES, pH 7.9, 100 mM KCl, 0.2 mM EDTA, 6.0 mM $MgCl_2$, 0.5 mM dithiothreitol, and 20 % glycerol, in a final volume of 10 μl. P11.60 (50 pmol) or non-radiolabelled R199G (50 pmol) were added to certain reactions, where indicated. Reaction mixtures were irradiated for 20 min on ice in UV Stratalinker 2400

(Stratagene) at a wavelength of 365 nm. Following addition of 10 µl of 2X SDS loading dye (100 mM Tris–HCl, pH 6.8, 4 % SDS, 0.1 % bromophenol blue and 20 % glycerol), RNA–protein complexes were resolved by 10 % SDS-PAGE, and visualized by autoradiography. To identify the proteins in the complex, the experiment was repeated with non-radiolabelled RNA, the gel was stained with methylene blue to visualize the RNA, the resulting bands were excised, and three samples were sent individually to WEMB Biochem Inc. (Toronto, Canada) for protein analysis by LC-MS/MS, as previously described (Greco-Stewart *et al*., 2006).

2.4 Electrophoretic mobility shift assay

^{32}P-labelled RNA (100 fmoles) was mixed with 0.5 µg of purified, GST-tagged protein. Reactions were carried out in a final volume of 10 µl containing 20 mM Tris-HCl, pH 7.5, 100 mM KCl, 1 mM EDTA, 1 mM dithiothreitol, 0.1 mg/ml BSA, and 20 mM $MgCl_2$. PolyA (10 pmoles) was used as a non-specific competitor. Following a 30-min incubation at 4 ^{o}C, 2 µl of 6X agarose gel loading buffer (30 % glycerol, 0.25 % bromophenol blue, 0.25 % xylene cyanol) were added, and the samples were subjected to non-denaturing 5 % polyacrylamide gel electrophoresis (49:1, acrylamide:bis-acrylamide) at 40 volts in 1X Tris-Borate-EDTA (TBE) buffer (90 mM Tris-HCl, pH 8.3, 90 mM boric acid, 2 mM EDTA) at room temperature. Following electrophoresis, the gel was exposed to a phosphor screen (GE Healthcare), and bands were visualized using the STORM 840 Phosphorimager system (Molecular Dynamics).

2.5 Co-immunoprecipitation assay

The co-immunoprecipitation experiments were carried out using the Protein G Immunoprecipitation Kit (Sigma), with a modified protocol. Radiolabelled R199G RNA (0.5 pmole) was incubated with 50 µg HeLa nuclear extract (Accurate Chemical and Scientific) in 1X RIPA buffer (50 mM Tris–HCl, pH 7.5, 1% Nonidet P-40 (NP-40), 0.5% sodium deoxycholate, 0.05% SDS, 1 mM EDTA, 150 mM NaCl) for 30 min at 4^{o}C. P11.60 RNA (50 pmol) or non-radiolabelled R199G RNA (50 pmol) were added to certain reactions, where indicated. Following the 30-min incubation, 5 µg of either anti-eEF1A1 (Abnova), anti-ASF/SF2 (Zymed), anti-p54^{nrb} (Upstate), anti-hnRNP-L (Abcam), anti-GAPDH (Santa Cruz), or anti-SMN (BD Transduction Laboratories) were added, and the reaction mixtures were incubated for 1 h at 4 ^{o}C before the addition of 30 µl pre-washed protein G agarose beads. After an overnight incubation at 4 ^{o}C, the beads were washed 5 times with 1X RIPA buffer and the RNA was eluted with 40 µl of acrylamide loading dye (95 % formamide, 0.025 % bromophenol blue, 0.025 % xylene cyanol, 0.5 mM EDTA). RNA was resolved on denaturing 5 % polyacrylamide (19:1, acrylamide:bis-acrylamide)/7 M urea gel, and visualized by autoradiography.

2.6 *In vitro* transcription assay

RNA templates (100 pmol) were incubated with 50 µg of HeLa NE (Accurate Chemical and Scientific) in transcription buffer (10 mM HEPES, pH 7.9, 50 mM KCl, 0.1 mM EDTA, 6.0 mM $MgCl_2$, 0.2 mM dithiothreitol and 10 % glycerol, 2 mM NTPs). For antibody inhibition experiments, HeLa NE was preincubated with 2.5 µg of either anti-RNAP

II CTD (clone 8WG16; Upstate), anti-TBP (Abcam), anti-eEF1A1 (Abnova), anti-ASF/SF2 (Zymed), anti-p54^{nrb} (Upstate), anti-SFPQ (Abcam), anti-hnRNP-L (Abcam), anti-GAPDH (Abcam), or anti-β-actin (Abcam), at 4^{o}C for 30 min prior to addition of RNA template; alternatively, immunodepleted HeLa NE was used (see below). Transcription reactions were carried out at 37 ^{o}C for 1 h, and purified using the TRIzol Reagent (Invitrogen) according to manufacturer's specifications. Purified RNA was resuspended in 20 µL of H_2O, and 5 µL were subjected to cDNA synthesis using the SuperScript® III Reverse Transcriptase (Invitrogen), according to manufacturer's protocol. The reverse transcription reaction was primed with a radiolabelled DNA oligonucleotide (5'-GGGCATTCGATCTACACCTG-3'), designed to specifically recognize transcription product(s). Following the reverse transcription reaction, samples were treated with 1 U of RNAse H and 1 U of RNase A for 30 min at 37 ^{o}C. Radiolabelled cDNA corresponding to transcription product(s) was resolved by denaturing 5 % polyacrylamide (19:1, acrylamide:bis-acrylamide)/7 M urea gel electrophoresis, and visualized by autoradiography. Intensities of the bands corresponding to the transcription products were measured using the ImageQuant TL v2003 software.

2.7 Immunodepletion

Forty µg of anti-SFPQ antibody (Abcam) were diluted in 500 µL of RIPA buffer (50 mM Tris–Cl, pH 7.5, 1% Nonidet P-40 (NP-40), 0.5 % sodium deoxycholate, 0.05 % SDS, 1 mM EDTA, 150 mM NaCl), supplemented with 10 mg/mL bovine serum albumin (BSA) and 0.1 % NP-40, and incubated with 50 µL of pre-washed protein G agarose beads (Sigma) at 4^{o}C overnight. The antibody-coupled beads were then washed 4 times with 600 µL of 1X

RIPA buffer; 200 µg of HeLa NE (Accurate Chemical and Scientific), diluted in 500 µL of 1X RIPA buffer supplemented with 0.05 % NP-40, were added to the beads, and incubated at 4^{o}C overnight. Following incubation, the beads were centrifuged at 4,000 x g to collect the supernatant. The 1 X RIPA buffer was then exchanged for protein storage buffer (20 mM Hepes, pH 7.9, 100 mM KCl, 0.2 mM EDTA, 1 mM DTT, 20 % glycerol) using a Microcon centrifugal filter device (Millipore), and protein concentration was determined by the Bio-Rad Protein Assay Kit II (Bio-Rad). The immunodepleted extract was subjected to Western blot analysis with the ONE-HOUR Western^{TM} Detection System (Genscript), according to manufacturer's instructions, using the following primary antibodies: mouse monoclonal anti-SFPQ antibody (Abcam), mouse monoclonal anti-RNAP II CTD antibody (clone 8GW16; Upstate), and mouse monoclonal anti-*β*-actin antibody (Abcam).

2.8 GST-ASF/SF2 expression and purification

Glutathione S-transferase-tagged ASF/SF2 was expressed from plasmid pGEX-ASF/SF2 transformed into *Escherichia coli* strain BL21(DE3)pLysS (Novagen). Bacterial cultures were grown for 18 h at 37 ^{o}C in 2X YTA medium (1.6 % tryptone, 1 % yeast extract, 0.5 % NaCl) supplemented with 100 µg/µL of ampicillin. Cells were then diluted 1:100 in fresh pre-warmed 2X YTA medium and grown at 37 ^{o}C until the culture reached an OD_{600} of 0.5. GST-ASF/SF2 expression was induced by further addition of 0.1 mM isopropyl *β*-D-1-thiogalactopyranoside (IPTG) and a further incubation of the bacterial culture for 4 h. Cells were then collected in 50-mL tubes following a 15-minute centrifugation at 6,000 x *g* at 4 ^{o}C. Pelleted cells were resuspended in 5 mL of BugBuster Protein Extranction Reagent

(Novagen) per 1 g of culture. The cell suspension was incubated with shaking at room temperature for 30 min and cell debris was collected by centrifugation at 16,000 x g for 20 min at 4^{o}C. GST-ASF/SF2 was purified from the supernatant using the BugBuster GST-Bind Purification Kit (Novagen) according to manufacturer's instructions. The purified GST-ASF/SF2 was then passed through a Microcon centrifugal filter device (Millipore) to concentrate the protein sample and to exchange the elution buffer for a protein storage buffer (20 mM Hepes, pH 7.9, 100 mM KCl, 0.2 mM EDTA, 1 mM DTT, 20 % glycerol). Protein purity was evaluated by SDS-PAGE and concentration was determined using the Bio-Rad Protein Assay Kit II (Bio-Rad), according to manufacturer's instructions. Protein aliquots were stored at -80 ^{o}C.

2.9 His-ASF/SF2 expression and purification

C-terminally hexahistidine (his) –tagged ASF/SF2 was expressed from plasmid pET-20b(+)-ASF transformed into *Escherichia coli* strain BL21(DE3)pLysS (Novagen). Bacterial cultures were grown for 18 h at 37 ^{o}C in Terrific Broth (Gibco) supplemented with 100 μg/μL of ampicillin, and cells were collected in 50-mL tubes following a 15-minute centrifugation at 6,000 x *g* at 4 ^{o}C. Pelleted cells were rotated in 1 mL of binding buffer (5 mM imidazole, 0.5 M NaCl, 20 mM Tris-HCl, pH 7.9, 8 M urea) for 60 min at room temperature, and cell lysate was cleared by centrifugation at 14,000 x *g* for 30 min. His-tagged ASF/SF2 was purified by immobilized metal affinity chromatography using the Ni-NTA Spin columns (Qiagen) according to manufacturer's instructions. The column-bound proteins were washed 5 times with binding buffer containing 40 mM of imidazole, and eluted

twice with 200 µl of elution buffer (500 mM imidazole, 0.5 M NaCl, 20 mM Tris-HCl, pH 7.9, 8 M urea). The protein extracts were dialyzed overnight at 4°C against 50 mM Tris-HCl, pH 7.9, 1 mM EDTA, 0.1 mM dithiothreitol, 50 mM NaCl, 50 % glycerol. Protein purity was evaluated by SDS-PAGE and concentration was determined using the Bio-Rad Protein Assay Kit II (Bio-Rad), according to manufacturer's instructions. Protein aliquots were stored at -80 ^{o}C.

2.10 Fluorescence spectroscopy

Intrinsic fluorescence was measured with a Cary Eclipse fluorescence spectrophotometer (Agilent Technologies) using the Cary Eclipse Scan Application software. All binding experiments were carried out at room temperature, using an excitation wavelength of 280 nm with a 10 nm slit width; the emission slit width was also 10 nm. To select the excitation wavelength, the maximum absorption wavelength of the ASF/SF2 sample was determined. Emission spectra were read between 300-400 nm. Binding experiments were carried out in 100 mM KCl, 20 mM Tris-HCl, pH 7.5. Background emission was eliminated by subtracting the signal of buffer alone, or buffer plus ASF/SF2. Binding assays were carried out at an ASF/SF2 concentration of 100 nM. Changes in ASF/SF2 fluorescence upon addition of RNA ligand were analysed using the GraphPad Prism 3.0 software.

2.11 Cell cultures and transient transfections

HeLa, HepG2, and 293-HDV cells were cultured in Dulbecco`s modified Eagle medium supplemented with 10 % fetal bovine serum. 293-HDV cells were maintained with 5 mg/mL blasticidin and 200 mg/mL hygromycin B. This cell line is derived from the human embryonic kidney cell line 293TRex; it expresses a single copy of HDAg-S cDNA under the control of a tetracycline (TET)-inducible promoter, and contains a mutated HDV RNA genome that is unable to produce HDAg (Chang *et al*., 2005).

HepG2 and HeLa cells were transiently transfected using Lipofectamine LTX and the PLUS Reagent (Invitrogen) according to manufacturer's standard protocol, using the following ratios: 1 μg plasmid DNA : 20 pmol RNA : 6 μl lipofectamine LTX : 1 μl PLUS Reagent. Cells were collected 3 days post-transfection and total RNA was extracted for reverse transcription (RT)-PCR analysis. Transfections of 293-HDV cells were performed using Lipofectamine 2000 (Invitrogen) following manufacturer's instructions. A ratio of 5 μl lipofectamine : 4 μg plasmid DNA was used. Expression of HDAg-S was induced 24 h post-transfection with TET at 1 μg/ml. Cells were collected 24 h post-induction, and RNA and protein were extracted for further analysis. Transfection efficiencies were estimated visually following co-transfection with a plasmid encoding the green fluorescent protein (pGFP), provided by Dr. E. G. Brown (University of Ottawa).

2.12 RNA/protein extraction

Extraction of RNA and proteins from cultured cells was performed using the TRIzol Reagent (Invitrogen), following instructions given by the manufacturer. Total RNA

concentration was estimated by spectrophotometry. RNA quality was verified by denaturing 1 % agarose/2.2 M formaldehyde gel electrophoresis. RNA samples were used directly for cDNA synthesis, or stored in aliquots at -80 ^{o}C. Protein concentration was determined using Bio-Rad Protein Assay Kit II (Bio-Rad), according to manufacturer's instructions, and the protein samples were stored in 1 % SDS at -20 ^{o}C.

2.13 Reverse transcription-PCR

Reverse transcription reactions to detect miniHDV or PSTVd RNA in human cells were carried out using the SuperScript® III Reverse Transcriptase (Invitrogen), according to manufacturer's protocol. To detect miniHDV RNA, reverse transcription was carried out using a genome-specific primer, 5'-^{770}GGTCCCATTCGCCATTACCG^{751}-3', or an antigenome-specific primer, 5'-^{771}CACAAATCTCTCTAGATTCC^{790}-3'. PSTVd RNA was detected using the (+) polarity-specific primer, 5'-^{358}GGAACCAACTGCGGTTCCAAGGGCTAAACACCC^{326}-3', or the (-) polarity-specific primer, 5'-^{2}GGAACTAAACTCGTGGTTCCTTGTGGTTC^{29}-3'. Amplification of cDNA products was carried out using the Platinum® *Taq* DNA Polymerase (Invitrogen), under the following conditions: initial denaturation at 95 °C for 5 min, followed by 30 cycles of 30 s at 95 °C, 15 s at 55 °C and 30 s at 72 °C. Products were resolved on a 1.5 % agarose gel, and visualized using SYBR Green II (Invitrogen) staining. Some RT-PCR products were eluted from the agarose gel using the QIAquick Gel Extraction Kit (Qiagen), and cloned into the pCR®2.1-TOPO® vector, using the TOPO TA Cloning® Kit (Invitrogen), according to

manufacturer's instructions. The inserts were sequenced at the StemCore-DNA Sequencing Facility of the Ottawa Health Research Institute.

2.14 ASF/SF2 knock-down

ASF/SF2 knockdown was achieved by transfection of 293-HDV cells (see above) with three different shRNA constructs (Sigma; clones NM_006924.x-879s1c1, NM_006924.x-1508s1c1 and NM_006924.x-1539s1c1). An empty vector (pKLO.1; Sigma) and a non-target shRNA construct (Sigma) were used as negative controls. To assess knock-down levels, 30 μg of total cellular protein were resolved by SDS-PAGE, and transferred to a nitrocellulose membrane (GenScript). Membrane was blocked in 5 % non-fat dry milk in TBS buffer (50 mM Tris-HCl, pH 7.5, 1.25 M NaCl) + 0.1 % tween 20, and probed with a mouse monoclonal anti-ASF/SF2 antibody (Invitrogen) or a mouse monoclonal anti-GAPDH antibody (Abcam). The membrane was then washed with TBS + 0.1 % tween 20, and incubated with a horse radish peroxidase-conjugated goat anti-mouse or goat anti-rabbit IgG antibody (Abcam). Protein expression was detected by incubation with the SuperSignal West Pico Chemiluminescent Substrate (Thermo Scientific), and visualized following exposure to X-ray film. Bands were quantified using the ImageJ software (downloaded from http://rsbweb.nih.gov/ij/).

2.15 Quantitative RT-PCR analysis

For quantitative RT-PCR (qRT-PCR) analysis, 1 µg of RNA extracted from 293-HDV cells was transcribed into cDNA using the iScript Select cDNA Synthesis Kit (Bio-Rad) and random primers in a 20 µl volume. The cDNA samples were subjected to qPCR with the following primers: HDV forward, 5'-GGAATTCTAATACGACTCACTATAGGGACTGCT CGAGGATCTCTTCTCTCC-3', HDV reverse, 5'- CACTCCCCTCTCGGTGCTG -3'; *β*-actin forward, 5′-CCATGTTTGTGATGGGTGTGAACCA -3', *β*-actin reverse, 5'-ACCAGTGGATGCAGGGATGATGTTC -3'. qPCR was performed by Chromo4 Real-Time Detector (Bio-Rad) using the iQ SYBR Green Supermix (Bio-Rad). The PCR reaction was set up as follows: initial denaturation at 95 °C for 3 min, followed by 40 cycles of 30 s at 95 °C, 20 s at 55 °C and 30 s at 72 °C. Following amplification, melting curve analysis was performed. The levels of HDV expression were quantified and normalized to *β*-actin expression using the $2^{-\Delta\Delta C}$T method (Livak and Schmittgen, 2001). Amplification efficiencies of the two primer pairs were tested by initial qPCR performed at different dilutions of the template.

2.16 Bioinformatics analysis

Sequences corresponding to the ASF/SF2 binding site from 92 HDV strains were obtained from the online Subviral RNA Database (http://subviral.med.uottawa.ca/cgi-bin/home.cgi). Sequences were aligned with the ClustalW multiple alignment program using default parameters (Thompson *et al*., 1994), and adjusted manually. A sequence logo was

produced from the multiple alignment using the web-based WebLogo application (http://weblogo.berkeley.edu/logo.cgi).

Chapter 3: HDV RNA interacts with eEF1A1, p54^{nrb}, hnRNP-L, GAPDH and ASF/SF2

Data included in sections 3.1 to 3.5 were published in Virology (2009) Vol. 390:71-78 (Appendix II)

Author Contributions

All experiments were performed by Dorota Sikora, with the exception of the following:

Purification of the splicing factor hnRNP-L (Figure 3.2) was performed by Ms. Emilie Lemay. *In vitro* co-immunoprecipitations of R199G with p54^{nrb}, eEF1A1, and GAPDH (Figure 3.4) were performed by Mr. Paul Miron, under the direct supervision of Dorota Sikora. Co-immunoprecipitations of HDV RNA from HeLa cells (Figure 3.5) were performed by Dr. Valerie Greco-Stewart.

3.1 Identification of HeLa NE proteins involved in the formation of a UV crosslinked complex with R199G HDV RNA

To identify human proteins that interact with the HDV RNA genome, and thus might be important for HDV biology, a 199-nt HDV-derived RNA fragment corresponding to the right terminal stem–loop domain of the genomic polarity (R199G; Fig. 1.2B) was used as bait. This RNA segment was selected because it contains the proposed initiation site for HDAg mRNA transcription (Gudima *et al*., 2000); it was shown to direct synthesis of antigenomic RNA in an *in vitro* transcription reaction (Beard *et al*., 1996; Abrahem and Pelchat, 2008); and the specific binding of RNAP II to R199G has been demonstrated (Greco-Stewart *et al.*, 2007; Abrahem and Pelchat, 2008). All these features suggest that this part of the HDV genome includes an RNA promoter for RNAP II, which might be involved in viral replication and/or transcription.

Recently, Dr. Pelchat's laboratory reported the formation of a single, high molecular weight ribonucleoprotein complex following UV crosslinking of HeLa NE proteins to R199G (Greco-Stewart *et al*., 2006). Although preliminary mass spectrometry analysis of this complex led to the identification of PSF/SFPQ (polypyrimidine tract-binding protein-associated splicing factor/splicing factor proline/glutamine-rich) as a novel HDV RNA-interacting protein (Greco-Stewart *et al*., 2006), the presence of other proteins in the complex was likely. To identify additional proteins binding to R199G, I revisited the crosslinking experiment. R199G was synthesized *in vitro* in the presence of [α-^{32}P] GTP, incubated with HeLa NE proteins, and the ribonucleoprotein complexes were UV crosslinked at 365 nm. Following UV irradiation, the mixtures were fractionated by SDS-PAGE and the complex was detected by autoradiography. In agreement with the previous report (Greco-Stewart *et*

al., 2006), a specific band migrating as a species of approximately 220 kDa was detected when the radiolabelled R199G was incubated with HeLa NE proteins and UV crosslinked (Figure 3.1). To test the specificity of the complex, its formation was challenged with P11.60, which is a small RNA fragment derived from the peach latent mosaic viroid that folds into a hairpin (Pelchat and Perreault, 2004), thus providing an excellent competitive RNA to test for non-specific affinity of the proteins to double-stranded RNA or stem–loop secondary structures. Challenges of the complex with a molecular excess of this non-specific competitor did not significantly alter its formation. However, complex formation was greatly reduced by the addition of excess of non-radiolabelled R199G RNA, and no complex was observed in the absence of NE or UV irradiation. Taken together, these observations demonstrate that NE protein(s) interact specifically with R199G.

The complexes from three independent experiments were excised and analyzed by mass spectrometry (LC-MS/MS, Wemb Biochem), as previously described (Greco-Stewart *et al*., 2006). As a negative control, UV irradiation was performed on samples without R199G and subjected to the same treatment. The protonated masses of those peptides were then used to search human protein sequence databases. To be cautious, only the proteins for which at least two peptides were identified in the three samples, and which were not found in the absence of R199G, were considered. A list of the putative HDV-interacting proteins is presented in Table 3.1. In accordance with previous reports (Abrahem and Pelchat, 2008; Greco-Stewart *et al*., 2006, 2007), peptides corresponding to both the largest subunit of RNAP II and to PSF were detected as constituents of the complex. In addition, numerous peptides corresponding to proteins involved in a wide range of cellular processes were

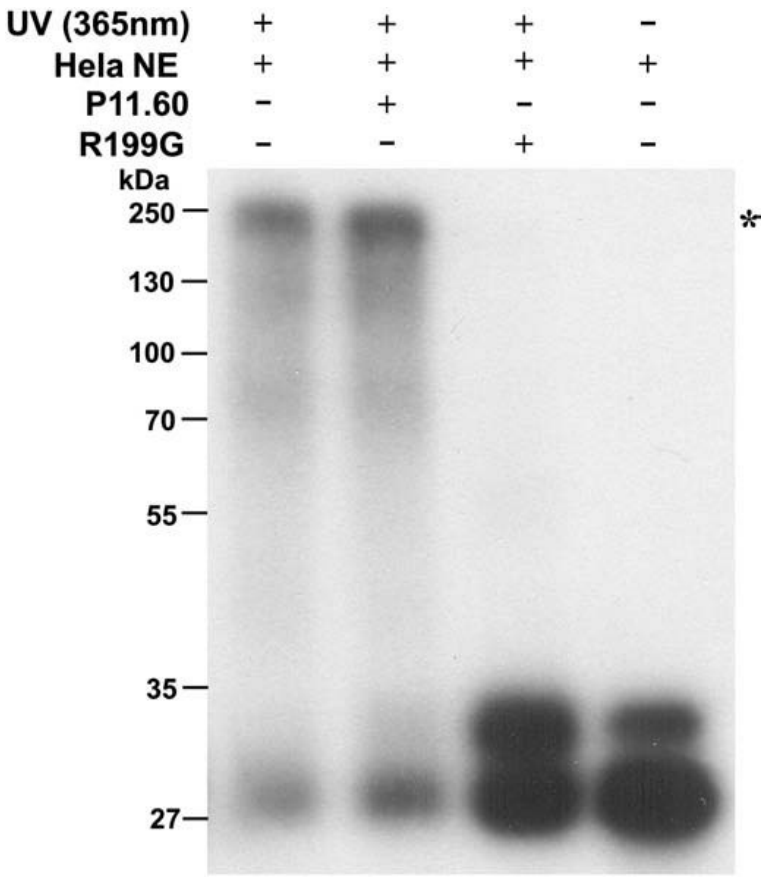
UV (365nm) + + + −
Hela NE + + + +
P11.60 − + − −
R199G − − + −
kDa
250
130
100
70
55
35
27
*

Figure 3.1: Detection of a specific UV crosslinked complex between R199G and HeLa nuclear extract proteins.

Radiolabelled R199G was incubated with HeLa NE and subjected to UV irradiation at a wavelength of 365 nm. Complexes were resolved on SDS-PAGE. Specificity of the interaction was verified by addition of 50X molar excess of either a specific (R199G) or non-specific (P11.60) RNA competitor. The asterisk indicates the excised complex.

Table 3.1: Proteins identified by LC-MS/MS following analysis of a ribonucleoprotein complex obtained from UV crosslinking experiment between HDV-derived RNA (R199G) and HeLa nuclear extract proteins.

Protein Identified	Cellular Function	Accession No.	Peptides Identified	MW (kDa)
Eukaryotic translation elongation factor 1A1	Translation	4503471	4	50
Polypyrimidine tract binding protein-associated splicing factor	Pre-mRNA processing	33879558	3	75
Nuclear mitotic apparatus protein 1	Mitotic spindle stabilization	68362740	3	238
$p54^{nrb}$	Pre-mRNA processing	543010	2	54
F-box and leucine-rich repeat protein 17	Protein-ubiquitin ligase complex constituent	42657267	2	34
ANKS6 protein	Unknown function	39963545	2	50
DNA-directed RNA polymerase II polypeptide A	Transcription	4505939	2	217
Kalirin/RhoGEF kinase isoform 3	Guanine nucleotide exchange factor	68362740	2	144

detected in the sample containing R199G, suggesting their interaction with the right terminal stem–loop region of genomic HDV RNA. Among those were peptides specific to the mRNA splicing factor $p54^{nrb}$, a cellular homologue of PSF (Dong *et al*., 1993); the eukaryotic translation elongation factor 1 *alpha* 1 (eEF1A1); the F-box and leucine-rich repeat protein 17; the isoform 3 of kalirin/RhoGEF kinase; and the nuclear mitotic apparatus protein 1.

3.2 Purification of the splicing factor hnRNP-L using R199G affinity chromatography

As an alternative to the UV crosslinking approach, an RNA affinity chromatography purification procedure was used, which involved chemical crosslinking of R199G to adipic acid dehydrazide agarose beads (Vioque and Altman, 1986). R199G was synthesized *in vitro* and oxidized prior to being covalently linked to the beads. Nucleic acid-coupled beads were then incubated with pre-cleared HeLa NE. To assess the specificity of the complexes, an excess amount of yeast total tRNA was added to the extract. In addition, uncoupled adipic acid dehydrazide agarose beads were tested for protein interaction to rule out non-specific binding of NE proteins to the beads. Following incubation and washing to remove unbound proteins, the proteins were eluted with SDS loading dye and resolved by SDS-PAGE. Silver staining of the gel revealed a band corresponding to a protein of approximately 55 kDa (Figure 3.2). This band was clearly absent from the negative control, which consisted of uncoupled beads. The band was excised from the gel, in-gel trypsin digested, and analyzed by mass spectrometry (LC-MSMS; Wemb Biochem). By searching human protein sequence databases, peptides matching the heterogeneous nuclear ribonucleoprotein L (60 kDa; hnRNP-L), a multi-functional RNA-binding protein with important roles in mRNA

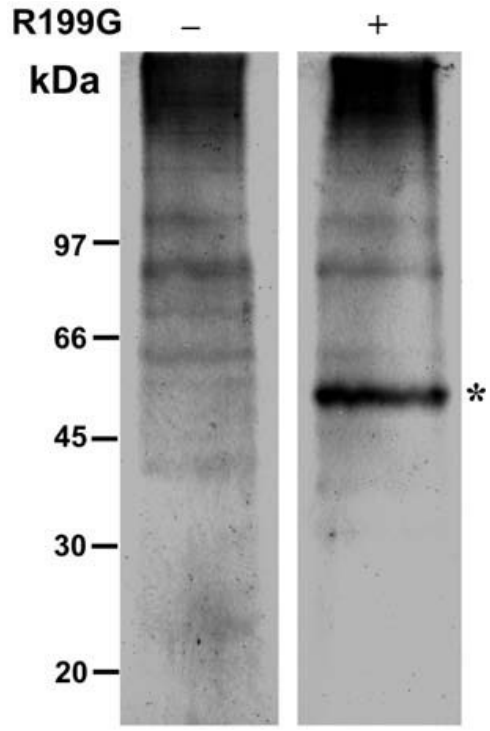
R199G
–
+
kDa
97
66
45
30
20
*

Figure 3.2: Interaction of hnRNP-L with R199G RNA.

RNA-coupled beads were incubated with HeLa nuclear extract. The bound proteins were eluted with SDS loading dye and resolved by SDS-PAGE. The gel was silver-stained and the band corresponding to a protein of approximately 55 kDa (asterisk), and absent from the negative control (uncoupled beads), was excised and identified by mass spectrometry as hnRNP-L.

processing, alternative splicing and translational regulation (Han *et al*., 2010), were detected in the sample.

3.3 Identification of the alternative splicing factor ASF/SF2 as a R199G binding protein by screening a library of proteins

HDV RNA was previously found to associate with the splicing factor SC35 and to co-localize with it in nuclear speckles (Abrahem and Pelchat, 2008; Bichko and Taylor, 1996). Work in Dr. Pelchat's laboratory led to the identification of three other pre-mRNA splicing factors as potential R199G-interacting partners, namely $p54^{nrb}$, hnRNP-L, and PSF (recently reported to interact specifically and directly with HDV RNA; Greco-Stewart *et al*., 2006). Accordingly, several purified recombinant proteins known to be involved in RNA metabolism, specifically during splicing events, were screened for their interaction with R199G by EMSA (Figure 3.3). I tested the Sm proteins B/B' and D1, which are ribonucleoproteins that collectively make up the Sm core of snRNPs (small nuclear ribonucleoproteins); the serine/arginine (SR)-rich proteins ASF/SF2 and SRp30, which play essential roles in constitutive as well as regulated splicing (Hastings and Krainer, 2001); Sam68, a member of the signal transduction and activation of RNA (STAR) family of proteins implicated in alternative splicing (Hartmann *et al.*, 1999); and the Tudor domain, which is found in several splicing factors and RNA-binding proteins (Ponting, 1997).

Radiolabelled R199G was synthesized *in vitro* and was allowed to bind to the purified recombinant proteins. To ensure specificity of the interactions, the samples were incubated either in the presence or absence of poly(A), a non-specific competitor. Following a 30-

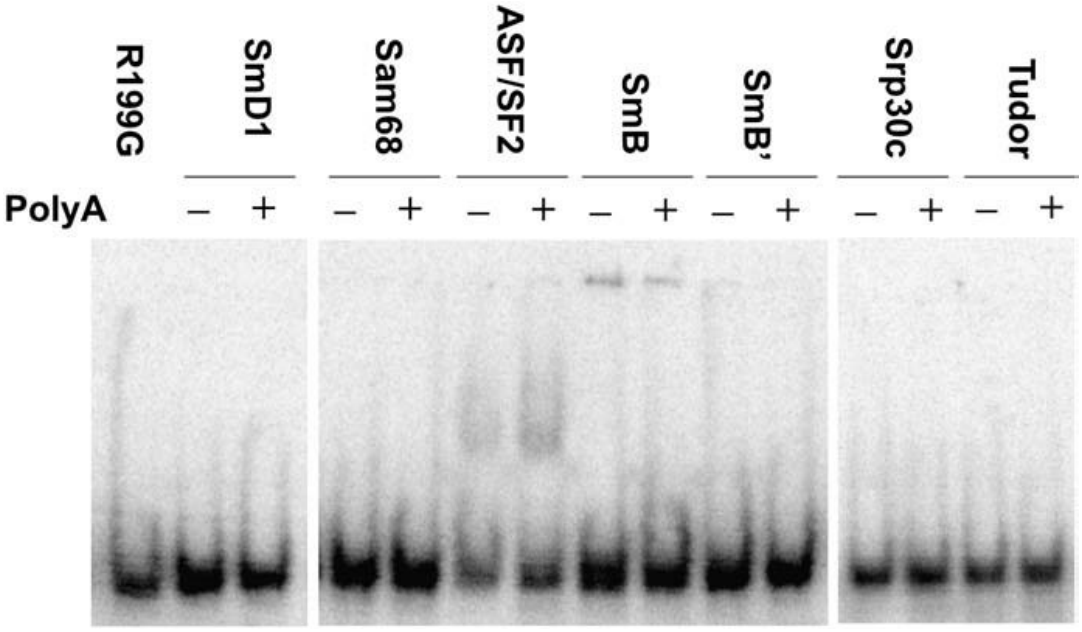
R199G
SmD1
Sam68
ASF/SF2
SmB
SmB'
Srp30c
Tudor
PolyA
– + – + – + – + – + – + – +

Figure 3.3: Direct interaction of R199G with GST-ASF/SF2 *in vitro*.

Electrophoretic gel shift assays (EMSAs) were performed to analyze interaction of the genomic HDV RNA promoter with several recombinant human proteins. Radiolabelled R199G was incubated with 0.5 μg of either SmD1, Sam68, ASF/SF2, SmB, SmB', Srp30c, or the Tudor domain, in the presence or absence of the non-specific competitor poly(A) (100 ng), and resolved by 5 % non-denaturing polyacrylamide gel electrophoresis.

minute incubation at 4 °C, the samples were subjected to electrophoresis through a non-denaturing 5 % polyacrylamide gel. Under these conditions, retardation of the migration of R199G was observed with ASF/SF2, both in the presence and absence of molecular excess of poly(A), indicating the specific binding of this purified protein to the HDV-derived RNA molecule. Similar experiments showed that ASF/SF2 does not bind to P11.60 (data not shown), confirming that the binding of ASF/SF2 to R199G was not due to non-specific affinity to double-stranded RNA or stem–loop secondary structures. Finally, an apparent shift of the radiolabelled R199G in the presence of SmB was observed. However, because the RNA was trapped in the wells of the gel, this finding was considered inconclusive. No apparent binding of R199G to the other proteins was observed, although activity of these proteins was not tested.

3.4 Interaction of p54^{nrb}, eEF1A1, GAPDH, hnRNP-L, and ASF/SF2 with R199G in HeLa NE

To confirm the interactions between R199G and the newly identified R199G-interacting proteins, co-immunoprecipitation experiments were performed with R199G and nuclear extract proteins. Because my analysis was limited to commercial availability of antibodies, only p54^{nrb}, eEF1A1, hnRNP-L, and ASF/SF2 were analyzed. I also included GAPDH in our analysis, based on previous findings indicating GAPDH association with the opposite extremity of the HDV genome (Lin *et al*., 2000), which also interacts with RNAP II (Filipovska and Konarska, 2000; Greco-Stewart *et al*., 2007). Radiolabelled R199G was incubated with HeLa NE proteins in the presence or absence of molecular excess of P11.60 RNA or unlabelled R199G RNA, to verify the specificity of the interaction. Following co-

immunoprecipitation using specific antibodies against those five proteins, the resulting mixture was resolved on denaturing PAGE and visualized by autoradiography (Figure 3.4).

R199G co-immunoprecipitated with $p54^{nrb}$, eEF1A1, GAPDH, hnRNP-L, and ASF/SF2. The presence of molecular excess of the non-specific competitor P11.60 did not significantly alter the amount of R199G that was co-immunoprecipitated. However, the interactions were greatly reduced by the addition of molecular excess of non-radiolabelled R199G RNA, and no R199G RNA was detected in the absence of nuclear extract. Finally, no R199G was co-immunoprecipitated using an anti-IgG antibody (data not shown), or an antibody specific for SMN (Figure 3.4), a protein containing a Tudor domain, which has shown no interaction with HDV RNA by EMSA (Figure 3.3). Taken together, my observations demonstrate that these proteins interact specifically with R199G within HeLa NE.

3.5 Interaction of $p54^{nrb}$, eEF1A1, GAPDH, hnRNP-L and ASF/SF2 with both polarities of HDV RNA in HeLa cells replicating HDV RNA

To establish the significance of these interactions in a physiological context, HeLa cells replicating HDV RNA were subjected to a ribonucleoprotein immunoprecipitation assay (RIPA; Niranjanakumari *et al*., 2002). This technique is both sensitive and specific, and has recently been employed by Dr. Pelchat's laboratory to demonstrate cellular interactions of PSF and RNAPs I, II and III with HDV RNA (Greco-Stewart *et al*., 2006, 2007, 2009).

HeLa cells were co-transfected with a dimeric HDV transcript of genomic polarity and a plasmid transiently expressing HDAg-S from a CMV promoter, since HDAg-S is

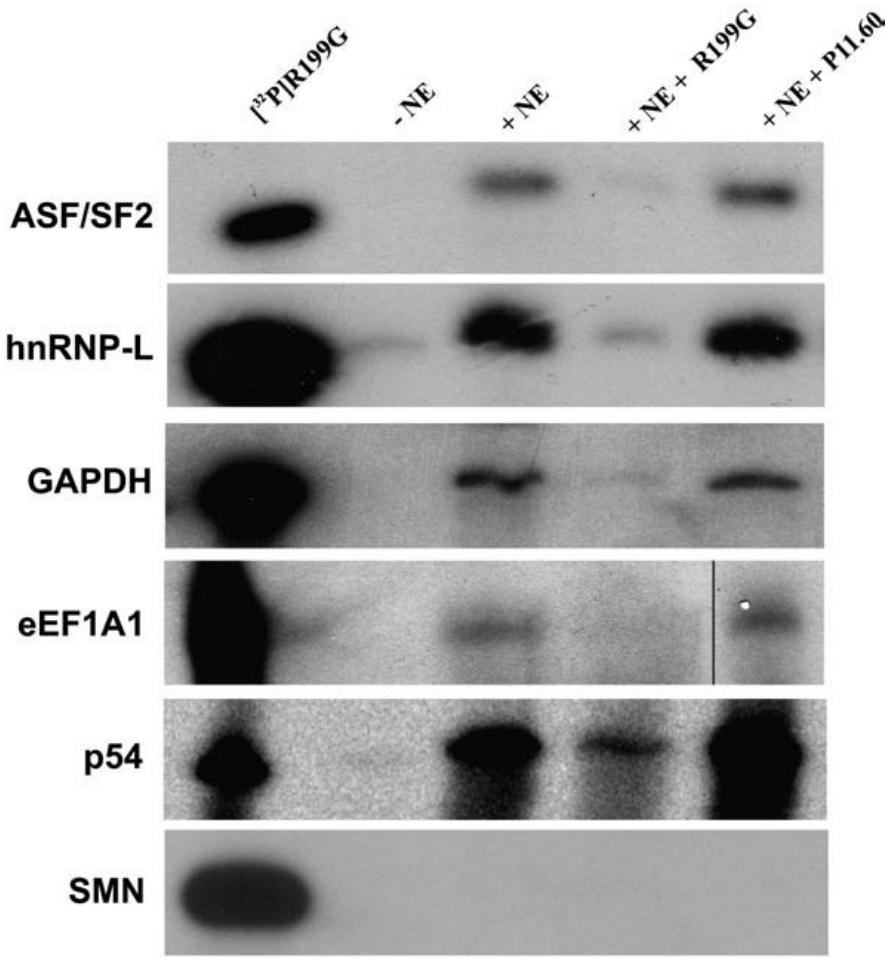
[32P]R199G
- NE
+ NE
+ NE + R199G
+ NE + P11.60
ASF/SF2
hnRNP-L
GAPDH
eEF1A1
p54
SMN

Figure 3.4: Interaction of R199G with various nuclear factors in HeLa nuclear extract.

Radiolabelled R199G RNA was co-immunoprecipitated with each eEF1A1, $p54^{nrb}$, hnRNP-L, GAPDH, ASF/SF2 and SMN from HeLa nuclear extract using the corresponding antibody. Specificity of the interaction was verified by addition of 50X molar excess of either a specific (R199G) or non-specific (P11.60) RNA competitor. RNA was resolved by 5 % denaturing PAGE. First lane ('[^{32}P]R199G') contains a 1:100 dilution of R199G RNA used in each co-immunoprecipitation reaction, and was used as a size marker.

required to initiate HDV RNA replication (Kuo *et al*., 1989). Four days post-transfection, the cells were treated with formaldehyde, a reversible crosslinking agent. Following cell lysis and co-immunoprecipitation of the RNA-protein complexes using specific antibodies, the crosslinks were heat-reversed. The RNA was isolated and analyzed by RT-PCR for the HDV RNA genome (Figure 3.5). Bands corresponding to the R199 cDNA (i.e. 232 bp) were detected when the crosslinked extract was subjected to co-immunoprecipitation with antibodies against $p54^{nrb}$, eEF1A1, GAPDH, hnRNP-L, and ASF/SF2. R199 cDNA was not detected in the absence of antibody, or in the presence of anti-IgG antibody, indicating that the RT-PCR products obtained were not the result of non-specific binding of HDV RNA to either the antibody or the protein G agarose beads. Furthermore, no HDV RNA–protein complexes were recovered from non-crosslinked HeLa lysates. However, in the case of eEF1A1 and ASF/SF2, a small amount of PCR product was recovered after the amplification reactions, which might indicate strong associations of these proteins with HDV RNA. Taken together, these data indicate the specific interactions of these proteins with HDV RNA within HeLa cells.

Additionally, the primers used for the reverse transcription reactions were designed to distinguish between the polarities of HDV RNA. For instance, the antisense primer used to generate the R199G cDNA was only able to reverse transcribe from the genomic polarity of HDV RNA (Figure 3.5, HDVG RNA lanes). Because RNA fragments corresponding to both polarities of HDV were detected when the crosslinked extract was co-immunoprecipitated with specific antibodies against $p54^{nrb}$, eEF1A1, GAPDH, hnRNP-L, and ASF/SF2, it can be concluded that these proteins associate with both polarities of HDV RNA within HeLa cells. These data indicate that each polarity of the HDV genome has at least one region that

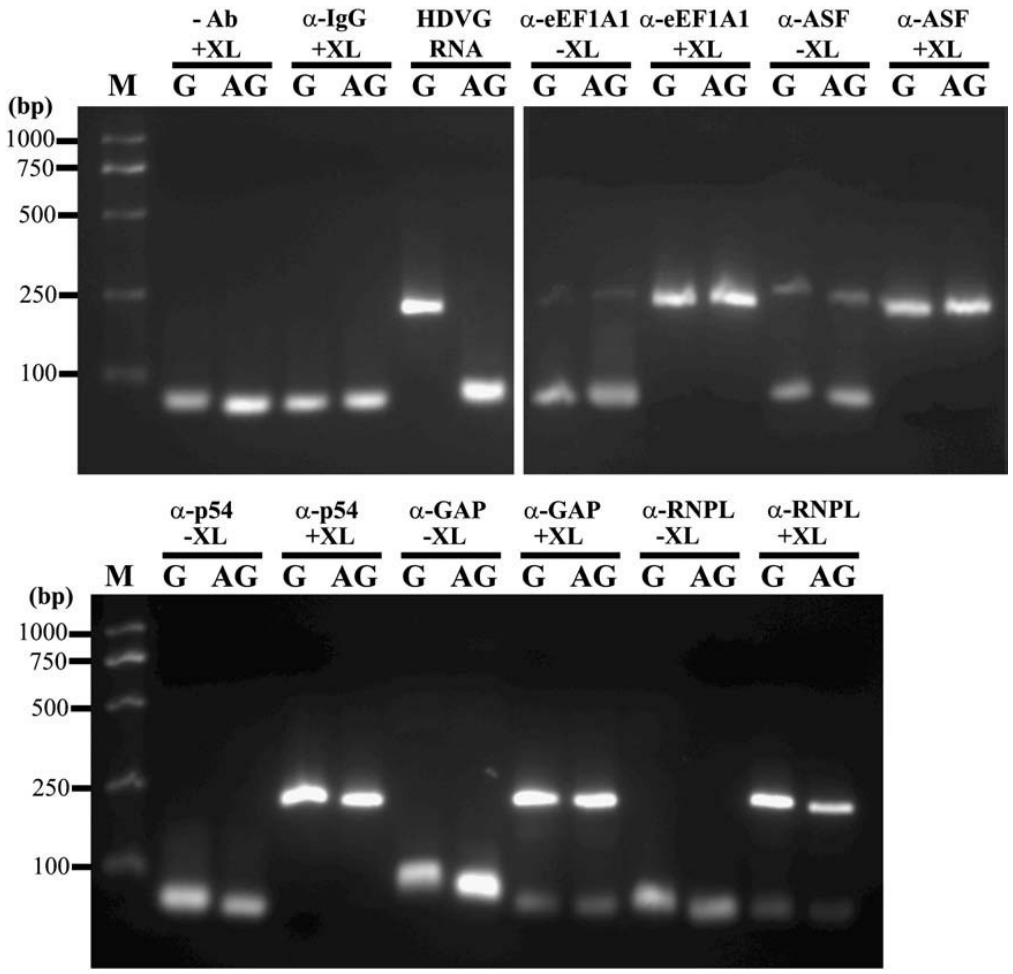
- Ab +XL
α-IgG +XL
HDVG RNA
α-eEF1A1 -XL
α-eEF1A1 +XL
α-ASF -XL
α-ASF +XL
M
G AG G AG G AG G AG G AG G AG G AG
(bp)
1000
750
500
250
100
α-p54 -XL
α-p54 +XL
α-GAP -XL
α-GAP +XL
α-RNPL -XL
α-RNPL +XL
M
G AG G AG G AG G AG G AG G AG
(bp)
1000
750
500
250
100

Figure 3.5: Interaction of HDV RNA with various cellular factors in cultured HeLa cells.

Ribonucleoprotein immunoprecipitation assays were performed to confirm the interaction of HDV RNA of both genomic and antigenomic polarity (G or AG) with the candidate host proteins in HDV infected HeLa cells. HDV RNA was co-immunoprecipitated from lysates of formaldehyde crosslinked HDV-replicating cells with the indicated proteins using the corresponding antibodies. HDV RNA was detected by reverse transcription using strand-specific primers to produce R199G cDNA. Co-immunoprecipitations from non-crosslinked cell lysates serve as specificity controls. HDVG RNA lanes are controls using *in vitro* transcribed HDV RNA of genomic polarity. Lane 'M' contains the Gelpilot Midrange DNA ladder (Qiagen).

interacts with these proteins, and that these interactions occur in a cellular context during HDV replication.

3.6 Involvement of host proteins in *in vitro* transcription of HDV RNA

The present study has identified novel HDV RNA interacting partners, and demonstrated their specific association with an HDV RNA fragment believed to contain an RNA promoter (R199G; Abrahem and Pelchat, 2008). Thus, it is possible that some of these proteins function as transcription factors. To examine the possible involvement of the five identified HDV binding proteins in HDV replication, an *in vitro* run-off transcription assay was carried out in HeLa nuclear extract (NE), and the potential inhibitory effect of antibodies directed against each protein was investigated. The *in vitro* transcription assay was initially performed using the R199G RNA fragment as template; to detect products of transcription, reverse transcription (RT) was performed using a primer that bound specifically to the product. However, because of the complementary nature of the 5' and 3' ends of R199G (Figure 1.2B), an RT primer designed to bind to the 3' end of the product was not able to distinguish between the highly similar sequences of product and template (data not shown). Hence, the R199G RNA fragment was modified by addition of a 20-nucleotide non-HDV sequence at its 5'-end (Y-R199G; Figure 3.6A) to allow for the specific detection of transcription product.

Using the modified Y-R199G RNA fragment as a template, transcription reactions were carried out in HeLa NE, or HeLa NE pre-incubated with an antibody against the protein of interest. Transcription products were reverse transcribed using a radiolabelled DNA

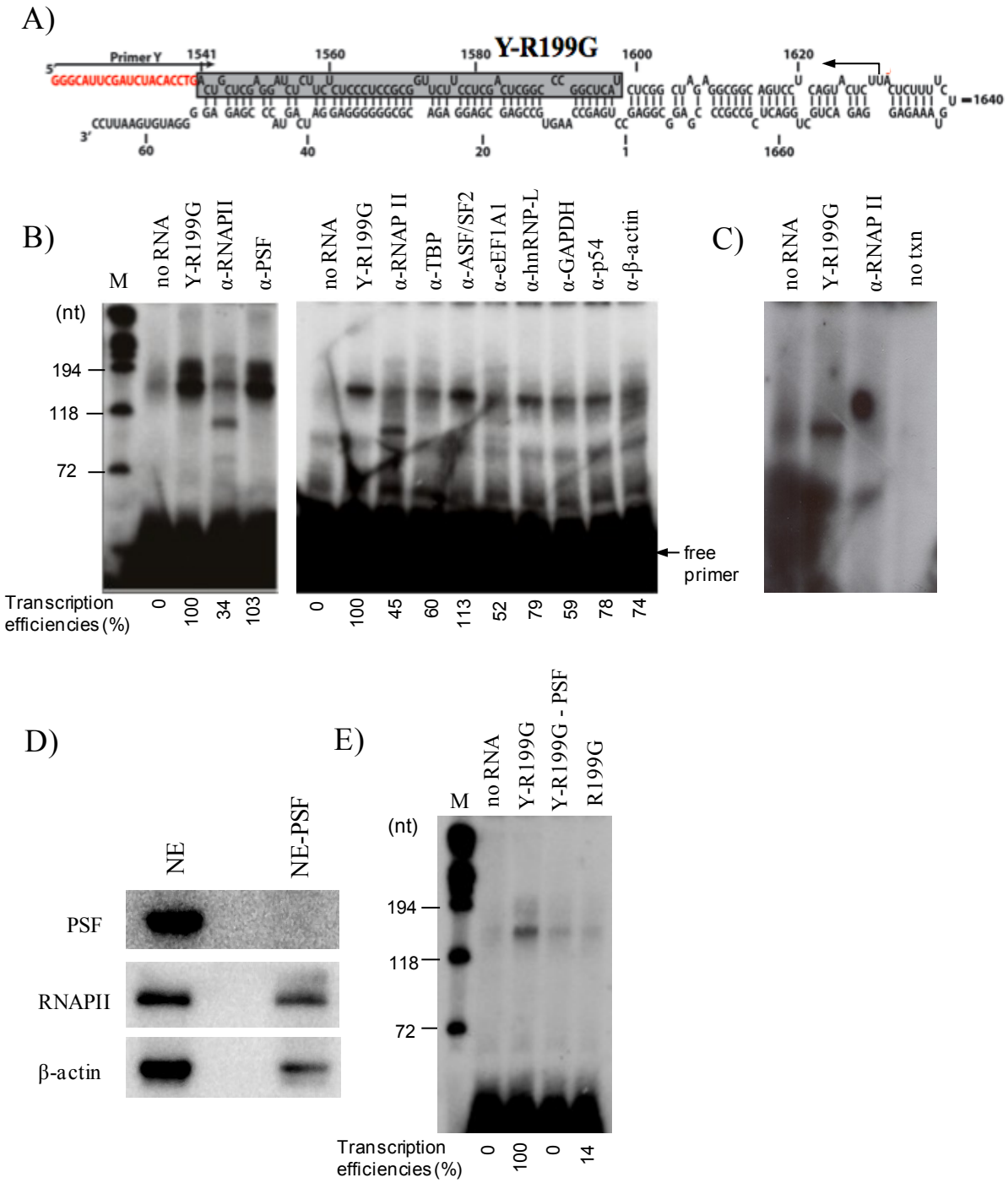
A)
Y-R199G
Primer Y
B)
M
no RNA
Y-R199G
α-RNAPII
α-PSF
(nt)
194
118
72
Transcription efficiencies (%)
0
100
34
103
α-RNAP II
α-TBP
α-ASF/SF2
α-eEF1A1
α-hnRNP-L
α-GAPDH
α-p54
α-β-actin
45
60
113
52
79
59
78
74
free primer
C)
no txn
D)
NE
NE-PSF
PSF
RNAPII
β-actin
E)
Y-R199G - PSF
R199G

Figure 3.6: Potential involvement of host proteins in the transcription of HDV RNA.

In vitro transcription assays were performed in HeLa NE using a modified R199G (Y-R199G) RNA as template. (A) Secondary structure of Y-R199G RNA. The initiation site for the transcription of HDAg mRNA is indicated with an arrow. The boxed region corresponds to the 5' end of HDAg ORF. A 20-nt non-HDV sequence ('Y') was added to the 5' end of R199G to allow for the specific detection of transcription product by reverse transcription (RT) with a radiolabelled primer Y. (B) Denaturing polyacrylamide gel electrophoresis of transcription products, detected by RT. Lane M contains the ΦX174 DNA/*Hae* III fragments. A non-templated reaction ('no RNA' lane) was performed as a negative control. The 'Y-R199G' lane contains the product(s) of Y-R199G-templated transcription. Inhibition of transcription by indicated antibodies was examined by pre-incubation of HeLa NE with 2.5 μg of an anti-RNAP II, -PSF, -TBP, -ASF/SF2, -eEF1A1, -hnRNP-L, -GAPDH, -$p54^{nrb}$, or –*β*-actin antibody. (C) *In vitro* transcription was repeated with an additional negative control, in which the RT was performed on Y-R199G RNA without prior *in vitro* transcription reaction ('no txn' lane). (D) Western blot following PSF-immunodepletion of HeLa NE. Protein levels of PSF, RNAP II and *β*-actin were compared pre- and post- immunodepletion of HeLa NE with an anti-PSF antibody. (E) Denaturing polyacrylamide gel electrophoresis of transcription products following *in vitro* transcription in HeLa NE (lane 'Y-R199G'), or PSF-immunodepleted HeLa NE (lane 'Y-R199G-PSF'). R199G-templated transcription (lane 'R199G) was included as a negative control to ensure that product formation is dependent on 'Y'-primed RT.

primer corresponding to the sequence of the 5' extension (primer Y; Figure 3.6A), and the radiolabelled cDNAs were resolved by denaturing PAGE (Figure 3.6B). An excess of primer was used as demonstrated by the non-incorporated primer at the bottom of the gel. Although *in vitro* transcription from HDV-derived RNA fragments has been shown to be inefficient, particularly in the absence of HDAg-S (Abrahem and Pelchat, 2008; Filipovska and Konarska, 2000; Yamaguchi *et al*., 2001), the present assay was sufficiently sensitive to detect a transcription product; a major band, with an apparent molecular size of about 130 nt, was observed following PAGE ('Y-R199G' lane). The appearance of this band was template-dependent, as it was absent from the negative control, from which the RNA template was missing (Figure 3.6B, 'no RNA' lane). As a further confirmation that the observed 130 nt band is a genuine product of Y-R199G-templated transcription, two additional control samples have been included in the analysis. First, reverse transcription using the radiolabelled primer Y was performed on the template Y-R199G RNA, without having subjected it to the *in vitro* transcription reaction. No band was detected in the control sample (Figure 3.6C, 'no txn' lane), indicating that the 130 nt band corresponds to a product of the *in vitro* transcription reaction, and is not the result of reverse transcription from the Y-R199G template. Second, to verify the specificity of the primer used to detect the product of the Y-R199G-templated transcription, the assay was also performed using the original R199G fragment (without the 5' extension) as a template (Figure 3.6E, 'R199G' lane). No product was detected, indicating that the 130 nt band is a specific product of the "Y"-primed reverse transcription reaction. Altogether, these findings indicate that the observed RT product truly represents the Y-R199G-templated transcription product.

Following the development of a working *in vitro* HDV RNA transcription assay, I wanted to assess the potential role of HDV RNA-interacting proteins in HDV transcription. To achieve this, the transcription reactions were carried out in nuclear extract pre-incubated with the specified antibody (Figure 3.6B). Transcription efficiencies (%) were estimated relative to the negative control (no RNA template – 0 %) and the untreated sample (no antibody – 100 %), based on the intensity of the band corresponding to the 130-nt product. An observed decrease in product formation following inhibition of the protein suggested its involvement in the *in vitro* transcription of HDV RNA, although a quantitative analysis was not possible without determining the amount of the protein of interest in the nuclear extract.

The transcription reaction was inhibited by more than 50 % in NE pre-incubated with the anti-RNAP II CTD antibody, as compared to the no antibody control, indicating that the observed 130-nt band is a product of RNAP II-mediated transcription. This is consistent with similar findings observed by Abraham and Pelchat (2008). Interestingly, a lower-molecular weight product (~100 nt) appeared in the anti-RNAP II antibody-treated sample, suggesting that this product may have been generated by another polymerase in the absence of functional RNAP II; alternatively, a different initiation site might have been used by RNAP II in the presence of the anti-RNAP II antibody. Since recognition of the HDV promoter by RNAP II has been suggested to occur through the TATA binding protein (TBP; Abrahem and Pelchat, 2008), I also examined the effect of an anti-TBP antibody on HDV transcription. Not surprisingly, the transcription reaction was estimated to be only 60 % efficient when the NE was pre-incubated with the anti-TBP antibody. After pre-incubation with an anti-eEF1A1 antibody, the transcription reaction was only half as efficient, pointing to a potential involvement of eEF1A1 in HDV transcription. A similar decrease in transcription efficiency

was also observed following pre-incubation with the anti-GAPDH antibody, suggesting that GAPDH may be enhancing HDV transcription. Pre-treatment with anti-ASF/SF2, -hnRNP-L, -p54^{nrb}, and -PSF antibodies had no considerable effect on product accumulation; these transcription reactions were all over 70 % efficient, comparable to the anti-β-actin-treated control, which had an efficiency of 74 %. However, the potential involvement of these proteins in HDV transcription cannot be dismissed, as it is possible that insufficient antibody was used to achieve a significant inhibition. This could be the case particularly with ASF/SF2 and hnRNP-L, two highly abundant proteins (Han *et al*., 2010; Lin and Fu, 2007).

It is also possible that antibody binding did not interfere with the function of the protein. Since the epitopes recognized by anti-hnRNP-L, -p54^{nrb}, and -PSF antibodies are unknown, there is a chance that antibody binding did not inhibit protein activity. The anti-ASF/SF2 antibody is known to target amino acids 1 to 97 of the protein. This part of ASF/SF2 contains one of two RNA recognition motifs (RRMs; Figure 4.1); although either RRM can bind to RNA by itself, optimal interaction of ASF/SF2 with RNA requires both RRMs (Caceres and Krainer, 1993; Zuo and Manley, 1993). Thus, it is unlikely that ASF/SF2 is directly involved in HDV transcription, since interfering with the protein's RNA binding activity had no effect on product accumulation following *in vitro* HDV transcription; however, it is presently unknown what region of ASF/SF2 is involved in the binding to HDV RNA.

Antibody binding to p54^{nrb} or its cellular homologue PSF had no effect on product accumulation. This finding was surprising, since previous findings (Greco-Stewart, 2009) demonstrated the simultaneous presence of both PSF and RNAP II on the R199G RNA fragment, and suggested that PSF may be involved in the recruitment of the HDV template to

the RNAP II complex. However, it is possible that antibody binding did not inhibit PSF function; therefore, a modified approach was used to reconsider its involvement in HDV transcription. Prior to the transcription reaction, HeLa NE was successfully immunodepleted of PSF; Western blot analysis verified that PSF was removed from the NE without altering the amount of RNAP II (Figure 3.6D). Because the NE was diluted during the process of immunodepletion, the volume of the extract was adjusted accordingly. When the HDV transcription assay was carried out in the immunodepleted extract, very little product was observed (Figure 3.6E), suggesting that PSF is needed for HDV transcription. Ideally, the *in vitro* transcription experiment would be repeated in PSF-immunodepleted extract supplemented with purified PSF to verify that the loss of activity was related to PSF removal, rather than the removal of co-immunodepleted factors. However, previous attempts in our laboratory at bacterial expression and purification of PSF have been only marginally successful (Greco-Stewart, 2009).

Taken together, the data obtained from the *in vitro* transcription experiments indicate that PSF, GAPDH and eEF1A1 may participate in the transcription of HDV RNA, and confirm the involvement of RNAP II and TBP in this process. While ASF/SF2 and hnRNP-L appear to be dispensable for R199G RNA-templated transcription, their involvement in HDV transcription *in vivo* cannot be excluded.

Chapter 4: The role of ASF/SF2 in HDV biology

Author Contributions

All experiments were performed by Dorota Sikora, with the exception of the following:

Binding of ASF/SF2 to the R177GΔASF mutant (Figure 4.6) was performed by Mr. Ali Tanara.

.

4.1 ASF/SF2 knock-down affects accumulation of HDV RNA in cell culture

Previous experiments have identified ASF/SF2 as a direct binding partner of HDV RNA (Figure 3.3). Although ASF/SF2 appeared to be dispensable for *in vitro* HDV RNA transcription (Figure 3.6), its direct and specific association with a fragment of HDV comprising an RNA promoter suggests that it plays an important role in HDV biology. ASF/SF2 is a multifunctional protein belonging to the family of serine/arginine-rich (SR) splicing factors. Structurally, ASF/SF2 has one classical RNA recognition motif (RRM) in its N-terminal region, followed by an additional degenerate RRM (Figure 4.1A); the two RRMs are separated by an arginine/glycine-rich (RGG) linker region. An arginine/serine (RS) domain is found in its C-terminus, and is involved in protein-protein interactions (Birney *et al*., 1993). ASF/SF2 plays an essential role in constitutive splicing (Zahler *et al*., 1992), and also regulates alternative splicing in a concentration-dependent manner (Zahler *et al*., 1993), by promoting exon inclusion through binding to exonic splicing enhancers (ESEs; Graveley, 2000). In addition to its roles in pre-mRNA splicing, ASF/SF2 has also been shown to function in mRNA export (Cáceres *et al*., 1998; Huang and Steitz, 2005), mRNA translation (Sanford *et al*., 2004), and mRNA stability (Lemaire *et al*., 2002). In the current study, I wanted to further investigate the *in vivo* significance of the interaction between ASF/SF2 and HDV RNA.

To examine the potential involvement of ASF/SF2 in the life cycle of HDV, an HDV replication system developed by Chang *et al*. (2005) was used. This replication system was created by stably transfecting a human embryonic kidney cell line with a single copy of the small *delta* antigen cDNA under the control of a tetracycline (TET)-inducible promoter. These cells were then transfected with a mutated HDV RNA unable to produce HDAg-S, to

A)

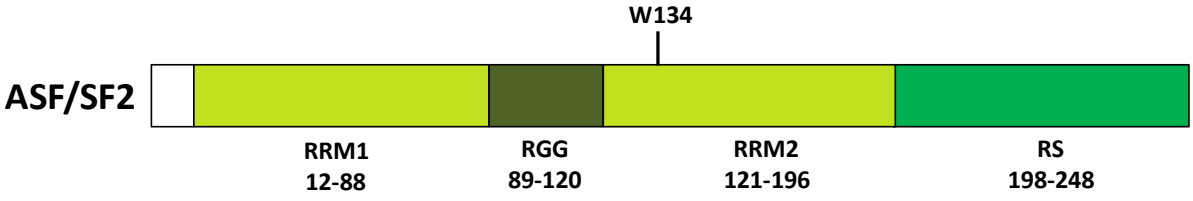
W134
ASF/SF2
RRM1
12-88
RGG
89-120
RRM2
121-196
RS
198-248

B)

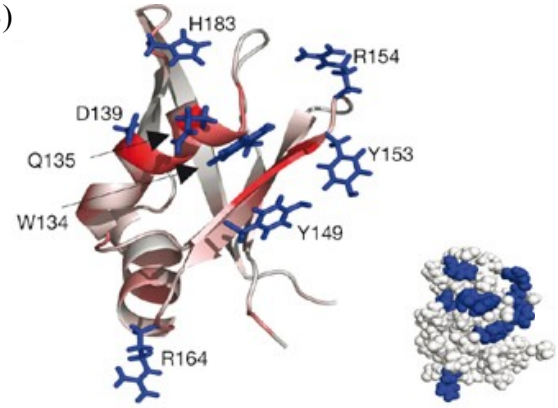
H183
R154
D139
Q135
Y153
W134
Y149
R164

Figure 4.1: Structure of ASF/SF2.

(A) Schematic representation of ASF/SF2. Structural motifs are indicated as follows: RRM (RNA recognition motif), RGG (arginine-glycine rich region), RS (serine-arginine rich region). Position of the tryptophan (W) residue is shown. (B) Tertiary structure of RRM2, determined by nuclear magnetic resonance (NMR) spectroscopy (Tintaru *et al*., 2007), showing the surface-exposed tryptophan residue. Reprinted by permission from Macmillan Publishers Ltd: EMBO Reports 8:756, copyright 2007.

create a cell line (designated 293-HDV) in which replication of HDV RNA is under the control of the TET-inducible HDAg-S. These cells are able to maintain a stable basal level of HDV replication in the absence of TET.

Using the 293-HDV cell line as a model system for HDV replication, the cells were transfected with three different plasmids containing shRNA constructs directed against ASF/SF2. A non-target shRNA construct was used as the negative control. Transfection efficiency was monitored by co-transfection with a plasmid encoding the green fluorescent protein, and estimated visually at 70-80 %. The expression of HDAg-S was induced with TET (1 μg/μL) 16 hours post-transfection. Cells were collected 24 hours later, and ASF/SF2 knock-down was verified by Western blotting (Figure 4.2A). The percentage of ASF/SF2 knock-down was estimated by measuring the intensity of the bands corresponding to ASF/SF2 relative to the intensity of the bands corresponding to GAPDH. ASF/SF2 expression was reduced by only about 30 % with one shRNA construct (sh1), while ASF/SF2 was not detectable following transfection with the other two shRNAs (sh2 and sh3).

The effect of ASF/SF2 knock-down on the accumulation of HDV RNA was assessed by quantitative RT-PCR (qRT-PCR). The quality of the RNA used in the Q-PCR analysis was confirmed by denaturing 1 % agarose/2.2 M formaldehyde gel electrophoresis. The amount of HDV RNA was normalized to the level of β-actin mRNA. Three technical replicates were performed for each sample. The abundance of HDV RNA in anti-ASF/SF2 shRNA-transfected cells relative to non-target shRNA-transfected cells ranged from 90 % (sh1) to about 50 % (sh2 and sh3; Figure 4.2B). These values were consistent with the amount of ASF/SF2 knockdown (Figure 4.2A). These results suggest that ASF/SF2 enhances

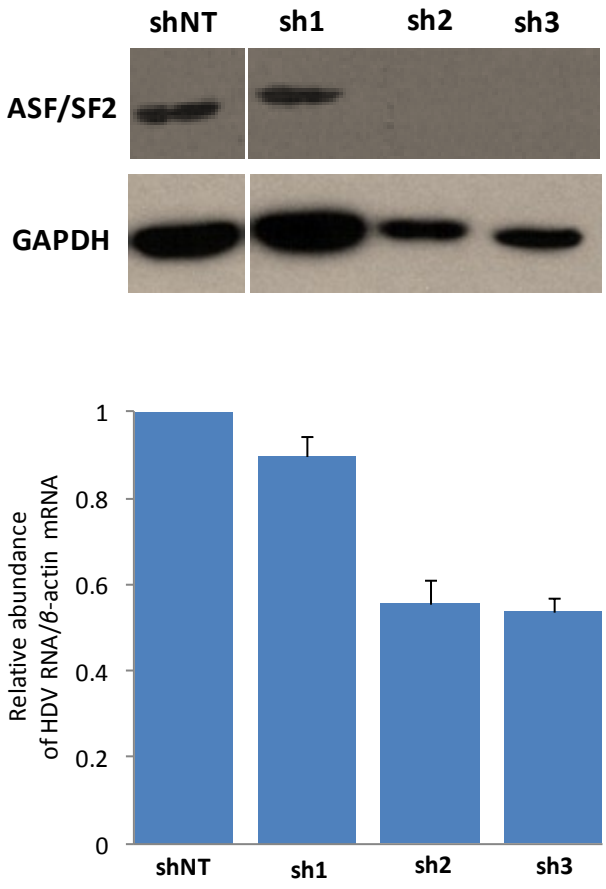
shNT
sh1
sh2
sh3
ASF/SF2
GAPDH
Relative abundance of HDV RNA/β-actin mRNA
1
0.8
0.6
0.4
0.2
0
shNT
sh1
sh2
sh3

Figure 4.2: Involvement of ASF/SF2 in the life cycle of HDV.

HDV-replicating 293 cells were transfected with plasmids harbouring different shRNA constructs against ASF/SF2 (sh1-3), or a non-target shRNA-encoding plasmid (shNT). (A) ASF/SF2 knock-down efficiency was verified by Western blotting, using GAPDH as a loading control. (B) HDV RNA accumulation was normalized to the amount of β-actin mRNA and quantified relative to the negative control (non-target shRNA) by qRT-PCR analysis. A mean of three technical replicates is presented for each shRNA-treated sample.

the accumulation of HDV RNA in the 293 cells, although it is not necessary for HDV replication.

4.2 Characterization of ASF/SF2 binding to HDV RNA

My results thus far have established a direct interaction between ASF/SF2 and HDV RNA. ASF/SF2 was also demonstrated to play a role in the accumulation of HDV RNA in a cell culture system, albeit probably not by direct stimulation of transcription, as suggested by the *in vitro* transcription assay. To further characterize the ASF/SF2-HDV interaction, the binding of *in vitro*-synthesized HDV RNA to purified ASF/SF2 was studied using a fluorescence binding assay.

4.2.1 Overexpression and purification of ASF/SF2

A pure preparation of ASF/SF2 was essential for performing binding experiments using fluorescence spectrophotometry. For this reason, the GST-tagged ASF/SF2 preparation used in previous binding experiments was not suitable, as it was purified under native conditions. Furthermore, the large GST tag was impractical for this assay. Thus, GST-ASF/SF2 was replaced by a histidine-tagged protein. The his-tagged ASF/SF2 (His-ASF/SF2) was overexpressed in *E. coli* and purified under denaturing conditions. Firstly, the *E. coli* BL21 strain was transformed with the expression vector pET-20b harbouring an ASF/SF2 cDNA insert. This expression vector is designed to produce a fusion protein containing 6 histidine residues at the C-terminus, to allow for protein purification by metal

chelate affinity chromatography. It also contains N-terminal *pelB* secretion signal sequence that allows for periplasmic translocalization of the pre-protein. Use of secretion signal peptides in bacterial expression systems was shown to greatly enhance protein expression levels (Sletta *et al*., 2007), and is particularly valuable in the expression of ASF/SF2, since this protein is normally insoluble in *E. coli* (Ge *et al*., 1991; Krainer *et al*., 1991), and accumulates in inclusion bodies (Yue *et al*., 2000). Transformed *E. coli* were grown overnight and expression of His-ASF/SF2 was assessed by 10 % SDS-PAGE electrophoresis. A band of ~ 33 kDa was observed in the sample from transformed *E. coli*, but was absent from the non-transformed cells (Figure 4.3A). While the calculated molecular weight of His-ASF/SF2 is 28.7 kDa, it typically migrates at 33 kDa (Ge *et al*., 1991; Krainer *et al*., 1991). Although protein expression from the pET-20b vector is under the control of an isopropyl-*β*-D-thiogalactoside (IPTG) –inducible promoter, induction was not necessary to obtain a high level of ASF/SF2 overexpression. The *E.coli*-expressed ASF/SF2 was then bound to a Ni^{2+}-nitrilotriacetic acid affinity column, washed, and eluted with an excess of imidazole (Figure 4.3B), which displaces the Ni^{2+}-bound histidine, thereby freeing the protein. The purification was carried out under denaturing conditions (in the presence of 8 M urea) to obtain a pure sample. The urea was removed by stepwise dialysis against buffer containing sequentially decreasing concentrations of urea, and the protein was eventually stored in dialysis buffer containing 1.5 M urea, to maintain protein solubility. During the renaturation process, most of the protein was precipitating out of solution; formation of aggregates is a common feature of SR proteins that tend to self-associate via their RS domains (Nikolakaki *et al*., 2008). To overcome the problem of aggregation, the concentration of His-ASF/SF2 was reduced to ~10 pmol/μL prior to dialysis. At concentrations below 10 pmol/μL, no further precipitate was observed. The purified protein was analyzed by SDS-PAGE, and estimated by densitometry

A)

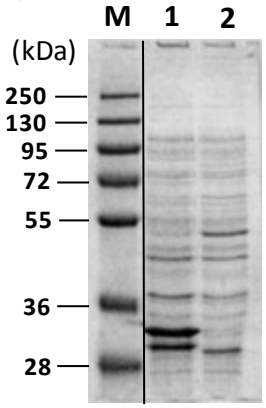
M
1
2
(kDa)
250
130
95
72
55
36
28

B)

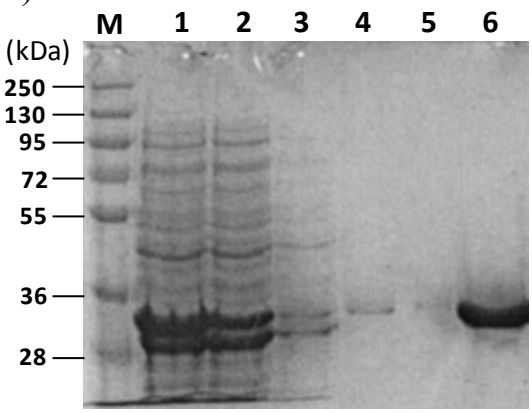
M
1
2
3
4
5
6
(kDa)
250
130
95
72
55
36
28

C)

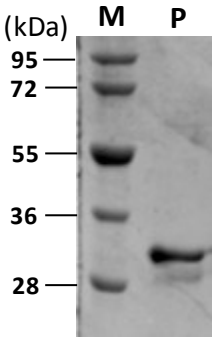
M
P
(kDa)
95
72
55
36
28

Figure 4.3: Expression and purification of ASF/SF2.

(A) SDS-PAGE analysis showing overexpression of His-ASF/SF2 in *E. coli* BL21(DE3)pLysS bacterial cells cultured at 37 ^{o}C for 18 hours in LB medium. Lane M: PageRuler Plus Prestained Protein Ladder; lane 1: pET20-b(ASF/SF)–transformed cells; lane 2: untransformed cells. (B) SDS-PAGE analysis of His-ASF/SF2 binding to and elution from a Ni^{2+}-nitrilotriacetic acid affinity column. Lane 1: cell lysate; lane 2: flowthrough; lanes 3-5: sequential washes with 40 mM imidazole; lane 6: elution with 250 mM imidazole. (C) SDS-PAGE of purified His-ASF/SF2 following dialysis in 50 mM Tris-HCl, pH 7.9, 1 mM EDTA, 0.1 mM dithiothreitol, 50 mM NaCl, 50 % glycerol, 1.5 M urea (lane P).

to be over 95 % pure (Figure 4.3C); its identity was verified by Western blotting using a mouse monoclonal anti-ASF/SF2 antibody (data not shown).

4.2.2 Fluorescence properties of ASF/SF2

A fluorescence binding assay was used to further characterize the binding of HDV RNA to His-ASF/SF2. Fluorescence spectroscopy exploits the intrinsic fluorescence property of proteins; owing to the presence of three aromatic amino acid residues, tryptophan, tyrosine and phenylalanine, proteins are innately fluorescent, and changes in fluorescence can be used to monitor structural changes in a protein. Although all three amino acids may contribute to the fluorescence of a protein, tryptophan is by far the dominant fluorophore, and most of the emissions are due to excitation of tryptophan residues, with limited emissions resulting from excitation of tyrosine and phenylalanine. Due to the distinct fluorescence characteristics of the three residues and to resonance energy transfer from proximal phenylalanine to tyrosine and from tyrosine to tryptophan, the fluorescence spectrum of a protein containing all three residues will usually resemble that of tryptophan (Eftink, 1991; Lakowicz, 2006).

Intrinsic tryptophan fluorescence has been used extensively to investigate the interactions of different proteins with their ligands (Benzaghou *et al*., 2006; Bougie *et al*., 2004; Elton *et al*., 1999; Flowers *et al*., 2003; Lima *et al*., 2006; Zhou *et al*., 1995). ASF/SF2 is a good candidate protein for binding studies using fluorescence spectroscopy, as it has only one tryptophan residue, located in RRM2 (Figure 4.1), which makes the interpretation of fluorescence data more accurate; in multiple-tryptophan proteins, the signal-to-noise response to ligand binding may be decreased, since each tryptophan will respond differently

A)

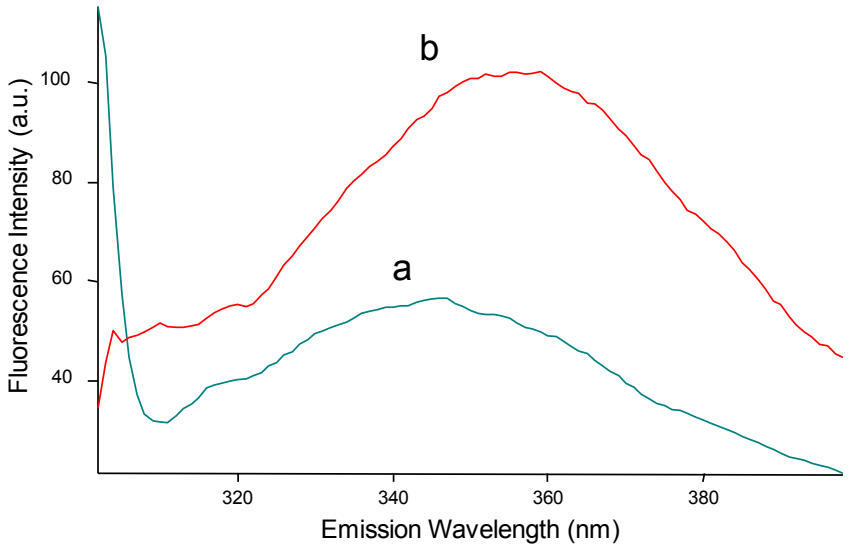
b
a
Fluorescence Intensity (a.u.)
100
80
60
40
320
340
360
380
Emission Wavelength (nm)

B)

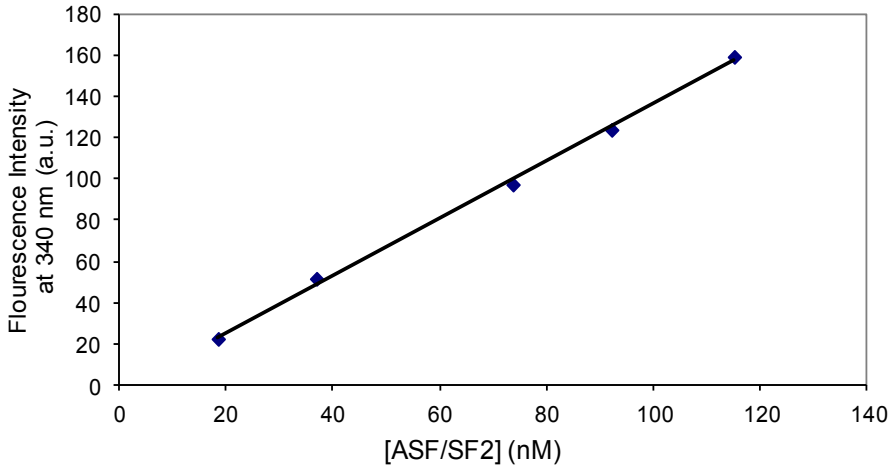
Flourescence Intensity at 340 nm (a.u.)
180
160
140
120
100
80
60
40
20
0
0
20
40
60
80
100
120
140
[ASF/SF2] (nM)

Figure 4.4: Fluorescence properties of ASF/SF2.

(A) Emission spectrum of ASF/SF2 (100 nM) at an excitation wavelength of 280 nm. a, purified protein in 20 mM Tris-HCl, 100 mM KCl, pH 7.5; b, purified protein after a 2h incubation in 20 mM Tris-HCl, 100 mM KCl, pH 7.5, and 8 M urea at 25 ^{o}C. (B) Molar fluorescence of ASF/SF2. ASF/SF2 was excited at 280 nm and fluorescence intensity at increasing concentration of ASF/SF2 was measured at an emission wavelength of 340 nm.

depending on their position in the protein (Zhou and Rosen, 1997). An emission spectrum of purified His-ASF/SF2 is shown in Figure 4.4A (curve 'a'). The emission spectrum was obtained following excitation at 280 nm; this excitation wavelength was determined to produce the maximal emission peak after scanning the absorption spectrum of His-ASF/SF2. Emission maximum was observed at about 340 nm. Although the emission maximum of free tryptophan is 348 nm, it is not uncommon to observe lower emission maxima in native proteins, as tryptophan fluorescence is easily shifted in response to minor changes in its microenvironment. Emission maxima of native proteins depend on the position of the tryptophan residues in the folded protein. Typically, surface residues that are exposed to a polar solvent will have an emission wavelength close to that of free tryptophan, whereas residues that are buried in the interior of the protein will be blue-shifted (Eftink and Ghiron, 1976). Thus, the observed 340 nm emission maximum of His-ASF/SF2 indicates that the tryptophan is partially exposed to the solvent; this is in agreement with the solution structure of RMM2 of ASF/SF2 (Tintaru *et al*., 2007), in which the tryptophan residue is surface-exposed (Figure 4.1B). Consistent with these observations, upon denaturation of the protein in 8M urea, the emission maximum was red-shifted (Figure 4.3A, curve 'b'), indicating that the unfolding of the protein fully exposed the tryptophan residue to the polar solvent (Eftink and Ghiron, 1976). The fluorescence intensity increased as a result of denaturation; although exposure to polar solvent usually quenches tryptophan fluorescence (Eftink and Ghiron, 1976, Lakowicz, 2006), increase in tryptophan fluorescence has also been reported upon denaturation in urea (Benzaghou *et al*., 2006; Soulière *et al*., 2008).

To verify that the intrinsic protein fluorescence is directly proportional to protein concentration, molar fluorescence of ASF/SF2 was analyzed (Figure 4.4B). Fluorescence was

measured at increasing concentrations of ASF/SF2, and was observed to be changing at a constant rate in the assayed concentration range (20-120 nM), indicating negligible loss of active protein through aggregation and/or adhesion. Based on these observations, all subsequent binding experiments were performed at an ASF/SF2 concentration of 100 nM. This concentration was both large enough to obtain a practicable fluorescence signal, and low enough to allow for an accurate estimation of the apparent dissociation constant ($AppK_D$) between an HDV RNA fragment and ASF/SF2.

4.2.3 Identification of an ASF/SF2 binding site on R199G RNA

The interaction of ASF/SF2 and R199G RNA was studied by observing the response of tryptophan fluorescence to the addition of RNA. The binding experiments were carried out by adding increasing amounts of RNA to a fixed amount of ASF/SF2 (100 nM), and observing a change in the emission spectra. Figure 4.5A shows typical emission spectra generated after the addition of RNA. The interaction of R199G RNA with ASF/SF2 caused a decrease in the fluorescence intensity but did not affect the position of the emission maximum (at 340 nm), indicating that the fluorescence of tryptophan was quenched by the interaction with RNA.

The binding curve produced from the observed change in the emission spectra of ASF/SF2 upon addition of increasing amounts of RNA is shown in Figure 4.5B. The difference in ASF/SF2 fluorescence was plotted as a function of increasing RNA concentration, and analysed using the GraphPad Prism 3.0 software by fitting the points to a

A)

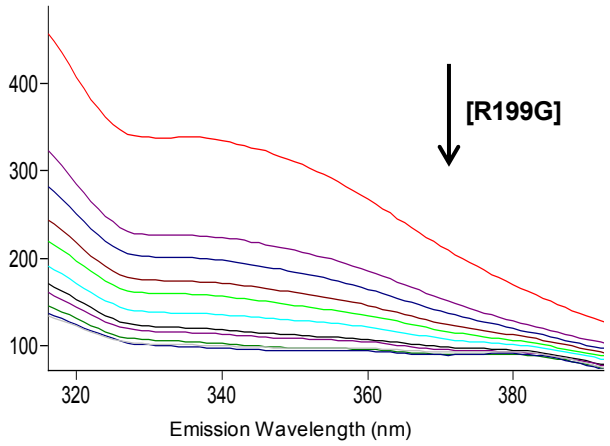
400
300
200
100
[R199G]
320
340
360
380
Emission Wavelength (nm)

B)

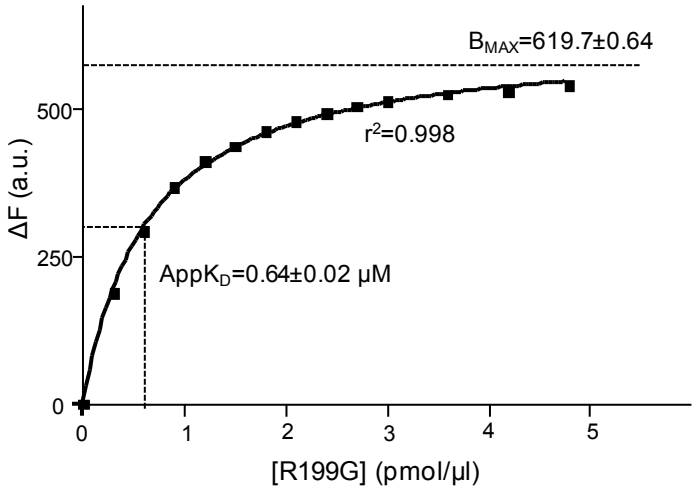
B_{MAX}=619.7±0.64
500
250
0
r^2=0.998
ΔF (a.u.)
AppK_D=0.64±0.02 μM
0
1
2
3
4
5
[R199G] (pmol/μl)

C)

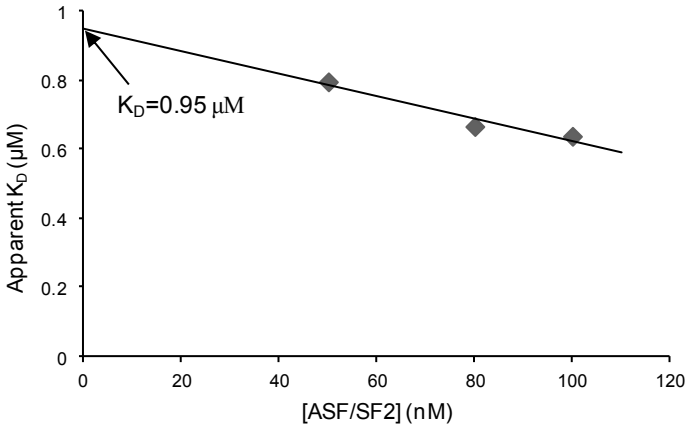
1
0.8
0.6
0.4
0.2
0
K_D=0.95 μM
Apparent K_D (μM)
0
20
40
60
80
100
120
[ASF/SF2] (nM)

Figure 4.5: Quantification of the binding of R199G RNA to ASF/SF2 using a fluorescence binding assay.

(A) Typical ASF/SF2 emission spectra generated after the addition of RNA. Excitation was carried out at 280 nm; red curve (top) corresponds to the fluorescence of ASF/SF2 alone. Addition of RNA resulted in a decrease in ASF/SF2 fluorescence (background buffer emission was not subtracted). (B) A binding curve was generated by plotting the observed change in fluorescence of ASF/SF2 at 340 nm as a function of increasing concentration of HDV RNA. The binding was analyzed by the GraphPad Prism 3.0 software using the one-site binding model, and the apparent K_D ($AppK_D$) and B_{max} values were calculated. (C) Apparent K_D versus ASF/SF2 concentration. K_D's for the interaction of R199G and ASF/SF2 were measured at different concentrations of ASF/SF2. The points were fitted to a linear regression line ($y = -0.0032x + 0.95$, $r^2=0.946$).

one-site binding curve, with the square of the correlation coefficient (r^2) = 0.998. The binding between R199G and ASF/SF2 was specific, as is could be saturated by increasing amounts of RNA (a binding maximum (B_{MAX}) was observed at 619.7±0.64 a.u.). An apparent dissociation constant ($AppK_D$) for the interaction, the concentration of the RNA at which 50 % of the protein was bound, was calculated to be 0.64 ± 0.02 μM under my experimental conditions. To monitor how the $AppK_D$ changes depending on the concentration of ASF/SF2, the binding experiment was repeated at 80 nM and 50 nM of ASF/SF2. The graph of the apparent K_D versus ASF/SF2 concentration is shown in Figure 4.5C. The points were fitted to a linear regression line (r^2=0.946), and the y-intercept was determined at 0.95 μM, suggesting that the equilibrium K_D for the reaction is closer this value.

Having developed a working binding assay, I subsequently used it to further characterize the ASF/SF2 – HDV RNA interaction. To determine the location of the ASF/SF2 binding site on R199G, truncation mutants were constructed and their interaction with ASF/SF2 was compared to that of R199G. Examination of the binding affinity of R199G truncation mutants to ASF/SF2 revealed that shortening the stem of R199G to produce R177G did not interfere with its ability to bind the protein (Figure 4.6), although it increased the $AppK_D$ to 0.88±0.13 μM. Similar affinity was observed between R161G RNA and ASF/SF2 ($AppK_D$=0.93±0.10 μM). However, reducing the stem further, to produce R156G, resulted in loss of binding to ASF/SF2. Based on these results, and previous findings that ASF/SF2 specifically binds polypurine stretches (Graveley, 2000), the potential ASF/SF2 target sequence was proposed to be GGGAGGA (indicated by the red rectangle in Figure 4.6). To verify that this region is involved in ASF/SF2 binding, the R177G RNA fragment was modified by removing the GGGAGGA sequence, along with the region it


R199G
AppK$_D$ = 0.64±0.02
[R199G] (pmol/ul)
R177G
AppK$_D$ = 0.88±0.13
[R177G] (pmol/ul)
R161G
AppK$_D$ = 0.93±0.10
[R161G] (pmol/ul)
R156G
[R156G] (pmol/ul)
R177GΔASF
[R177GΔASF] (pmol/ul)
R47G
[R47G] (pmol/ul)
P11.60
[P11.60] (pmol/ul)
deltaF (a.u.)

Figure 4.6: Identification of a putative ASF/SF2 binding site on R199G RNA.

The binding of four R199G truncation mutants (R177G, R161G, R156G and R177GΔASF) to ASF/SF2 was analyzed using the fluorescence binding assay. The boxed nucleotides in R177ΔASF represent a deletion. Excitation was performed at 280 nm, and emission was monitored at 340 nm. The proposed ASF/SF2 binding site is indicated by the red rectangle. R47G and P11.60 RNAs were used as negative controls. The binding was analyzed by the GraphPad Prism 3.0 software using the one-site binding model, and an apparent K_D ($AppK_D$) was calculated where indicated.

hybridizes to when forming the stem structure, producing the R177GΔASF mutant. This mutant was unable to bind ASF/SF2. Non-specific binding was observed between ASF/SF2 and the R47G truncation mutant, as indicated by a linear binding curve. Binding of this RNA species increased the fluorescence of ASF/SF2, suggesting that R47G and R199G bind at distinct sites on the protein. Similar results were observed with the P11.60 RNA (a 60-nucleotide hairpin derived from the peach latent mosaic viroid); this RNA has been used as a non-specific competitor in previous binding experiments (Figure 3.4). Taken together, these results suggest that ASF/SF2 is binding HDV RNA at a distinct site downstream of the proposed transcription initiation site and RNAP II binding region (Figure 1.2B).

To investigate whether the proposed ASF/SF2 target sequence is conserved among different HDV strains, the region of HDV RNA containing the potential ASF/SF2 binding site was aligned across 92 strains of HDV using the ClustalW multiple alignment program, and corrected manually (sequences obtained from the online Subviral RNA Database, available at http://subviral.med.uottawa.ca/cgi-bin/home.cgi; Figure 4.7A). The alignment revealed a purine-rich consensus sequence at the proposed ASF/SF2 binding site. The percentage of purine versus pyrimidine content at each nucleotide position was calculated (Figure 4.7A, bottom), and shows a strong enrichment in purine content at the proposed ASF/SF2 binding site across the aligned sequences. The obtained consensus sequence also strongly corresponds to the published ASF/SF2 recognition sequence (Sanford *et al*., 2009), which was determined by a cross-linking immunoprecipitation and high-throughput sequencing (CLIP-seq) approach in cultured human embryonic kidney cells (Figure 4.7B), suggesting that it is a genuine ASF/SF2 target.

A)

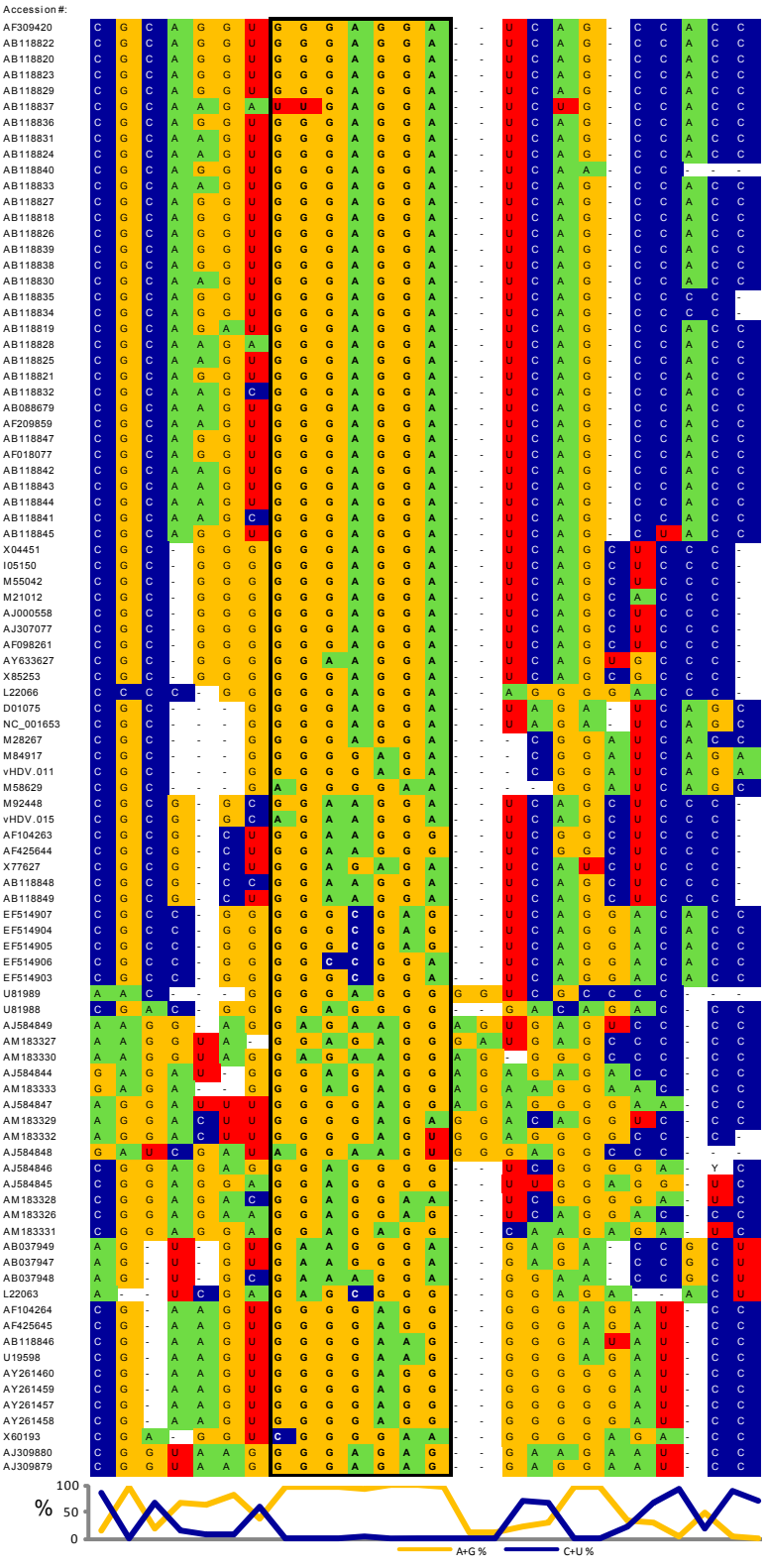
Accession #:
AF309420
AB118822
AB118820
AB118823
AB118829
AB118837
AB118836
AB118831
AB118824
AB118840
AB118833
AB118827
AB118818
AB118826
AB118839
AB118838
AB118830
AB118835
AB118834
AB118819
AB118828
AB118825
AB118821
AB118832
AB088679
AF209859
AB118847
AF018077
AB118842
AB118843
AB118844
AB118841
AB118845
X04451
I05150
M55042
M21012
AJ000558
AJ307077
AF098261
AY633627
X85253
L22066
D01075
NC_001653
M28267
M84917
vHDV.011
M58629
M92448
vHDV.015
AF104263
AF425644
X77627
AB118848
AB118849
EF514907
EF514904
EF514905
EF514906
EF514903
U81989
U81988
AJ584849
AM183327
AM183330
AJ584844
AM183333
AJ584847
AM183329
AM183332
AJ584848
AJ584846
AJ584845
AM183328
AM183326
AM183331
AB037949
AB037947
AB037948
L22063
AF104264
AF425645
AB118846
U19598
AY261460
AY261459
AY261457
AY261458
X60193
AJ309880
AJ309879
100
%
50
0
A+G %
C+U %

B)

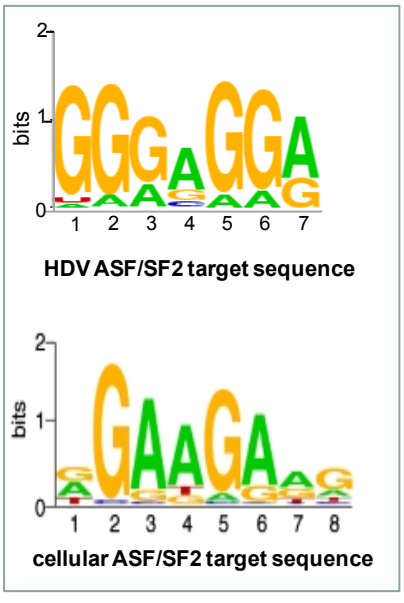
bits
2
1
0
1 2 3 4 5 6 7
HDV ASF/SF2 target sequence
bits
2
1
0
1 2 3 4 5 6 7 8
cellular ASF/SF2 target sequence

Figure 4.7: Sequence alignment of the proposed ASF/SF2 recognition site on HDV RNA.

(A) Multiple alignment of sequences corresponding to 92 HDV strains. The purine versus pyrimidine content (%) at each position is plotted below the alignment. (B) Logo representation of the consensus ASF/SF2 binding sequence created from the HDV sequence alignment (using the web-based WebLogo application) compared to a published consensus ASF/SF2 recognition sequence obtained from a pool of cellular RNAs (Sanford *et al*., 2009). Reprinted from Sanford *et al*., Genome Research 19:381, copyright 2009, used under a Creative Commons Attribution-NonCommercial 3.0 Unported license (http://creativecommons.org/licenses/by-nc/3.0).

Based on my results, ASF/SF2 appears to be involved in the life cycle of HDV, and enhance HDV RNA accumulation in cells. The role of ASF/SF2 is likely mediated by the direct interaction between ASF/SF2 and its proposed target sequence on HDV RNA located downstream of the HDAg mRNA transcription initiation site. However, the existence of additional ASF/SF2 binding sites on HDV RNA is probable.

Chapter 5: Evolutionary relationship between HDV and viroids

Author Contributions

All experiments were performed by Dorota Sikora, with the exception of the following:

MiniHDV reverse transcription-PCR reactions and cloning of miniHDV cDNA products were performed by Ms. Ji Yin (Figures 5.4 and 5.5) under the direct guidance of Dorota Sikora.

5.1 The human ASF/SF2 interacts directly with PSTVd RNA

The current study identified a number of host factors that interact with HDV RNA, and are thus expected to play unique roles in HDV biology. HDV relies on several host proteins to complete its life cycle. Interestingly, viroids have been observed to interact with orthologous proteins in their hosts. RNA-templated transcription of both HDV and pospiviroid genomes is carried out by the cellular RNAP II (Flores, 2011; Taylor, 2009), and the rod-like conformation of each species is believed to be important for RNAP II template recognition. Both HDV and PSTVd RNA have also been found to interact with RNAP III-associated transcription factors *in vitro* (Eiras *et al*., 2011; Greco-Stewart *et al*., 2009), suggesting the involvement of RNAP III in their replication. In addition, HDV and viroids interact with similar cellular components; while eEF1A1 and GAPDH were identified as HDV RNA interacting partners in the present study, PSTVd was also suggested to interact with the plant orthologues of these two proteins (Bojić, 2009). All these observations suggest that HDV and viroids are replicated by analogous mechanisms in their respective hosts. To further examine the parallels between HDV and PSTVd, I sought to determine if PSTVd RNA would interact with ASF/SF2. Two ASF/SF2-like proteins, atSR30 and atSR34/SR1, have been identified in plants (Lazar *et al*., 1995; Lopato *et al*., 1999); these proteins were readily immunodetected by a specific monoclonal antibody raised against human ASF/SF2 (Lopato *et al*., 1996). Because I did not have direct access to either ASF/SF2 plant orthologue, I considered the binding between PSTVd RNA and the human ASF/SF2. For this purpose, radiolabelled full-length PSTVd RNAs of each polarity were synthesized *in vitro*, and each was incubated for 30 minutes with purified human GST-tagged ASF/SF2. The

samples were then subjected to electrophoresis through a non-denaturing 5 % polyacrylamide gel (Figure 5.1). Migration of

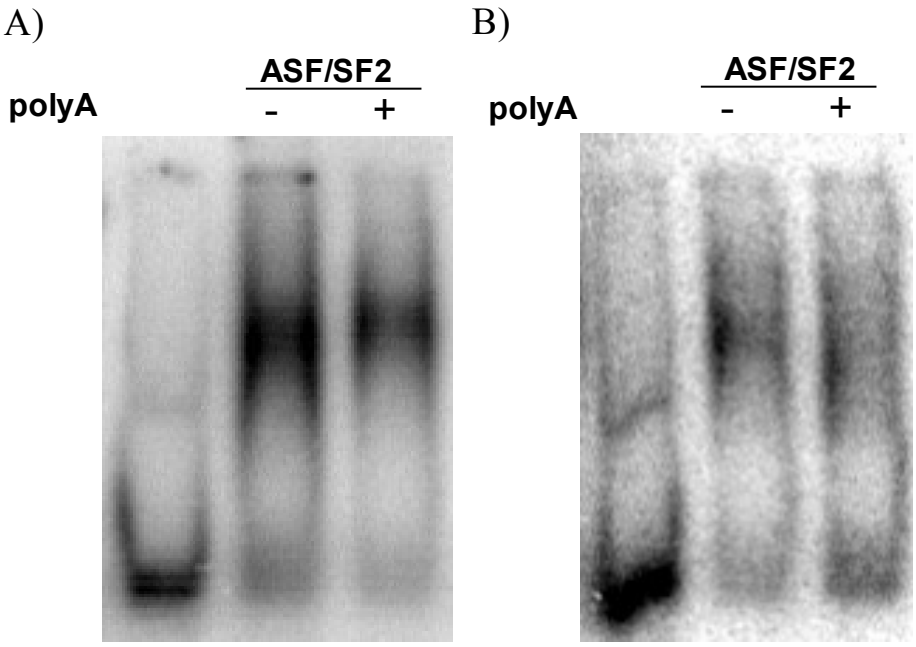

Figure 5.1: Direct interaction of PSTVd RNA with human ASF/SF2.

EMSA was performed to analyze the direct binding of PSTVd(-) RNA (A), and PSTVd(+) RNA (B). Radiolabelled linear PSTVd RNA monomer was incubated with 0.5 μg of purified GST-ASF/SF2 in the presence or absence of poly(A) (100 ng), and resolved by non-denaturing polyacrylamide gel electrophoresis.

both PSTVd(+) and PSTVd(-) RNAs was retarded in the presence of ASF/SF2; the RNAs were also shifted in the presence of molecular excess of poly(A), indicating the direct and specific binding of the human ASF/SF2 to PSTVd RNA. This finding, together with previous findings that HDV and viroids interact with common cellular factors, suggests that these similar RNA pathogens use analogous strategies to exploit their respective host for their replication.

5.2 PSTVd replicates in human hepatocytes

In addition to the numerous orthologous host factors that HDV and viroids interact with, this study has established that PSTVd interacts directly and specifically with the human SR protein ASF/SF2 *in vitro*. Interestingly, PSTVd RNA has also been shown to interact specifically with the human RNAP II in HeLa NE (Bojić, 2009). These findings suggested the potential of PSTVd to replicate in a human cell system. To examine the possibility that PSTVd can use human factors to replicate its genome, human hepatocytes (HepG2) were transfected with a trimer of *in vitro*-synthesized PSTVd RNA of the (+) polarity. A trimer rather than a monomer of PSTVd RNA was used to transfect HepG2 cells, because monomeric PSTVd constructs are known to be only marginally infectious, since they are not efficiently processed by cleavage and ligation (Diener, 1986). Cells were collected 3 days post-transfection, and the presence of PSTVd RNA was analyzed by reverse transcription (RT)-PCR using strand-specific primers (Figure 5.2). PCR performed on a plasmid harbouring PSTVd cDNA amplified a product of about 390 nt, and served as a size marker. Non-templated PCR (Figure 5.2, 'H_20' lane) was also performed to exclude the possibility of

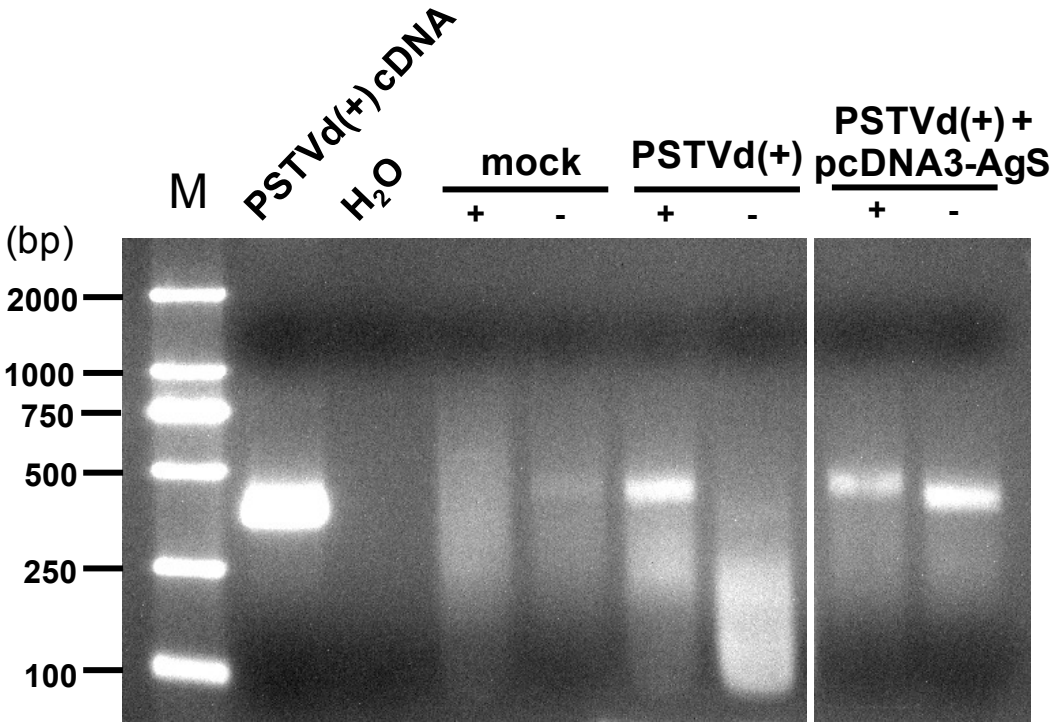
M
PSTVd(+) cDNA
H2O
mock
PSTVd(+)
PSTVd(+) + pcDNA3-AgS
+
-
+
-
+
-
(bp)
2000
1000
750
500
250
100

Figure 5.2: Replication of PSTVd in human hepatocytes.

Human HepG2 cells were transfected with either a trimer of PSTVd(+) RNA alone, or PSTVd(+) RNA along with a plasmid encoding the small *delta* antigen (pcDNA3-AgS). A mock transfection was performed as a negative control. Presence of PSTVd RNA was assessed by reverse transcription using either a (+) strand-specific or (-) strand-specific primer, followed by PCR with both primers. PCR was also performed on a plasmid containing a trimer of PSTVd cDNA to served as a size indicator ('PSTVd cDNA' lane), and a 'no-template' PCR ('H_2O' lane) was included as a control. Lane 'M' contains the Gelpilot Midrange DNA ladder (Qiagen).

contamination. Following RT with a primer complementary to the (+) strand, PSTVd RNA was successfully detected in cells transfected with the PSTVd(+) trimer, but not in mock-transfected cells. However, when RT was performed with a (-) strand-specific primer, no band was detected at the expected size, indicating that PSTVd (+) to (-) strand synthesis was not occurring in the hepatocytes, and that the (+) strand-specific primer detected the PSTVd(+) RNA that was introduced into the cells.

I next considered the possibility that PSTVd requires HDAg-S to successfully replicate in the human host. HDAg-S is necessary for HDV replication and has been proposed to stimulate HDV transcription by direct binding to RNAP II and displacement of the negative elongation factor (NELF) (Yamaguchi *et al*., 2001). However, NELF homologues have not been found in plants (Narita *et al*., 2003), which may explain why the non-coding viroid RNA is able to replicate in a plant host, but may require the HDV-derived protein to replicate in human cells. To explore the possibility that HDAg-S may serve a similar function in PSTVd replication inside the human cell, the experiment was repeated by co-transfection of hepatocytes with the PSTVd(+) RNA and a plasmid encoding HDAg-S (Figure 5.2). Following RT-PCR analysis, the presence of both polarities of PSTVd RNA was detected, suggesting that PSTVd(-) RNA was produced from the (+) template in human cells in the presence of HDAg-S. Surprisingly, the band corresponding to the (-) polarity migrated slightly lower than expected; sequencing analysis will be necessary to confirm the identity of the band. Taken together, these results suggest that PSTVd RNA can replicate using human factors. However, based on this finding it is unclear whether *de novo* synthesis of (+) strand RNA was occurring from the newly produced PSTVd(-) RNA. Furthermore, it remains to be determined whether the PSTVd RNA is processed inside human cells.

5.3 MiniHDV replicates in HeLa cells

To further explore the possibility that HDV and viroids are evolutionarily related, I wanted to assess the replication ability of a viroid-like mutant of HDV. Although the genomes of HDV and viroids are structurally similar, the HDV genome is about five times larger than an average viroid genome, and this difference can presumably be attributed to the HDAg coding sequence. To create an HDV molecule that would more closely resemble a viroid, the HDV RNA was truncated by removing the HDAg coding sequence and the polyadenylation signal, along with the region it hybridizes to when it adopts the rod-like conformation (Figure 5.3). The *delta* ribozyme motifs were kept intact, since they are essential for the processing of HDV RNA during the replication cycle. The two terminal stem-loop domains were also retained, as they have been proposed to comprise RNA promoters (Abrahem and Pelchat, 2008; Beard *et al*., 1996; Filipovska and Konarska, 2000; Greco-Stewart *et al*., 2007, 2009). This truncation effectively reduced the size of HDV from 1679 to 342 nucleotides (Figure 5.4A), creating a non-coding RNA molecule, very similar in size and structure to PSTVd. The sequence corresponding to 1.4 times the size of miniHDV (Figure 5.4B) was cloned into a pUC57 vector (Genscript). This sequence contained two copies of the genomic *delta* ribozyme to ensure successful processing of the linear RNA into circles. The ability of this mutant (miniHDV) to replicate in human cells was assessed by transfecting HeLa cells with *in vitro*-synthesized genomic miniHDV RNA corresponding to 1.4 times the length of a monomer. Presence of miniHDV RNA inside the cells 3 days post-transfection was assessed by RT-PCR with strand-specific primers. A band was observed

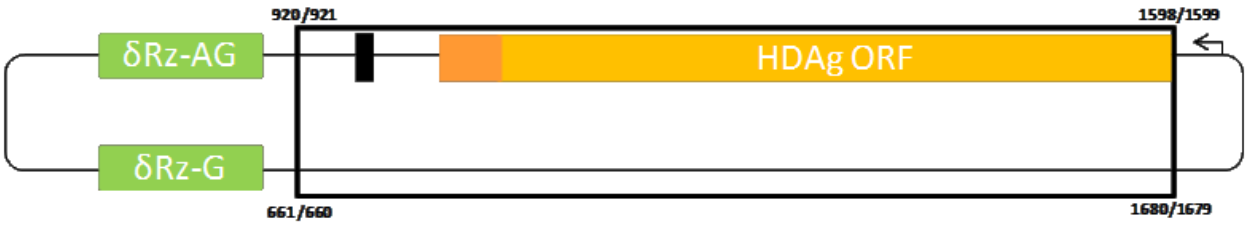
920/921
1598/1599
δRz-AG
HDAg ORF
δRz-G
661/660
1680/1679

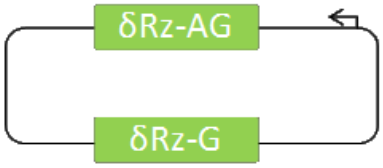
δRz-AG
δRz-G

Figure 5.3: Structural comparison of HDV and miniHDV RNA genomes.

Genomic and antigenomic polarities of HDV RNA are superimposed. Locations of genomic (G) and antigenomic (AG) *delta* ribozymes (*δ*Rz) are shown. Predicted HDAg mRNA transcription start site is indicated by an arrow. The boxed region of HDV, including the HDAg ORF and the polyadenylation site as well as the region it hybridizes to when it adopts the rod-like conformation (black box), was removed to produce a truncated mutant of HDV – miniHDV. The miniHDV molecule consists of the two terminal hairpin domains of HDV, reported to act as RNA promoters (Abrahem and Pelchat, 2008; Beard *et al*., 1996; Filipovska and Konarska, 2000; Greco-Stewart *et al*., 2007, 2009), and both G and AG ribozyme motifs.

A)

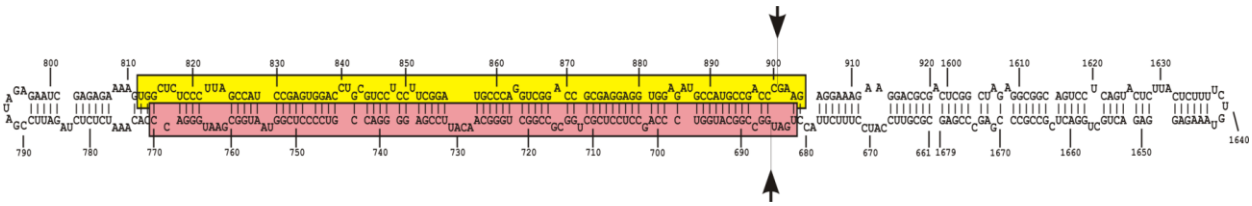

B)

Clone sequence:

5’GAATTCTAATACGACTCACTATAGGGACTCGCCG**CTGCAG**CCC**GGTACC**GTT
CCATCCTTTCTTACCTGATGGCCGGCATGGTCCCAGCCTCCTCGCTGGCGCCGGC
TGGGCAACATTCCGAGGGGACCGTCCCCTCGGTAATGGCGAATGGGACCCACAA
ATCTCTCTAGATTCCGATAGAGAATCGAGAGAAAAGTGGCTCTCCCTTAGCCATC
CGAGTGGACCTGCGTCCTCCTTCGGATGCCCAGGTCGGACCGCGAGGAGGTGGA
GATGCCATGCCGACCCGAAGAGGAAAGAAGGACGCGACTCGGCTAGAGGCGGC
AGTCCTCAGTACTCTTACTCTTTTCTGTAAAGAGGAGACTGCTGGACTCGCCGCC
CGAGCCCGAGCGCGTTCCATCCTTTCTTACCTGATGGCCGGCATGGTCCCAGCCT
CCTCGCTGGCGCCGGCTGGGCAACATTCCGAGGGGACCGTCCCCTCGGTAATGG
CGAATGGGACCCACAAAT**CT**GCAGA**GGATCC**GAATTC -3’

C)

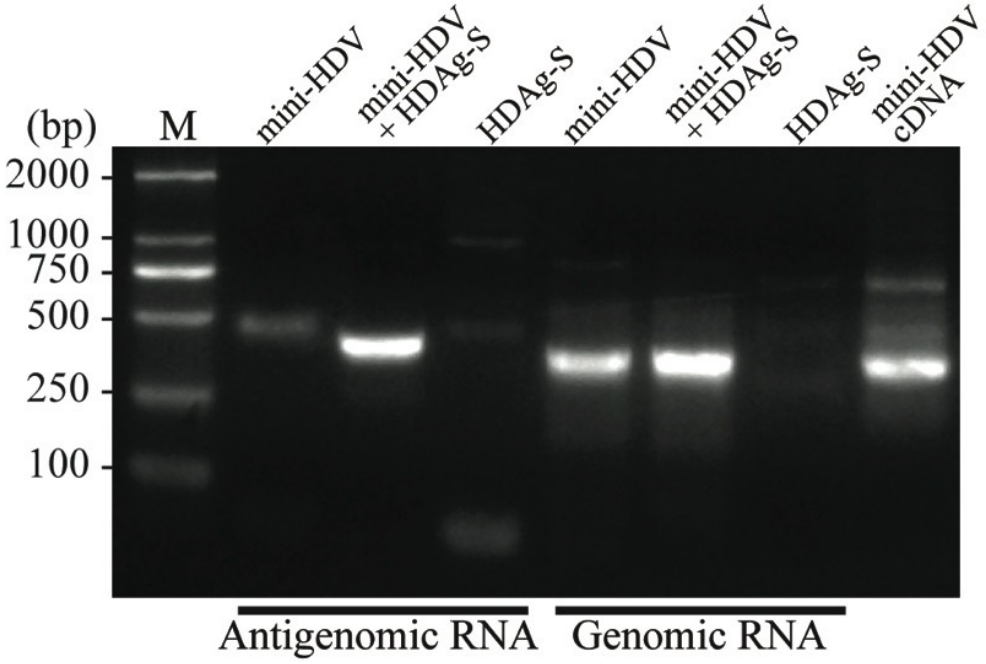

Figure 5.4: Replication of miniHDV in HeLa cells.

(A) Secondary structure of miniHDV. Regions corresponding to genomic and antigenomic ribozymes are highlighted in pink and yellow, respectively. Arrows indicate ribozyme cleavage sites. (B) Sequence of the miniHDV clone used to generate the 1.4-mer of miniHDV RNA. Nucleotides highlighted in green represent non-HDV residues introduced into the sequence to create restriction sites (shown in bold), to facilitate subsequent cloning. (C) Detection of miniHDV RNA in HeLa cells. HeLa cells were transfected with either a miniHDV RNA of genomic polarity (corresponding to 1.4X its length), or a plasmid encoding the small *delta* antigen (HDAg-S), or co-transfected with both. Presence of miniHDV RNA was detected by reverse transcription using a primer designed to specifically detect either the genomic or antigenomic miniHDV RNA, followed by PCR with both primers. PCR was also performed on a plasmid containing a 1.4-mer of miniHDV cDNA, and served as a size indicator (‘mini-HDV cDNA’ lane). Lane 'M’ contains the Gelpilot Midrange DNA ladder (Qiagen).

when the RT was performed with a genome (G)-specific primer (Figure 5.4C), and migrated at the expected size as compared to the product of PCR off the miniHDV plasmid ('miniHDV cDNA' lane), but a corresponding band was not observed following RT with an antigenome (AG)-specific primer. This finding suggested that miniHDV RNA G to AG synthesis did not occur, and that the band observed following RT with a G-specific primer resulted from amplification of the miniHDV RNA introduced into the cells during transfection. However, successful HDV replication in the human host requires the presence of HDAg-S (Kuo *et al*., 1989). To test whether miniHDV replication in human cells could be stimulated by HDAg-S, the cells were co-transfected with genomic miniHDV RNA and a plasmid encoding HDAg-S. This time, bands corresponding to both genomic and antigenomic miniHDV RNA were observed. However, when cells were transfected with the HDAg-S plasmid alone, no product was observed following RT with miniHDV-specific primers. The presence of the antigenomic miniHDV molecule in HeLa cells suggests that this minimal HDV RNA molecule can still replicate in the human host, as long as HDAg-S is provided *in trans*. However, from these results it cannot be ascertained whether AG to G RNA synthesis is also occurring; therefore it is not clear whether miniHDV is replicating by a rolling circle mechanism.

The band corresponding to the antigenomic miniHDV was extracted from the gel, cloned, and sequenced. Sequencing results from six different clones identified the band as miniHDV (Figure 5.5A), confirming the specific amplification of this RNA from human cells. An A to G point mutation and a single nucleotide deletion were detected in clones C and F, respectively. These mutations were likely introduced by the *Taq* DNA polymerase during PCR. Although the cDNA was amplified using a high fidelity enzyme mixture

A)

```
mini  AAATCTCTCT AGATTCCGAT AGAGAATCGA GAGAAAAGTG GCTCTCCCTT AGCCATCCGA
A     AAATCTCTCT AGATTCCGAT AGAGAATCGA GAGAAAAGTG GCTCTCCCTT AGCCATCCGA
B     AAATCTCTCT AGATTCCGAT AGAGAATCGA GAGAAAAGTG GCTCTCCCTT AGCCATCCGA
C     AAATCTCTCT AGATTCCGAT AGAGAATCGA GAGAAAAGTG GCTCTCCCTT AGCCATCCGA
D     AAATCTCTCT AGATTCCGAT AGAGAATCGA GAGAAAAGTG GCTCTCCCTT AGCCATCCGA
E     AAATCTCTCT AGATTCCGAT AGAGAATCGA GAGAAAAGTG GCTCTCCCTT AGCCATCCGA
F     AAAT-TCTCT AGANNCNNNN NGANNNTCNN NNNAAAANTG GCTCTCCCTT AGCCATCCGA

mini  GTGGACCTGC GTCCTCCTTC GGATGCCCAG GTCGGACCGC GAGGAGGTGG AGATGCCATG
A     GTGGACCTGC GTCCTCCTTC GGATGCCCAG GTCGGACCGC GAGGAGGTGG AGATGCCATG
B     GTGGACCTGC GTCCTCCTTC GGATGCCCAG GTCGGACCGC GAGGAGGTGG AGATGCCATG
C     GTGGACCTGC GTCCTCCTTC GGATGCCCAG GTCGGACCGC GAGGAGGTGG AGATGCCATG
D     GTGGACCTGC GTCCTCCTTC GGATGCCCAG GTCGGACCGC GAGGAGGTGG AGATGCCATG
E     GTGGACCTGC GTCCTCCTTC GGATGCCCAG GTCGGACCGC GAGGAGGTGG AGATGCCATG
F     GTGGACCTGN GNCCTCCTTC GGATGCCCAG GTCGGACCGN GANNAGGTGG AGATGCCATG

mini  CCGACCCGAA GAGGAAAGAA GGACGCGACT CGGCTAGAGG CGGCAGTCCT CAGTACTCTT
A     CCGACCCGAA GAGGAAAGAA GGACGCGACT CGGCTAGAGG CGGCAGTCCT CAGTACTCTT
B     CCGACCCGAA GAGGAAAGAA GGACGCGACT CGGCTAGAGG CGGCAGTCCT CAGTACTCTT
C     CCGGCCCGAA GAGGAAAGAA GGACGCGACT CGGCTAGAGG CGGCAGTCCT CAGTACTCTT
D     CCGACCCGAA GAGGAAAGAA GGACGCGACT CGGCTAGAGG CGGCAGTCCT CAGTACTCTT
E     CCGACCCGAA GAGGAAAGAA GGACGCGACT CGGCTAGAGG CGGCAGTCCT CAGTACTCTT
F     CCGACCCGAA GAGGAAANAA GGACGCGNCT CGGNTAGAGN CGGNNNNCCT CAGTACTCTT

mini  ACTCTTTTCT GTAAAGAGGA GACTGCTGGA CTCGCCGCCC GAGCCCGAGC GCGTTCCATC
A     ACTCTTTTCT GTAAAGAGGA GACTGCTGGA CTCGCCGCCC GAGCCCGAGC GCGTTCCATC
B     ACTCTTTTCT GTAAAGAGGA GACTGCTGGA CTCGCCGCCC GAGCCCGAGC GCGTTCCATC
C     ACTCTTTTCT GTAAAGAGGA GACTGCTGGA CTCGCCGCCC GAGCCCGAGC GCGTTCCATC
D     ACTCTTTTCT GTAAAGAGGA GACTGCTGGA CTCGCCGCCC GAGCCCGAGC GCGTTCCATC
E     ACTCTTTTCT GTAAAGAGGA GACTGCTGGA CTCGCCGCCC GAGCCCGAGC GCGTTCCATC
F     ACTCTTTTCT GTAAAGANGA NACTGCTGGA CTCNCCGCCN GAGCCCGAGC GCGTTCCATC

mini  CTTTCTTACC TGATGGCCGG CATGGTCCCA GCCTCCTCGC TGGCGCCGGC TGGGCAACAT
A     CTTTCTTACC TGATGGCCGG CATGGTCCCA GCCTCCTCGC TGGCGCCGGC TGGGCAACAT
B     CTTTCTTACC TGATGGCCGG CATGGTCCCA GCCTCCTCGC TGGCGCCGGC TGGGCAACAT
C     CTTTCTTACC TGATGGCCGG CATGGTCCCA GCCTCCTCGC TGGCGCCGGC TGGGCAACAT
D     CTTTCTTACC TGATGGCCGG CATGGTCCCA GCCTCCTCGC TGGCGCCGGC TGGGCAACAT
E     CTTTCTTACC TGATGGCCGG CATGGTCCCA GCCTCCTCGC TGGCGCCGGC TGGGCAACAT
F     CTTTCTTACC TGATGGCCGG NATGGCCCCA GCCTCCTCGC TGGCGCCGGC TGGNCAACAT

mini  TCCGAGGGGA CCGTCCCCTC GGTAATGGCG AATGGGACC
A     TCCGAGGGGA CCGTCCCCTC GGTAATGGCG AATGGGACC
B     TCCGAGGGGA CCGTCCCCTC GGTAATGGCG AATGGGACC
C     TCCGAGGGGA CCGTCCCCTC GGTAATGGCG AATGGGACC
D     TCCGAGGGGA CCGTCCCCTC GGTAATGGCG AATGGGACC
E     TCCGAGGGGA CCGTCCCCTC GGTAATGGCG AATGGGANN
F     TCCGAGGGGA CCGTCCCCTC GGTAATGGCG AATGGGACC
```

B)

C)

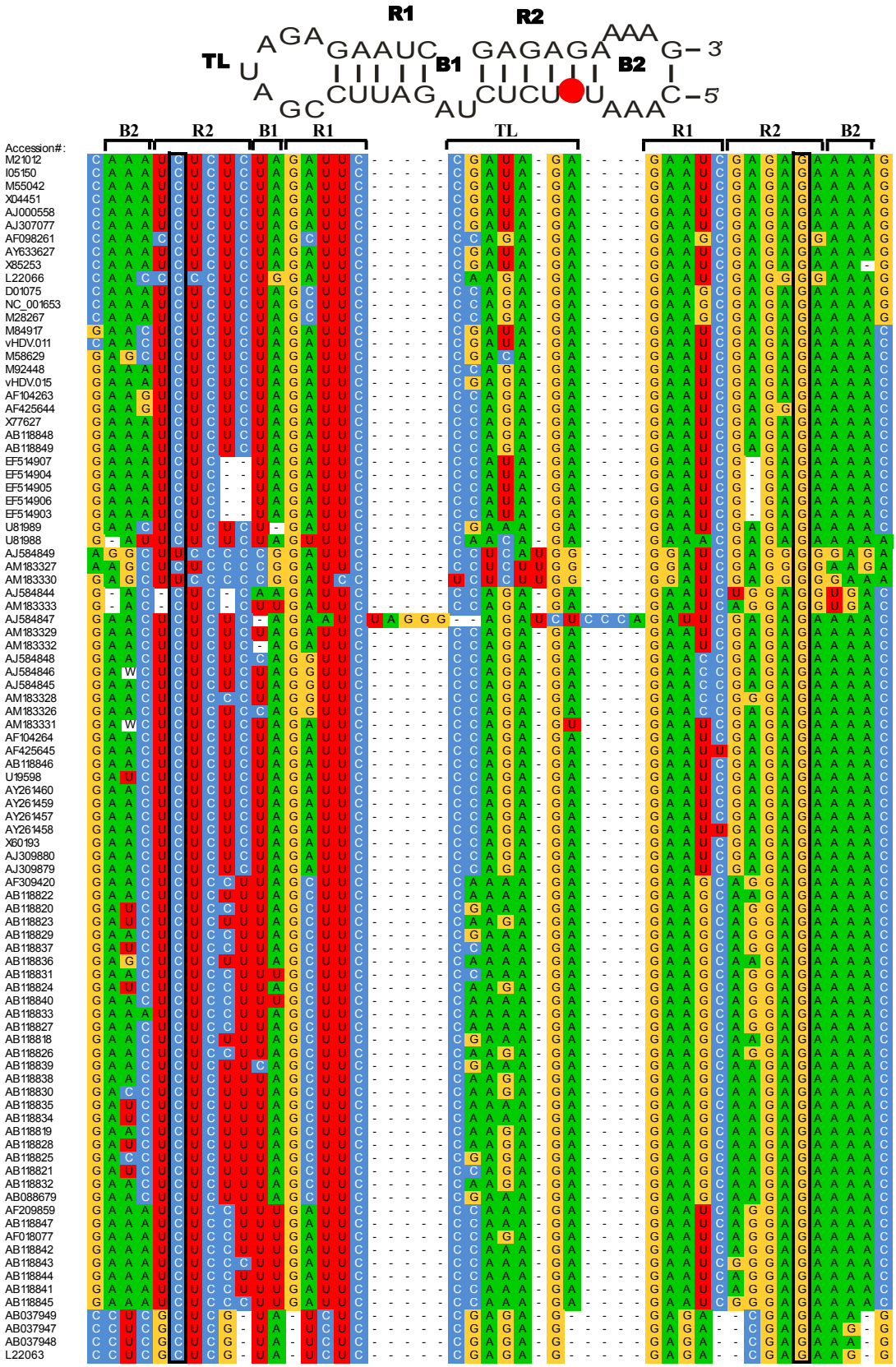

Figure 5.5: Analysis of the sequence of six clones of miniHDV cDNA amplified from miniHDV-replicating HeLa cells, and sequence comparison to known HDV variants.

(A) ClustalW (Thompson *et al*., 1994) alignment of miniHDV and the sequenced clones. Mutations are shown in red. Secondary structures of the antigenomic *delta* ribozyme (B) and of the left terminal stem-loop domain of genomic polarity (C) show the positions of the mutated residues in red. Multiple alignments of the corresponding regions of 92 HDV sequences are shown; boxed positions indicate to the base pairs affected by the observed mutations. The first sequence in the alignment corresponds to the HDV strain used in the current study.

(consisting of *Taq* DNA polymerase and *Pyrococcus species* GB-D polymerase, which possesses a 3' to 5' proofreading activity) to decrease the rate of mutation, errors are still possible (Flaman *et al*., 1994; Lundberg *et al*., 1991). It is improbable that these mutations represent viral adaptations. The A to G point mutation in clone C results in a U to C mutation in the P1 stem of the antigenomic *delta* ribozyme (Figure 5.5B). Multiple alignment of all available HDV sequences (obtained from the Subviral RNA Database) was performed using the ClustalW program (Thompson *et al*., 1994), and manually corrected. The alignment revealed that this mutation is located at a position that is 100 % conserved across the HDV strains (Figure 5.5B). Even though the activity of the *delta* ribozyme is almost entirely determined by its secondary and tertiary structure, with only a few functionally essential nucleotides (Webb and Lupták, 2011), the primary sequence of the naturally occurring HDV ribozymes is highly conserved (Been and Wickham, 1997; Figure 5.5B). This is likely due to the additional selective pressure on the HDV genome to maintain the rod-like conformation.

The second identified mutation, the deletion in clone F, is located in the left terminal stem-loop domain of HDV (Figure 5.5C, highlighted C residue). A ClustalW multiple sequence alignment of 92 HDV sequences was performed and corrected manually to ensure proper alignment of the structural motifs (i.e. stems, loops, bulges). The deleted nucleotide corresponds to a highly conserved C (substituted by U in a few sequences), which participates in the formation of a conserved base pair with a G in the descending strand of the RNA hairpin (Greco-Stewart *et al*., 2007; Figure 5.5C). This region has been shown to interact with RNAP II (Greco-Stewart *et al*., 2007), and may comprise an RNA promoter (Filipovska and Konarska, 2000), hence it is unlikely to tolerate mutations that disrupt its secondary structure.

The finding that the viroid-like miniHDV RNA can successfully replicate in human cells, provided that HDAg-S is present, suggests that the HDV sequence that was removed to produce the truncated molecule does not contain motifs required for replication, and that the main function of the region complementary to the HDAg coding sequence is to maintain the rod-like conformation. Taken together, the results presented in this chapter support the hypothesis that HDV and viroids are evolutionarily related.

Chapter 6: Discussion

6.1 Summary of major findings

HDV is unique among human pathogens, in that it relies almost solely on host factors to propagate. This study was aimed at identifying potential HDV interacting proteins to broaden our understanding of HDV biology. Five HDV-interacting partners were identified: eEF1A1, $p54^{nrb}$, hnRNP-L, GAPDH and ASF/SF2, and their involvement in the replication of HDV was explored. ASF/SF2 was found to play a role in the accumulation of HDV RNA in cultured cells, but was apparently not required for *in vitro* transcription from a fragment of HDV RNA. A putative ASF/SF2 binding site was identified downstream of the transcription initiation site. This study also addressed the potential evolutionary relationship between HDV and viroids. PSTVd and a viroid-like mutant of HDV were apparently able to replicate in human cells as long as the small *delta* antigen was supplied in *trans*, suggesting that HDV, miniHDV and PSTVd use common cellular machineries to replicate; these findings support the hypothesis that HDV evolved from a viroid-like element through the capture of a cellular transcript.

6.2 Identification of HDV-interacting proteins

HDV has a very limited coding capacity, and thus must rely on host factors for its replication. In addition, because the HDV RNA genome interacts with several host proteins, it is likely that these interactions affect normal host functions. Despite their functional importance in both viral replication and pathogenicity, only a few cellular proteins have been reported to interact with HDV RNA. Accordingly, this study was undertaken to identify additional host factors that interact specifically with HDV RNA, and that might be involved

in HDV transcription and/or replication. I used an HDV RNA fragment corresponding to the right stem–loop domain of the genomic polarity, which has previously been shown to comprise an RNA promoter for RNAP II, with a role in viral replication and/or transcription of the HDAg mRNA (Abrahem and Pelchat, 2008; Beard *et al*., 1996; Greco-Stewart *et al*., 2007; Gudima *et al*., 2000). Using a UV crosslinking approach and RNA affinity chromatography, we have identified several HDV RNA-interacting partners. As reported previously (Greco-Stewart *et al*., 2006), UV crosslinking of HeLa NE to R199G did not yield complexes corresponding to the molecular weights of the individual proteins. It is likely that several of these proteins might have crosslinked to R199G simultaneously, which would account for the detection of a single high molecular weight complex.

Because a number of the identified proteins are known to be involved in splicing events, I screened additional purified recombinant splicing factors using an electrophoretic mobility shift assay, which revealed ASF/SF2 as another HDV RNA-interacting partner. The interactions between HDV RNA and these proteins were further validated by co-immunoprecipitations both *in vitro* and in HeLa cells replicating HDV RNA. In addition to PSF and RNAP II (Abrahem and Pelchat, 2008; Greco-Stewart *et al*., 2006, 2007), the results presented here demonstrate the interactions of eEF1A1, $p54^{nrb}$, hnRNP-L, GAPDH and ASF/SF2 with HDV RNA. Interestingly, different proteins were identified using these various experimental approaches, suggesting that those proteins might represent only a small subset of the host proteins interacting with HDV RNA. However, I might have been too cautious in the analysis of the mass spectrometry results, as single peptides for both hnRNP-L and ASF/SF2 were also detected in some of the UV crosslinked complexes.

6.2.1 Potential roles of eEF1A1, p54^{nrb}, hnRNP-L, GAPDH and ASF/SF2 in HDV's life cycle

The proteins identified in this study are frequently linked to viral replication and/or transcription. Their potential involvement in HDV replication was examined in an *in vitro* antibody inhibition assay, and the results suggested that both eEF1A1 and GAPDH are important for HDV RNA synthesis. GAPDH, a key metabolic enzyme, is involved in many additional cellular activities, including apoptosis, endocytosis, nuclear tRNA transport, DNA replication and repair, mRNA stabilization (Sirover, 1999; Tristan *et al*., 2011). Moreover, GAPDH has previously been identified as a key component of a transcription co-activation complex (Zheng *et al*., 2003); it was shown to greatly stimulate transcription by RNAP II in *Xenopus laevis* oocytes (Morgenegg *et al*., 1986); and has been reported to associate with RNAP II in *Schizosaccharomyces pombe* through a direct interaction with the Rpb7 subunit of the polymerase (Mitsuzawa *et al*., 2005). GAPDH was also reported to influence viral replication by binding to AU-rich sequences found in many RNA viruses, including the hepatitis A virus (Dollenmeier and Weitz, 2003; Schultz *et al*., 1996), hepatitis C virus (Petrik *et al*., 1999; Randall *et al*., 2007), human parainfluenza virus-3 (De *et al*., 1996), transmissible gastroenteritis coronavirus (Galán *et al*., 2007), and Japanese encephalitis virus (Yang *et al*., 2009). More recently, the plant GAPDH was shown to be a constituent of the tomato bushy stunt virus (TBSV) replicase complex, and to be involved in viral replication through direct stimulation of RNA synthesis, a function that was dependent on the direct association of GAPDH with viral RNA (Wang and Nagy, 2008; Huang and Nagy, 2011).

The translation elongation factor eEF1A is a highly abundant cellular protein involved in delivering aminoacyl-tRNA to the elongating ribosome in a GTP-dependent

manner. Additional functions of eEF1A include quality control of newly produced proteins, ubiquitin-dependent protein degradation, and organization of the actin cytoskeleton (Chuang *et al*., 2005; Gross and Kinzy, 2005). eEF1A also plays a key role in the replication of several RNA viruses. It has been reported to associate with the RNA-dependent RNA polymerase activities of numerous RNA viruses, including poliovirus (Harris *et al*., 1994), vesicular stomatitis virus (Das *et al*., 1998), turnip yellow mosaic virus (Joshi *et al*., 1986), West Nile virus (Blackwell and Brinton, 1997), turnip mosaic virus (Thivierge *et al*., 2008), tobacco mosaic virus (Yamaji *et al*., 2010), and TBSV (Li *et al*., 2009, 2010). Interestingly, eEF1A and GAPDH were identified as host constituents of the same TBSV replicase complex (Li *et al*., 2009; Wang and Nagy, 2008). eEF1A was shown to facilitate the assembly of the TBSV replicase complex and the recruitment of template RNA to the complex, and to enhance RNA synthesis by promoting transcription initiation. It is possible that eEF1A and GAPDH are also associated with the RNA-dependent RNA replication of HDV by enhancing RNA synthesis by the host polymerase, potentially acting as transcription co-activators. Investigating the effects of overexpression or downregulation of these proteins on HDV accumulation in cells would shed some light on their significance in HDV replication. It would also be worthwhile to investigate cellular localization of these proteins in HDV-replicating cells, particularly of eEF1A, since it is a primarily cytoplasmic protein, and HDV replication takes place exclusively in the nucleus.

Neither $p54^{nrb}$ nor its cellular homologue PSF appeared to be necessary for HDV RNA accumulation in the antibody inhibition experiments. However, when the transcription reaction was performed in a nuclear extract immunodepleted of PSF, a considerable reduction in HDV-specific product accumulation was observed. PSF has previously been

reported to interact specifically and directly with HDV RNA domains also bound by RNAP II (Greco-Stewart *et al*., 2006, 2007). *In vivo*, PSF forms heterodimers with $p54^{nrb}$ (Straub *et al*., 1998; Zhang *et al*., 1993); together, they participate in pre-mRNA splicing (Patton *et al*., 1993; Peng *et al*., 2002; Shav-Tal and Zipori, 2002), transcription regulation (Dong *et al*., 2005; Mathur *et al*., 2001; Urban *et al*., 2000), nuclear retention of hyperedited RNAs (Zhang and Carmichael, 2001), DNA recombination (Akhmedov and Lopez, 2000), and repair of DNA double-strand breaks (Bladen *et al*., 2005). In addition, the PSF/$p54^{nrb}$ heterodimer was shown to interact with the CTD of RNAP II, and to promote the binding of RNA to the CTD (Emili *et al*., 2002). PSF was also reported to interact with RNAP II and HDV RNA simultaneously (Greco-Stewart, 2009); it has been suggested that PSF is involved in HDV replication by serving as a physical link between the RNA template and the polymerase during template recognition (Greco-Stewart, 2009; Greco-Stewart *et al*., 2006).

HnRNP-L belongs to a family of abundant, predominantly nuclear proteins involved in many aspects of mRNA processing, such as pre-mRNA splicing, mRNA transport and translation regulation (Han *et al*., 2010). Although pre-incubation of HeLa NE with an anti-hnRNP-L antibody did not have an effect on HDV RNA accumulation in the *in vitro* transcription assay, it is possible that antibody binding did not interfere with hnRNP-L's activity. Hence, the involvement of hnRNP-L in HDV replication cannot be definitely excluded. Members of the hnRNP protein family are frequently linked to viral replication (reviewed in Lai, 1998; Shi and Lai, 2005). While hnRNP-L has never been shown to be directly involved in viral replication, it has been reported to bind several viral RNAs (Guang *et al.*, 2005; Gutiérrez-Escolano *et al*., 2000; Hahm *et al*., 1998; Hwang *et al*., 2009; Liu and Mertz, 1995), and to function in nuclear export and translational regulation of these RNAs. It

remains to be determined if hnRNP-L is involved in HDV RNA nucleocytoplasmic transport and/or HDAg mRNA translation.

ASF/SF2 is a member of a large family of proteins known as the SR (serine arginine-rich) proteins, which play essential roles in constitutive splicing (Zahler *et al*., 1992), and also regulate alternative splicing in a concentration-dependent manner (Zahler *et al*., 1993). In addition to splicing, ASF/SF2 plays important roles in several mRNA-processing pathways, such as mRNA export (Cáceres *et al*., 1998), mRNA stability (Lemaire *et al*., 2002) and mRNA translation (Sanford *et al*., 2004). During alternative splicing, ASF/SF2 promotes exon inclusion by recognizing and binding to exonic splicing enhancers (ESEs); this binding is suggested to be modulated by the C-terminal domain (CTD) of the largest subunit of RNAP II (Cramer *et al*., 1999; McCracken *et al*., 1997). Although ASF/SF2 associates with the hyperphosphorylated (elongating) form of CTD (Kim *et al*., 1997; Yuryev *et al*., 1996), it has never been shown to participate directly in transcription; rather, the CTD-ASF/SF2 interaction is involved in coupled transcription-splicing regulation, in which the CTD facilitates the assembly of early spliceosome complexes (Millhouse and Manley, 2005). Moreover, hyperphosphorylated RNAP II (RNAP IIO) was shown to localize to discrete subnuclear speckle domains, often referred to as SC35 foci; the splicing factor SC35 is a marker for these domains, which are sites of high concentrations of proteins involved in mRNA processing. RNAP IIO remained localized to these domains even in the absence of active transcription (Bergman *et al*., 1995). A tight association between splicing factors, including SR proteins, and the CTD of RNAP IIO was demonstrated (Kim *et al*., 1997). This association was maintained in the absence of pre-mRNA, and the hyperphosphorylated polymerase did not have to be transcriptionally engaged to associate with splicing factors in

the speckle domains (Kim *et al*., 1997). Interestingly, HDV RNA and HDAg-S were found to co-localize to the same speckles in cells replicating HDV (Bichko and Taylor, 1996). Thus, the role of ASF/SF2 in HDV replication might be to target the replication complexes formed on the HDV RNA template to the subnuclear speckle domains, which are storage sites of many mRNA processing factors, to facilitate efficient transcription and/or processing of HDV RNA. This hypothesis is supported by the findings of the current study. ASF/SF2 was found to be dispensable for HDV transcription, as addition of antibody did not have an effect on product formation in the *in vitro* transcription experiment. The identification of the ASF/SF2 binding site away from the proposed RNAP II binding site is also consistent with the idea that ASF/SF2 is likely not involved in promoter recognition and/or transcription initiation. However, downregulation of ASF/SF2 in cells replicating HDV resulted in a decrease in HDV RNA accumulation, suggesting a role for ASF/SF2 in the accumulation of HDV *in vivo*.

ASF/SF2 could also be affecting HDV RNA accumulation by influencing the posttranslational modification of HDAg-S by SUMO1. ASF/SF2 was recently shown to be a regulator of the sumoylation pathway (Pelish *et al*., 2010). ASF/SF2 interacted with Ubc9, a SUMO E2 conjugating enzyme, and enhanced sumoylation of specific substrates; its knockdown resulted in inhibition of overall SUMO conjugation. HDAg-S has been shown to interact directly with SUMO1 and Ubc9, and to be sumoylated at multiple lysine residues; this modification enhanced synthesis of genomic HDV RNA as well as HDAg mRNA (Tseng *et al*., 2010). It is possible that ASF/SF2 is involved in the sumoylation of HDAg-S; the observed decrease in HDV RNA accumulation in response to ASF/SF2 knockdown could be

a result of inefficient sumoylation of HDAg-S. Clearly, additional experiments are needed to assess the role of ASF/SF2 in HDV's life cycle.

6.2.2 A role for HDV RNA-interacting partners in HDV pathogenesis

HDV has been shown to accumulate at up to 300,000 copies of genomic RNA per average cell in the livers of infected chimpanzees or woodchucks (Chen *et al*., 1986). The high amount of HDV RNA in infected cells suggests that the interaction of HDV RNA with these factors might interfere with several of their normal cellular functions, thereby eliciting the virus' pathogenic effect. For instance, it is possible that HDV alters ASF/SF2, PSF, $p54^{nrb}$ and/or hnRNP-L-mediated alternative splicing, since deregulated splicing has been associated with many types of cancer (Castiglioni *et al*., 2006; Lee *et al*., 2006; Pospisil *et al*., 2006), and HDV is known to be associated with liver cancer (Fattovich *et al*., 2004; Romeo *et al*., 2009; Su *et al*., 2006). In particular, ASF/SF2 was shown to be upregulated in a number of human tumours, and a two-fold overexpression of ASF/SF2 resulted in altered splicing patterns of a number of genes involved in transformation and apoptosis (Ezpodna *et al*., 2010; Karni *et al*., 2007). ASF/SF2 has also been shown to play a significant role in protecting chromosomal DNA from the damaging effects of R-loops that form between nascent RNA transcripts and template DNA; inactivation of this protein leads to genomic instability (Li and Manley, 2005). PSF represses the expression of numerous oncogenes (Song *et al*., 2004). The interaction of PSF with HDV RNA might reverse this repression and promote metastasis (Song *et al*., 2002, 2004, 2005). eEF1A1 has been shown to bind the non-coding RNA HSR1 and to activate the heat shock transcription factor 1 (HSF1), which

induces the expression of heat shock proteins. Interestingly, Hsp105 was reported to be downregulated in Huh7 cells transiently transfected with a plasmid encoding genomic HDV RNA (Mota *et al*., 2008). It is possible that HDV RNA might compete with HSR1 for eEF1A binding, thereby impeding a heat shock response. GAPDH has been proposed to play an essential role in apoptosis (Barbini *et al*., 2007; Fukuhara *et al*., 2001; Ishitani and Chuang, 1996; Ishitani *et al*., 1998). The potential deregulation of this important process by HDV might also contribute to liver disease. Although these proteins are very abundant, their essential nature suggests that interfering with their ability to perform their cellular activities would have an ill effect on many aspects of cellular functioning.

6.2.3 Binding of ASF/SF2 to HDV RNA

The direct interaction between ASF/SF2 and the R199G fragment of HDV RNA was investigated using a fluorescence binding assay. After testing a number of truncation mutants, the ASF/SF2 binding site was narrowed down to a short purine-rich region (Figure 4.4). Sequence-specific binding of ASF/SF2 to short, purine-rich regions of RNA has been demonstrated, both *in vitro* (Tacke and Manley, 1995; Smith *et al*., 2006) and *in vivo* (Sanford *et al*., 2008, 2009). The identified ASF/SF2 binding site on HDV RNA most highly resembles the ASF/SF2 target sequence identified in the study by Sanford *et al*. (2009); unlike the other studies, which limited their search for ASF/SF2 targets to exonic splicing enhancer sequences, this study focused on the whole transcriptome, and identified ASF/SF2 binding sites in many types of functionally distinct transcripts, including mRNAs, microRNAs, small nucleolar RNAs and non-coding RNAs. A comparison between the consensus ASF/SF2 binding sequence identified by Sanford *et al*. (2009) and that identified

in HDV RNA by the current study is shown in Figure 4.7B. The similarity between these two sequences supports the claim that the identified ASF/SF2 recognition sequence on HDV RNA represents a physiological target of ASF/SF2. Mutational analysis of this sequence coupled with *in vitro* and *in vivo* binding studies will be required to validate its authenticity. Curiously, the R199G RNA fragment contains multiple purine-rich regions that could theoretically serve as ASF/SF2 recognition sites. However, sequence specific recognition of single-stranded RNA by several RRMs has been shown to be strongly reliant on the structural context of the target sequence (reviewed in Maris *et al*., 2005). It has been suggested that the interaction of the protein with the RNA structure induces conformational changes that allow for the sequence-specific RNA-RRM binding to occur (Allain *et al*., 1996; Showalter and Hall, 2004). It is therefore possible that the identified purine-rich sequence on R199G is recognized by ASF/SF2 because it is found in a structurally optimal context.

The fluorescence binding assay used to characterize the ASF/SF2-HDV RNA interaction is a technique frequently used to investigate protein-ligand interactions (Bougie and Bisaillon, 2007; Bougie *et al*., 2004; Elton *et al*., 1999; Flowers *et al*., 2003; Lima *et al*., 2006). It provides an easy method of calculating an apparent K_D for the interaction by adding increasing amounts of RNA to a fixed amount of protein and observing the resulting quenching of the intrinsic tryptophan fluorescence of the protein. ASF/SF2 has a single partially surface-exposed tryptophan residue located in one of its two RRMs (Figure 4.1B). This tryptophan was previously demonstrated to be directly involved in binding to a short purine-rich RNA oligonucleotide (Tintaru *et al*., 2007). Indeed, aromatic residues have been shown to be involved in single stranded nucleic acid binding in a number of proteins, either by polar interactions or by planar stacking interactions of the aromatic side chain with

exposed bases (Brun *et al*., 1975; Elton *et al*., 1999; Gorlach *et al*., 1992; Jessen *et al*., 1991; Predki *et al*., 1995; Oubridge *et al*., 1994; Ueda *et al*., 1991). Hence, it is likely that the tryptophan of ASF/SF2 is also directly involved in binding to R199G RNA, although it is also possible that the RNA is binding somewhere else on the protein and affects its conformation, resulting in quenching of tryptophan fluorescence by other residues.

ASF/SF2 has two RNA recognition motifs (RRMs) in its N-terminus, a canonical motif (RRM1) followed by a degenerate motif (RRM2; Birney *et al*., 1993). Both are involved in sequence-specific binding to RNA (Tacke and Manley, 1995). Although each motif can bind RNA by itself, optimal interaction of ASF/SF2 with RNA requires both RRM1 and RRM2 (Cáceres and Krainer, 1993; Zuo and Manley, 1993), and the combined action of both RRMs was shown to ensure substrate specificity of ASF/SF2 (Tacke and Manley, 1995). The interaction between HDV and ASF/SF2 likely involves both RRMs; mutational analysis is required to determine which regions and/or residues of ASF/SF2 are involved in binding to HDV RNA.

6.2.4 Model and Perspectives

I have identified five proteins that interact specifically with HDV RNA: eEF1A1, $p54^{nrb}$, hnRNP-L, ASF/SF2 and GAPDH. Similar to what is observed for other RNA viruses, normal cellular components associated with mRNA-processing pathways appear to be exploited by HDV (Lai, 1998). Although their precise functions in HDV biology are not fully understood, their interactions with the HDV RNA genome are consistent with their known biological properties. Based on the findings of this study, these proteins serve potential

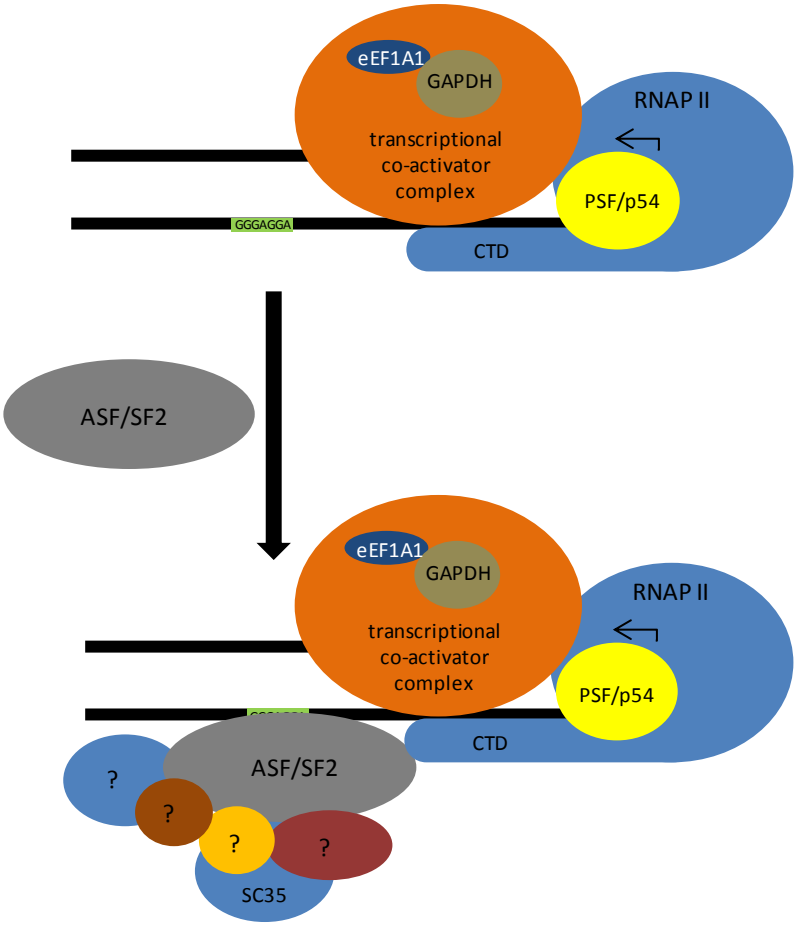
eEF1A1
GAPDH
transcriptional
co-activator
complex
RNAP II
PSF/p54
GGGAGGA
CTD
ASF/SF2
eEF1A1
GAPDH
transcriptional
co-activator
complex
RNAP II
PSF/p54
CTD
?
ASF/SF2
?
?
?
SC35

Figure 6.1: Hypothetical model of the involvement of host proteins in HDV replication.

The PSF/p54^{nrb} complex potentially interacts with the HDV promoter and the CTD of RNAP II during assembly of the transcription pre-initiation complex. GAPDH and eEF1A1 might be constituents of a transcriptional co-activator complex and function to stimulate RNAP II-directed transcription. Possible role of ASF/SF2 in HDV replication is to enhance RNAP II elongation and/or RNA processing through targeting of the replication complex to SC-35 speckles.

functions at different steps of HDV transcription. In the proposed **hypothetical** model (Figure 6.1), the $p54^{nrb}$/PSF heterodimer likely functions in recruitment of the RNA template to the RNAP II pre-initiation complex, as previously proposed (Greco-Stewart *et al*., 2006; Greco-Stewart, 2008). The potential roles of GAPDH and eEF1A1 are to stimulate the RNAP II-directed transcription of HDV RNA, possibly by acting as constituents of a transcriptional co-activator complex. The ASF/SF2-HDV RNA interaction, although apparently not necessary for *in vitro* HDV transcription, may enhance HDV replication *in vivo* by stimulating RNAP II elongation and/or RNA processing through targeting of the replication complex to SC-35 speckles.

Further investigation of the interactions of these proteins with HDV RNA is crucial to validate the proposed model. Functional studies of these interactions and their consequences on the various cellular processes mediated by these proteins might lead to a better comprehension of both HDV replication and pathogenicity.

6.3 Evolutionary relationship between HDV and viroids

Many features of HDV set it apart from other animal viruses, including its genome structure and mode of replication. Although HDV is a satellite virus of HBV, it replicates independently of the helper virus, relying solely on HDAg and host proteins. Many have speculated on the origin of HDV, and it is generally accepted that HDV likely shares its origins with plant viroids (Diener, 2001; Pelchat and Taylor, 2010; Taylor, 1999, 2009). While HDV shares common characteristics with both *Pospiviroidae* and *Avsunviroidae* families of viroids (see Figure 1.7 and Table 1.3), the present study used PSTVd, the type

species of the pospiviroids, to explore the evolutionary relationship between the two pathogens.

The circular RNA genomes of both PSTVd and HDV fold into similar unbranched rod-like structures (Figure 1.7). Although the genome of HDV is about 5 times larger than that of PSTVd, this difference can be attributed to the HDAg coding region. While HDV relies on its protein product to complete its life cycle, PSTVd and other viroids are entirely non-coding. Coding capacity appears to be the main difference between HDV and viroids; HDV has been suggested to have evolved from a viroid-like RNA following capture of a cellular transcript, which allowed it to replicate in an animal host, although it is also possible that viroids are remnants of coding genomes. Much debate still exists as to the cellular source of the genetic material (Long *et al*., 1997; Veretnik and Gribskov, 1998), potential human homologues of HDAg include the *delta*-interacting protein A (DIPA) (Brazas and Ganem, 1996), and the HMG (High Mobility Group) box of the DNA-binding protein SRY (Veretnik and Gribskov, 1998).

To further explore the idea that HDV and viroids are evolutionarily related, the current study investigated the possibility that these two pathogens interact with common host factors during their replication cycle. Both PSTVd and HDV are proposed to replicate by similar rolling-circle mechanisms, and are reported to be transcribed by RNAP II in the nucleus of the host cell (Flores, 2011; Taylor, 2009). Both RNAs have also been shown to interact with RNAP III-associated factors, eEF1A and GAPDH in their respective hosts (this study; Bojić, 2009; Eiras *et al*., 2011; Greco-Stewart *et al*., 2009), and PSTVd(+) RNA has been shown to co-immunoprecipitate with the human RNAP II from HeLa nuclear extract (Bojić, 2009). The current study showed that PSTVd RNA of both polarities is also able to

interact directly with the human ASF/SF2 *in vitro*, suggesting that PSTVd also interacts with the plant orthologues of ASF/SF2. It is possible that these interactions play analogous roles in the life cycles of these species.

Based on the findings that HDV and PSTVd interact with common host factors, I investigated the possibility that PSTVd has the ability to use the human host for its replication. Following transfection of HepG2 cells with a trimer of PSTVd(+) RNA, RT-PCR analysis was used to detect the (-) polarity. Initially, no PSTVd(-) RNA was detected; however, when HepG2 cells were transfected with the PSTVd(+) trimer and a plasmid expressing HDAg-S, PSTVd(-) RNA was readily detected, suggesting that PSTVd(-) RNA was successfully synthesized from the PSTVd(+) RNA template in human cells. This result strengthens the hypothesis that HDAg is an evolutionary adaptation that allowed HDV to replicate in a human host. During HDV replication *in vivo*, one of HDAg-S' essential roles is to bind RNAP II directly and inhibit RNAP II association with the A subunit of the negative elongation factor (NELF-A; Yamaguchi *et al*., 2001), thereby stimulating RNAP II elongation. However, no NELF-A homologue has been found in plants; hence viroids do not require an HDAg-like protein to replicate in a plant host, but need the HDAg-S activity to successfully use a the human RNAP II.

To further validate the hypothesis that viroids and HDV are evolutionarily related, I constructed a truncation mutant of HDV, by removing the entire coding sequence including the polyadenylation signal, as well as the corresponding sequence it hybridizes to during formation of the rod-like molecule (miniHDV; refer to Figure 5.3). This truncation created a molecule $1/5^{th}$ the size of the original HDV genome, and approximately the size of the PSTVd genome. HeLa cells were transfected with an RNA corresponding to 1.4X the size of

miniHDV of genomic polarity. As expected, RT-PCR analysis did not detect antigenomic miniHDV RNA in cells transfected with RNA alone, since HDAg-S is required for HDV replication *in vivo*. However, following co-transfection with miniHDV RNA and a plasmid encoding HDAg-S, antigenomic miniHDV RNA was detected, indicating successful synthesis of antigenomic miniHDV RNA from the genomic RNA template in HeLa cells. The observation that the viroid-like HDV molecule is replication-competent is consistent with reports that the putative RNA promoter elements/RNAP binding sites are located in the two stem-loop domains of HDV's rod-like genome (Abrahem and Pelchat, 2008; Beard *et al*., 1996; Filipovska and Konarska, 2000; Greco-Stewart *et al*., 2007, 2009). At the same time, this finding suggests that the removed region does not contain motifs required for replication, and that the main function of the region complementary to the HDAg coding sequence is to maintain the rod-like conformation. The miniHDV RNA molecule may represent a minimal HDV sequence needed to achieve replication. However, since the efficiency of miniHDV replication compared to that of wild-type HDV was not tested in this study, it is possible that the removed region contained motifs that modulated HDV replication. For instance, the ASF/SF2 binding site identified in the current study is absent from miniHDV; since ASF/SF2 seems to stimulate HDV replication in cell culture, the inability of miniHDV to interact with ASF/SF2 may decrease its replication efficiency. Indeed, attempts at detecting the replicating miniHDV or PSTVd RNAs in cells by Northern blot analysis were unsuccessful (data not shown), suggesting that their replication may be occurring below the assay's detection limit. All in all, this minimal HDV molecule is a promising model system to study HDV replication in human cells; at $1/5^{th}$ the size of HDV, miniHDV will be easier to manipulate to study the structure-function relationships.

The findings that a viroid and a minimal HDV molecule can still replicate in human cells, as long as the HDAg-S function is supplied, provide support to the notion that HDV and viroids are evolutionarily related. Further evidence of a common evolutionary origin between HDV and viroids comes from observations that HDV and miniHDV RNAs can replicate in a tomato plant (Bojić, 2009). The two may share a common ancestor, or one might have been a precursor of the other. However, based on current knowledge it is uncertain which scenario is more likely: that HDV evolved from a viroid-like RNA by acquiring a protein, or that a viroid evolved from an HDV-like molecule following loss of the protein function as it became dispensable in a plant host.

6.4 Conclusions

Hepatitis *delta* virus relies on host factors to complete its life cycle. The present study focused on identifying HDV RNA-interacting proteins in the human host. Specific interactions between HDV and RNA-processing factors have been demonstrated; these novel interactions likely play important roles in the biology of this pathogen. The study of the host's involvement in HDV's life cycle will contribute to the understanding of the unique replication and propagation strategies employed by this pathogen, and shed some light on HDV pathogenesis.

HDV belongs to a distinctive group of subviral RNA pathogens that also includes plant viroids and satellite RNAs. Although HDV and viroids have different natural hosts, these pathogens share structural and functional similarities that suggest a common evolutionary origin. The results of this study suggest that viroids and HDV use analogous

strategies to manipulate their hosts' cellular factors into replicating their RNA genomes. Both HDV and PSTVd were found to interact with common mRNA-processing factors, and PSTVd and a viroid-like HDV mutant lacking the HDAg coding region (miniHDV) were able to replicate in human cells. These findings support the hypothesis that HDV and viroids are evolutionarily related. Integration of the knowledge attained from HDV and viroid studies will expand our understanding of the mechanisms used by these subviral RNA agents during the course of infection.

References

Abrahem, A., Pelchat, M. 2008. Formation of an RNA polymerase II preinitiation complex on an RNA promoter derived from the hepatitis *delta* virus RNA genome. Nucleic Acids Res. 36:5201-5211

Aggarwal, B.B. 2004. Nuclear factor-*kappa*B: the enemy within. Cancer Cell 6:203-208

Akhmedov, A.T., Lopez, B.S. 2000. Human 100-kDa homologous DNA pairing protein is the splicing factor PSF and promotes DNA strand invasion. Nucleic Acids Res. 28:3022-3030

Alconada, A., Bauer, U., Hoflack, B. 1996. A tyrosine-based motif and a casein kinase II phosphorylation site regulate the intracellular trafficking of the varicella-zoster virus glycoprotein I, a protein localized in the trans-Golgi network. EMBO J. 15:6096-6110

Allain, F.H., Gubser, C.C., Howe, P.W., Nagai, K., Neuhaus, D., Varani, G. 1996. Specificity of ribonucleoprotein interaction determined by RNA folding during complex formulation. Nature 380:646-650

Alves, C., Freitas, N., Cunha, C. 2008. Characterization of the nuclear localization signal of the hepatitis *delta* virus antigen. Virology 370:12-21

Barbini, L., Rodriguez, J., Dominguez, F., Vega, F. 2007. Glyceraldehyde-3-phosphate dehydrogenase exerts different biologic activities in apoptotic and proliferating hepatocytes according to its subcellular localization. Mol. Cell. Biochem. 300:19-28

Baxi, M.D., Vishwanatha, J.K. 1999. Uracil DNA glycosylase/glyceraldehyde-3-phosphate dehydrogenase is an $A_{p4}A$ binding protein. Biochemistry 34:9700-9707

Beard, M.R., Macnaughton, T.B., Gowans ,E.J. 1996. Identification and characterization of a hepatitis *delta* virus RNA transcriptional promoter. J. Virol. 70:4986-4995

Been, M.D., Wickham, G.S. 1997. Self-cleaving ribozymes of the hepatitis *delta* virus RNA. Eur. J. Biochem. 247:741-753

Bell, P., Brazas, R., Ganem, D., Maul, G.G. 2000. Hepatitis *delta* virus replication generates complexes of large hepatitis *delta* antigen and antigenomic RNA that affiliate with and alter nuclear domain 10. J. Virol. 74:5329-5336

Benzaghou, I., Bougie, I., Picard-Jean, F., Bisaillon, M. 2006. Energetics of RNA binding by the West Nile virus RNA triphosphatase. FEBS Lett. 580:867-877

Bergman, D.B., Du, L., van der Zee, S., Warren, S.L. 1995. Transcription-dependent redistribution of the large subunit of RNA polymerase II to discrete nuclear domains. J. Cell Biol. 129:287-298

Bezy, O., Elabd, C., Cochet, O., Petersen, R.K., Kristiansen, K., Dani, C., Ailhaud, G., Amri, E.Z. 2005. *Delta*-interacting protein A, a new inhibitory partner of CCAAT/enhancer-binding protein *beta*, implicated in adipocyte differentiation. J. Biol. Chem. 280:11432-11438

Bichko, V.V., Taylor, J.M. 1996. Redistribution of the *delta* antigens in cells replicating the genome of hepatitis *delta* virus. J. Virol. 70:8064-8070

Bichko, V.V., Lemon, S.M., Wang, J.G., Hwang, S., Lai, M.M., Taylor, J.M. 1996. Epitopes exposed on hepatitis *delta* virus ribonucleoproteins. J. Virol. 70:5807-5811

Bichko, V., Barik, S., Taylor, J. 1997. Phosphorylation of the hepatitis *delta* virus antigens. J. Virol. 71:512-518

Birney, E., Kumar, S., Krainer, A.R. 1993. Analysis of the RNA-recognition motif and RS and RGG domains: conservation in metazoan pre-mRNA splicing factors. Nucleic Acids Res. 21:5803-5816

Blackwell, J.L., Brinton, M.A. 1997. Translation elongation factor-1 *alpha* interacts with the 3′ stem–loop region of West Nile virus genomic RNA. J. Virol. 71:6433-6444

Bladen, C.L., Udayakumar, D., Takeda, Y., Dynan, W.S. 2005. Identification of the plypyrimidine tract binding protein-associated splicing factor·p54(nrb) complex as a candidate DNA double-strand break rejoining factor. J. Biol. Chem. 280:5205-5210

Boggio, R., Chiocca, S. 2006. Viruses and sumoylation: recent highlights. Curr. Opin. Microbiol. 9:430-436

Bojić, T. 2009. Host involvement in the replication of potato spindle tuber viroid and the evolutionary Rrelationship between plant viroids and the hepatitis *delta* virus. Thesis, (MSc). University of Ottawa, Ottawa, Ontario, Canada

Bonino, F., Heermann, K.H., Rizzetto, M., Gerlich, W.H. 1986. Hepatitis *delta* virus: protein composition of *delta* antigen and its hepatitis B virus-derived envelope. J. Virol. 58:945-950

Bordier, B.B., Marion, P.L., Ohashi, K., Kay, M.A., Greenberg, H.B., Casey, J.L., Glenn, J.S. 2002. A prenylation inhibitor prevents production of infectious hepatitis *delta* virus particles. J. Virol. 76:10465-10472

Bordier, B.B., Ohkanda, J., Liu, P., Lee, S.Y., Salazar, F.H., Marion, P.L., Ohashi, K., Meuse, L., Kay, M.A., Casey, J.L., Sebti, S.M., Hamilton, A.D., Glenn, J.S. 2003. *In vivo*

antiviral efficacy of prenylation inhibitors against hepatitis *delta* virus. J. Clin. Invest. 112:407-414

Bougie, I., Bisaillon, M. 2007. Characterization of the RNA binding energetics of the *Candida albicans* poly(A) polymerase. Yeast 24:431-446

Bougie, I., Parent, A., Bisaillon, M. 2004. Thermodynamics of ligand binding by the yeast mRNA-capping enzyme reveals different modes of binding. Biochem. J. 384:411-420

Branch, A.D., Robertson, H.D. 1984. A replication cycle for viroids and small infectious RNAs. Science 223:450-455

Branch, A.D., Robertson, H.D. 1991. Efficient *trans* cleavage and a common structural motif for the ribozymes of the human hepatitis *delta* agent. Proc. Natl. Acad. Sci. U.S.A. 88:10163-10167

Brazas, R., Ganem, D. 1996. A cellular homolog of hepatitis *delta* antigen: implications for viral replication and evolution. Science 274:90-94

Brun, F., Toulmé, J.-J., Hélène, C. 1975. Interactions of aromatic residues of proteins with nucleic acids. Fluorescence studies of the binding of oligopeptides containing tryptophan and tyrosine residues to polynucleotides. Biochemistry 14:558-563

Bushnell, D.A., Cramer, P., Kornberg, R.D. 2002. Structural basis of transcription: *alpha*-amanitin−RNA polymerase II cocrystal at 2.8 Å resolution. Proc. Natl. Acad. Sci. U.S.A. 99:1218-1222

Cáceres, J.F., Krainer, A.R. 1993. Functional analysis of pre-mRNA splicing factor SF2/ASF structural domains. EMBO J. 12:4715-4726

Cáceres, J.F., Screaton, G.R., Krainer, A.R. 1998. A specific subset of SR proteins shuttles continuously between the nucleus and the cytoplasm. Genes Dev. 12:55-66

Cao, D., Haussecker, D., Huang, Y., Kay, M.A. 2009. Combined proteomic-RNAi screen for host factors involved in human hepatitis *delta* virus replication. RNA 15:1971-1979

Casey, J.L., Gerin, J.L. 1995. Hepatitis D virus RNA editing: specific modification of adenosine in the antigenomic RNA. J. Virol. 69:7593-7600

Castiglioni, F., Tagliabue, E., Campiglio, M., Pupa, S.M., Balsari, A., Menard, S. 2006. Role of exon-16-deleted HER2 in breast carcinomas. Endocr. Relat. Cancer 13:221-232

Castilla, A., Prieto, J., Fausto, N. 1991. Transforming growth factors *beta* 1 and *alpha* in chronic liver disease. Effects of interferon *alfa* therapy. N. Engl. J. Med. 324:933–940

Chambon, P. 1975. Eukaryotic nuclear RNA polymerases. Annu. Rev. Biochem. 44:613-638

Chang, F.L., Chen, P.J., Tu, S.J., Chiu, M.N., Wang, C.J., Chen, D.S. 1991. The large form of hepatitis δ antigen is crucial for the assembly of hepatitis δ virus. Proc. Natl. Acad. Sci. U.S.A. 88:8490-8494

Chang, J., Gudima, S.O., Tarn, C., Nie, X., Taylor, J.M. 2005. Development of a novel system to study hepatitis *delta* virus genome replication. J. Virol. 79:8182-8188

Chang, J., Nie, X., Gudima, S., Taylor, J. 2006. Action of inhibitors on accumulation of processed hepatitis *delta* virus RNAs. J. Virol. 80:3205-3214

Chang, J., Nie, X., Chang, H.E., Han, Z., Taylor, J. 2008. Transcription of hepatitis *delta* virus RNA by RNA polymerase II. J. Virol. 82:1118-1127

Chang, M.-F., Baker, S.C., Soe, L.H., Kamahora, T., Keck, J.G., Makino, S., Govindarajan, S., Lai, M.M.C. 1988. Human hepatitis *delta* antigen is a nuclear phosphoprotein with RNA binding activity. J. Virol. 62:2403-2410

Chang, M.F., Chen, C.J., Chang, S.C. 1994. Mutational analysis of *delta* antigen: effect on assembly and replication of hepatitis *delta* virus. J. Virol. 68:646-653

Chao, M., Hsieh, S.-Y., Taylor, J. 1990. Role of two forms of the hepatitis *delta* virus antigen: evidence for a mechanism of self-limiting genome replication. J. Virol. 64:5066-5069

Chen, C.W., Tsay, Y.G., Wu, H.L., Lee, C.H., Chen, D.S., Chen, P.J. 2002. The double-stranded RNA-activated kinase, PKR, can phosphorylate hepatitis D virus small *delta* antigen at functional serine and threonine residues. J. Biol. Chem. 277:33058-33067

Chen, P.-J., Kalpana, G., Goldberg, J., Mason, W., Werner, B., Gerin, J., Taylor, J. 1986. Structure and replication of the genome of hepatitis δ virus. Proc. Natl. Acad. Sci. U.S.A. 83:8774-8778

Chen, P.J., Chang, F.L., Wang, C.J., Lin, C.J., Sung, S.Y., Chen, D.S. 1992. Functional study of hepatitis *delta* virus large antigen in packaging and replication inhibition*:* role of the amino-terminal leucine zipper. J. Virol. 66:2853-2859

Chen, R., Linnstaedt, S.D., Casey, J.L. 2010. RNA editing and its control in hepatitis *delta* virus replication.Viruses 2:131-146

Chen, Y.S., Huang, W.H., Hong S.Y., Tsay, Y.G., Chen, P.J. 2008. ERK1/2-mediated phosphorylation of small hepatitis *delta* antigen at serine 177 enhances hepatitis *delta* virus antigenomic RNA replication. J. Virol. 82:9345-9358

Choi, S.H., Jeong, S.H., Hwang, S.B. 2007. Large hepatitis *delta* antigen modulates transforming growth factor-*beta* signaling cascades: implication of hepatitis *delta* virus-induced liver fibrosis. Gastroenterology 132:343-357

Chou, H.C., Hsieh, T.Y., Sheu, G.T., Lai, M.M. 1998. Hepatitis *delta* antigen mediates the nuclear import of hepatitis *delta* virus RNA. J. Virol. 72:3684-3690

Chuang, S.M., Chen, L., Lambertson, D., Anand, M., Kinzy, T.G., Madura, K. 2005. Proteasome-mediated degradation of cotranslationally damaged proteins involves translation elongation factor 1A. Mol. Cell. Biol. 25:403-413

Circle, D.A., Neel, O.D., Robertson, H.D., Clarke, P.A., Mathews, M.D. 1997. Surprising specificity of PKR binding to *delta* agent genomic RNA. RNA 3(4):438-448

Cole, S.M., Gowans, E.J., Macnaughton, T.B., Hall, P.D., Burrell, C.J. 1991. Direct evidence for cytotoxicity associated with expression of hepatitis *delta* virus antigen. Hepatology 13:845-851

Cramer, P., Caceres, J.F. Cazalla, D. Kadener S., Muro, A.F. Baralle F.E. and Kornblihtt, A.R. 1999. Coupling of transcription with alternative splicing: RNA pol II promoters modulate SF2/ASF and 9G8 effects on an exonic splicing enhancer. Mol. Cell 4:251-258

Das, T., Mathur, M., Gupta, A.K., Janssen, G.M., Banerjee, A.K. 1998. RNA polymerase of vesicular stomatitis virus specifically associates with translation elongation factor-1 *alpha beta gamma* for its activity. Proc. Natl. Acad. Sci. U.S A. 95:1449-1454

Dalmay, T., Horsefield, R., Braunstein, T.H., Baulcombe, D.C. 2001. SDE3 encodes an RNA helicase required for post-transcriptional gene silencing in *Arabidopsis*. EMBO J. 20:2069-2078

De, B.P., Gupta, S., Zhao, H., Drazba, J.A., Banerjee, A.K. 1996. Specific interaction *in vitro* and *in vivo* of glyceraldehyde-3-phosphate dehydrogenase and LA protein with *cis*-acting RNAs of human parainfluenza virus type 3. J. Biol. Chem. 271:24728-24735

Dennler, S., Prunnier, C., Ferrand, N., Gauthier, J.M., Atfi, A. 2000. c-Jun inhibits transforming growth factor *beta*-mediated transcription by repressing Smad3 transcriptional activity. J. Biol. Chem. 275:28858-28865

Derynck, R., Zhang, Y., Feng, X.H. 1998. Smads: transcriptional activators of TGF-*beta* responses. Cell 95:737-740

Derynck, R., Akhurst, R.J., Balmain, A. 2001. TGF-*beta* signaling in tumor suppression and cancer progression. Nat. Genet. 29:117-129

Diener, T.O. 1971. Potato spindle tuber "virus". IV. A replicating, low molecular weight RNA. Virology 45:411-28

Diener, T.O. 1986. Viroid processing: a model involving the central conserved region and hairpin I. Proc. Natl. Acad. Sci. U.S.A. 83:58-62

Diener, T.O. 2001. The viroid: biological oddity or evolutionary fossil? Adv. Virus Res. 57:137-184

Dijkstra, D.S., Broos, J., Lolkema, J.S., Enequist, H., Minke, W., Robillard, G.T. 1996. A fluorescence study of single tryptophan-containing mutants of enzyme IImtl of the *Escherichia coli* phosphoenolpyruvate-dependent mannitol transport system. Biochemistry 35:6628-6634

Ding, B., Itaya, A. 2007. Viroid: A useful model for studying the basic principles of infection and RNA biology. Mol. Plant Microbe Interact. 20:7-20

Dingle, K., Bichko, V., Zuccola, H., Hogle, J., Taylor, J. 1998. Initiation of hepatitis *delta* virus genome replication. J. Virol. 72:4783-4788

Dollenmaier, G., Weitz, M. 2003. Interaction of glyceraldehyde-3-phosphate dehydrogenase with secondary and tertiary RNA structural elements of the hepatitis A virus 3' translated and non-translated regions. J. Gen. Virol. 84:403-414

Dong, B., Horowitz, D.S., Kobayashi, R., Krainer, A.R. 1993. Purification and cDNA cloning of HeLa cell $p54^{nrb}$, a nuclear protein with two RNA recognition motifs and extensive homology to human splicing factor PSF and *Drosophila* NONA/BJ6, Nucleic Acids Res. 21:4085-4092

Dong, X., Shylnova, O., Challis, J.R., Lye, S.J. 2005. Identification and characterization of the protein-associated splicing factor as a negative co-regulator of the progesterone receptor. J Biol. Chem. 280:13329-13340

Du, X., Wang, Q., Hirohashi, Y., Greene, M.I. 2006. DIPA, which can localize to the centrosome, associates with p78/MCRS1/MSP58 and acts as a repressor of gene transcription. Exp. Mol. Pathol. 81:184-190

Dubé, A., Bisaillon, M., Perreault, J.P. 2009. Identification of proteins from *Prunus persica* that interact with peach latent mosaic viroid. J. Virol. 83:12057-12067

Eftink, M.R. 1991. Fluorescence techniques for studying protein structure. Methods Biochem. Anal. 35:127-205

Eftink, M.R., Ghiron, C.A. 1976. Exposure of tryptophanyl residues in proteins. Quantitative determination by fluorescence quenching studies. Biochemistry 15:672-680

Eiras, M., Nohales, M.A., Kitajima, E.W., Flores, R., Daròs, J.A. 2011. Ribosomal protein L5 and transcription factor IIIA from *Arabidopsis thaliana* bind *in vitro* specifically Potato spindle tuber viroid RNA. Arch. Virol. 156:529-533

Ehrlich, M., Boll, W., Van Oijen, A., Hariharan, R., Chandran, K., Nibert, M.L., Kirchhausen, T. 2004. Endocytosis by random initiation and stabilization of clathrin-coated pits. Cell 118:591-605

Elton, D., Medcalf, L., Bishop, K., Harrison, D., Digard, P. 1999. Identification of amino acid residues of influenza virus nucleoprotein essential for RNA binding. J. Virol. 73:7357-7367

Emili, A., Shales, M., McCracken, S., Xie, W., Tucker, P.W., Kobayashi, R., Blencowe, B.J., Ingles, C.J. 2002. Splicing and transcription-associated proteins PSF and p54^{nrb}/nonO bind to the RNA polymerase II CTD. RNA 8:1102–1111

Engelke, M., Mills, K., Seitz, S., Simon, P., Gripon, P., Schnölzer, M., Urban, S. 2006. Characterization of a hepatitis B and hepatitis *delta* virus receptor binding site. Hepatol. 43:750-760

Ezponda, T., Pajares, M.J., Agorreta, J., Echeveste, J.I., López-Picazo, J.M., Torre, W., Pio, R., Montuenga, L.M. 2010. The oncoprotein SF2/ASF promotes non-small cell lung cancer survival by enhancing survivin expression. Clin. Cancer Res. 16:4113-4125

Farci, P. 2003. *Delta* hepatitis: an update. J. Hepatol. 39(Suppl. 1):S212-S219

Farci, P., Roskams, T., Chessa, L., Peddis, G., Mazzoleni, A.P., Scioscia, R., Serra, G., Lai, M.E., Loy, M., Caruso, L., Desmet, V., Purcell, R.H., Balestrieri, A. 2004. Long-term benefit of interferon *alpha* therapy of chronic hepatitis D: regression of advanced hepatic fibrosis. Nat. Clin. Pract. Gastroenterol. Hepatol. 1(2):76-77

Fattovich, G., Giustina, G., Christensen, E., Pantalena, M., Zagni, I., Realdi, G., Schalm, S. W., the European Concerted Action on Viral Hepatitis (Eurohep). 2000. Influence of hepatitis *delta* virus infection on morbidity and mortality in compensated cirrhosis type B. Gut 46:420-426

Fattovich, G., Stroffolini, T., Zagni, I., Donato, F. 2004. Hepatocellular carcinoma in cirrhosis: incidence and risk factors. Gastroenterology 127:S35–S50

Ferré-D'Amaré, A.R., Zhou, K., Doudna, J.A. 1998. Crystal structure of a hepatitis *delta* virus ribozyme. Nature 395:567-574

Filipovska, J., Konarska, M.M. 2000. Specific HDV RNA-templated transcription by pol II *in vitro*. RNA 6:41-54

Flaman, J.M., Frebourg, T., Moreau, V., Charbonnier, F., Martin, C., Ishioka, C., Friend, S.H., Iggo, R. 1994. A rapid PCR fidelity assay. Nucleic Acids Res. 22:3259-3260

Flores, R., Delgado, S., Gas, M.-E., Carbonell, A. Molina, D., Gago, S. and De la Peña , M. 2004. Viroids: the minimal non-coding RNAs with autonomous replication. FEBS Lett. 567:42-48

Flores, R., Hernández, C., Martínez de Alba, A.E., Daròs, J.-A., Di Serio, F. 2005. Viroids and viroid-host interactions. Annu. Rev.Phytopathol. 43:117-139

Flores, R., Grubb, D., Elleuch, A., Nohales, M.Á., Delgado, S., Gago, S. 2011. Rolling-circle replication of viroids, viroid-like satellite RNAs and hepatitis *delta* virus: Variations on a theme. RNA Biol. 8:200-206

Flowers, S., Biswas, E.E., Biswas, S.B. 2003. Conformational dynamics of DnaB helicase upon DNA and nucleotide binding: analysis by intrinsic tryptophan fluorescence quenching. Biochemistry 42:1910-1921

Fu, T.-B., Taylor, J. 1993. The RNAs of hepatitis *delta* virus are copied by RNA polymerase II in nuclear homogenates. J. Virol. 67:6965-6972

Fukuhara, Y., Takeshima, T., Kashiwaya, Y., Shimoda, K., Ishitani, R., Nakashima, K. 2001. GAPDH knockdown rescues mesencephalic dopaminergic neurons from MPP+-induced apoptosis. Neuroreport 12:2049-2052

Galán, C., Sola, I., Nogales, A., Thomas, B., Akoulitchev, A., Enjuanes, L., Almazán, F. 2009. Host cell proteins interacting with the 3' end of TGEV coronavirus genome influence virus replication. Virology 391:304-314

Ganem, D. and Varmus, H.E. 1987. The molecular biology of the hepatitis B viruses. Annu. Rev. Biochem. 56:651-693

Gavin, A.C., Aloy, P., Grandi, P., Krause, R., Boesche, M., Marzioch, M., Rau, C., Jensen, L.J., Bastuck, S., Dümpelfeld, B., Edelmann, A., Heurtier, M.A., Hoffman, V., Hoefert, C., Klein, K., Hudak, M., Michon, A.M., Schelder, M., Schirle, M., Remor, M., Rudi, T., Hooper, S., Bauer, A., Bouwmeester, T., Casari, G., Drewes, G., Neubauer, G., Rick, J.M., Kuster, B., Bork, P., Russell, R.B., Superti-Furga, G. 2006. Proteome survey reveals modularity of the yeast cell machinery. Nature 440:631-636

Ge, H., Zuo, P., Manley, J.L. 1991. Primary structure of the human splicing factor ASF reveals similarities with *Drosophila* regulators. Cell 66:373-382

Ghosh, S., Karin, M. 2002. Missing pieces in the NF-*kappa*B puzzle. Cell 109:S81-S96

Glenn, J.S., Taylor, J.M., White, J.M. 1990. *In vitro*-synthesized hepatitis *delta* virus RNA initiates genome replication in cultured cells. J. Virol. 64:3104-3107

Glenn, J.S., Watson, J.A., Havel, C.M., White, J.M. 1992. Identification of a prenylation site in *delta* virus large antigen. Science 256:2955-2959

Gordon, S., Akopyan, G., Garban, H., Bonavida, B. 2006. Transcription factor YY1: structure, function, and therapeutic implications in cancer biology. Oncogene 25:1125-1142

Gorlach, M., Wittekind, M., Beckman, R.A., Mueller, L., Dreyfuss, G. 1992. Interaction of the RNA-binding domain of the hnRNP C proteins with RNA. EMBO J. 11:3289-329

Goto, T., Kato, N., Ono-Nita, S.K., Yoshida, H., Otsuka, M., Shiratori, Y., Omata, M. 2000. Large isoform of hepatitis *delta* antigen activates serum response factor-associated transcription. J. Biol. Chem. 275:37311-37316

Goto, T., Kato, N., Yoshida, H., Otsuka, M., Moriyama, M., Shiratori, Y., Koike, K., Matsumura, M., Omata, M. 2003. Synergistic activation of the serum response element-dependent pathway by hepatitis B virus x protein and large-isoform hepatitis *delta* antigen. J. Infect. Dis. 187:820-828

Graveley, B.R. 2000. Sorting out the complexity of SR protein functions. RNA 6:1197-1211

Greco-Stewart, V.S. 2009. Characterization of the interaction of human DNA-dependent RNA polymerases and transcription factors with RNA from the hepatitis *delta* virus: novel perspectives in HDV biology. Thesis, (PhD). University of Ottawa, Ottawa, Ontario, Canada

Greco-Stewart, V.S., St-Laurent Thibault, C., Pelchat, M. 2006. Binding of the polypyrimidine tract-binding protein-associated splicing factor (PSF) to the hepatitis *delta* virus RNA. Virology 356:35-44

Greco-Stewart, V.S., Miron, P., Abrahem, A., Pelchat M. 2007. The human RNA polymerase II interacts with the terminal stem-loop regions of the hepatitis *delta* virus RNA genome. Virology 357:68-78

Greco-Stewart, V.S., Schissel, E., Pelchat, M. 2009. The hepatitis *delta* virus RNA genome interacts with the human RNA polymerases I and III. Virology 386:12-15

Greco-Stewart, V.S., Pelchat, M. 2010. Interaction of host cellular proteins with components of the hepatitis *delta* virus. Viruses 2:189-212

Gross, S.R., Kinzy, T.G. 2005. Translation elongation factor 1A is essential for regulation of the actin cytoskeleton and cell morphology. Nat. Struct. Mol. Biol. 12:772-778

Guang, S., Felthauser, A.M., Mertz, J.E. 2005. Binding of hnRNP L to the pre-mRNA processing enhancer of the herpes simplex virus thymidine kinase gene enhances both polyadenylation and nucleocytoplasmic export of intronless mRNAs. Mol. Cell Biol. 25:6303-6313

Gudima, S., Dingle, K., Wu, T.-T., Moraleda, G., Taylor, J. 1999. Characterization of the 5'-ends for polyadenylated RNAs synthesized during the replication of hepatitis *delta* virus. J. Virol. 73:6533-6539

Gudima, S., Wu, S.Y., Chiang, C.M., Moraleda, G., Taylor, J. 2000. Origin of hepatitis *delta* virus mRNA. J. Virol. 74:7204-7210

Gudima, S., Chang, J., Moraleda, G., Azvolinsky, A., Taylor, J. 2002. Parameters of human hepatitis *delta* virus genome replication: the quantity, quality, and intracellular distribution of viral proteins and RNA. J. Virol. 76:3709-3719

Gudima, S., He, Y., Meier, A., Chang, J., Chen, R., Jarnik, M., Nicolas, E., Bruss, V., Taylor J. 2007. Assembly of hepatitis *delta* virus: particle characterization, including the ability to infect primary human hepatocytes. J. Virol. 81:3608-3617

Guilhot, S., Huang, S.N., Xia, Y.P., La Monica, N., Lai, M.M., Chisari, F.V. 1994. Expression of the hepatitis *delta* virus large and small antigens in transgenic mice. J. Virol. 68:1052-1058

Gutiérrez-Escolano, A.L., Brito, Z.U., del Angel, R.M., Jiang, X. 2000. Interaction of cellular proteins with the 5' end of Norwalk virus genomic RNA. J. Virol. 74:8558-8562

Hahm, B., Kim, Y.K., Kim, J.H., Kim, T.Y., Jang, S.K. 1998. Heterogeneous nuclear ribonucleoprotein L interacts with the 3' border of the internal ribosomal entry site of hepatitis C virus. J Virol. 72:8782-8788

Han, S.P., Tang, Y.H., Smith, R. 2010. Functional diversity of the hnRNPs: past, present and perspectives. Biochem. J. 430:379-392

Happel, N., Doenecke, D. 2009. Histone H1 and its isoforms: contribution to chromatin structure and function. Gene 431:1-12

Harris, K.S., Xiang, W., Alexander, L., Lane, W.S., Paul, A.V., Wimmer, E. 1994. Interaction of poliovirus polypeptide 3CDpro with the 5′ and 3′ termini of the poliovirus genome. Identification of viral and cellular cofactors needed for efficient binding. J. Biol. Chem. 269:27004-27014

Hartmann, A.M., Nayler, O., Schwaiger, F.W., Obermeier, A., Stamm, S. 2001. The interaction and colocalization of Sam68 with the splicing-associated factor YT521-B in nuclear dots is regulated by the Src family kinase p59(fyn), Mol. Biol. Cell. 10:3909-3926

Hastings, M.L., Krainer, A.R.2001. Pre-mRNA splicing in the new millennium. Curr. Opin. Cell. Biol. 13:302-309

Haussecker D, Cao D, Huang Y, Parameswaran P, Fire AZ, Kay MA. 2008. Capped small RNAs and MOV10 in human hepatitis *delta* virus replication. Nat. Struct. Mol. Biol. 15:714-721

He, L.F., Ford, E., Purcell, R.H., London, W.T., Phillips, J., Gerin, J.L. 1989. The size of the hepatitis *delta* agent. J. Med. Virol. 27:31-33

Hong, S.Y., Chen, P.J. 2010. Phosphorylation of serine 177 of the small hepatitis *delta* antigen regulates viral antigenomic RNA replication by interacting with the processive RNA polymerase II. J. Virol. 84:1430-1438

Hovanessian, A.G. 1993. Interferon-induced dsRNA-activated protein kinase (PKR)*: antiproliferative, antiviral and antitumoral functions. Semin. Virol. 4:237-245

Hsieh, S.-Y., Chao, M., Coates, L., Taylor, J. 1990. Hepatitis *delta* virus genome replication: a polyadenylated mRNA for *delta* antigen. J. Virol. 64:3192-3198

Hunter, T., Hunt, T., Jacosn, R.J., Robertson, H.D. 1975. The characteristics of inhibition of protein synthesis by double-stranded ribonucleic acid in reticulocyte lysates. J. Biol. Chem. 250:409-417

Huang, C., Chang, S.C., Yu, I.C., Tsay, Y.G., Chang, M.F. 2007. Large hepatitis *delta* antigen is a novel clathrin adaptor-like protein. J. Virol. 81 :5985-5994

Huang, C., Chang, S.C., Yang, H.C., Chien, C.L., Chang, M.F. 2009. Clathrin-mediated post-Golgi membrane trafficking in the morphogenesis of hepatitis *delta* virus. J. Virol. 83:12314-12324

Huang, T.-S., Nagy, P.D. 2011. Direct inhibition of tombusvirus plus-strand RNA synthesis by a dominant negative mutant of a host metabolic enzyme, glyceraldehyde-3-phosphate dehydrogenase, in yeast and plants. J. Virol. 85:9090-9102

Huang, W.H., Yung, B.Y., Syu, W.J., Lee, Y.H. 2001. The nucleolar phosphoprotein B23 interacts with hepatitis *delta* antigens and modulates the hepatitis *delta* virus RNA replication. J. Biol. Chem. 276:25166-25175

Huang, W.H., Chen, Y.S., Chen, P.J. 2008a. Nucleolar targeting of hepatitis *delta* antigen abolishes its ability to initiate viral antigenomic RNA replication. J. Virol. 82:692-699

Huang, W.H., Mai, R.T., Lee, Y.H. 2008b. Transcription factor YY1 and its associated acetyltransferases CBP and p300 interact with hepatitis *delta* antigens and modulate hepatitis *delta* virus RNA replication. J. Virol. 82:7313-7324

Huang, Y., Steitz, J.A. 2001. Splicing factors SRp20 and 9G8 promote the nucleocytoplasmic export of mRNA. Mol. Cell. 7:899-905

Huang, Y., Steitz, J.A. 2005. SRprises along a messenger's journey. Mol. Cell 17:613-615

Huang, Z.S., Wu, H.N. 1998. Identification and characterization of the RNA chaperone activity of hepatitis *delta* antigen peptides. J. Biol. Chem. 273:26455-26461

Hwang, S.B., Lai, M.M. 1993. Isoprenylation mediates direct protein-protein interactions between hepatitis large *delta* antigen and hepatitis B virus surface antigen. J. Virol. 67:7659-7662

Hwang, B., Lim, J.H., Hahm, B., Jang, S.K., Lee, S.W. 2009. hnRNP L is required for the translation mediated by HCV IRES. Biochem. Biophys. Res. Commun. 378:584-588

Hwang, S.B., Lai, M.M. 1994. Isoprenylation masks a conformational epitope and enhances trans-dominant inhibitory function of the large hepatitis *delta* antigen. J. Virol. 68:2958-2964

Hwang, S.B., Park, K.J. 1999. Cell cycle arrest mediated by hepatitis *delta* antigen. FEBS Lett. 449:41-44

Inagaki, Y., Mamura, M., Kanamaru, Y., Greenwel, P., Nemoto, T., Takehara, K., Ten Dijke, P., Nakao, A. 2001. Constitutive phosphorylation and nuclear localization of Smad3 are correlated with increased collagen gene transcription in activated hepatic stellate cells. J. Cell. Physiol. 187:117-123

Inouye, C.J., Seto, E. 1994. Relief of YY1-induced transcriptional repression by protein-protein interaction with the nucleolar phosphoprotein B23. J. Biol. Chem. 269:6506-6510

Ishitani, R., Chuang, D.M. 1996. Glyceraldehyde-3-phosphate dehydrogenase antisense oligodeoxynucleotides protect against cytosine arabinonucleoside-induced apoptosis in cultured cerebellar neurons. Proc. Natl. Acad. Sci. U.S.A. 93:9937-9941

Ishitani, R., Sunaga, K., Hirano, A., Saunders, P., Katsube, N., Chuang, D. M. 1996. Evidence that glyceraldehyde-3-phosphate dehydrogenase is involved in age-induced apoptosis in mature cerebellar neurons in culture. J. Neurochem. 66:928-935

Ishitani, R., Tanaka, M., Sunaga, K., Katsube, N., Chuang, D.M. 1998. Nuclear localization of overexpressed glyceraldehyde-3-phosphate dehydrogenase in cultured cerebellar neurons undergoing apoptosis. Mol. Pharmacol. 53:701-707

Jayan, G.C., Casey, J.L. 2005. Effects of conserved RNA secondary structures on hepatitis *delta* virus genotype I RNA editing, replication, and virus production. J. Virol. 79:11187-11193

Jessen, T.H., Oubridge, C., Teo, C.H., Pritchard, C., Nagai, K. 1991. Identification of molecular contacts between the U1 A small nuclear ribonucleoprotein and U1 RNA. EMBO J. 10:3447-3456

Joshi, R.L., Ravel, J.M., Haenni, A.L. 1986. Interaction of turnip yellow mosaic virus Val-RNA with eukaryotic elongation factor EF-1 [*alpha*]. Search for a function. EMBO J. 5:1143-1148

Kanai, Y., Dohmae N., Hirokawa, N. 2004. Kinesin transports RNA: isolation and characterization of an RNA-transporting granule. Neuron 43:513-525

Karin, M., Gallagher, E. 2005. From JNK to pay dirt: jun kinases, their biochemistry, physiology and clinical importance. IUBMB Life 57:283-295

Karin, M., Liu, Z.-G., Zandi, E. 1997. AP-1 function and regulation. Curr. Opin. Cell Biol. 9: 240–246

Karni, R., de Stanchina, E., Lowe, S.W., Sinha, R., Mu, D., Krainer, A.R. 2007. The gene encoding the splicing factor SF2/ASF is a proto-oncogene. Nat. Struct. Mol. Biol. 14:185-193

Kelly, C., Van Driel, R., Wilkinson, G.W. 1995. Disruption of PML-associated nuclear bodies during human cytomegalovirus infection. J. Gen. Virol. 76:2887-2893

Kim, J.B., Sharp, P.A. 2001. Positive transcription elongation factor b phosphorylates hSPT5 and RNA Polymerase II carboxyl-terminal domain independently of cyclin-dependent kinase-activating kinase. J. Biol. Chem. 276:123117-12323

Kim, E., Du, L., Bregman, D.B., Warren, S.L. 1997. Splicing factors associate with hyperphosphorylated RNA polymerase II in the absence of pre-mRNA. J. Cell Biol. 136:19-28

Kim, U., Wang, Y., Sanford, T., Zeng, Y., Nishikura, K. 1994. Molecular cloning of cDNA for double-stranded RNA adenosine deaminase, a candidate enzyme for nuclear RNA editing. Proc. Natl. Acad. Sci. USA 91:11457-11461

Kolonko, N., Bannach, O., Aschermann, K., Hu, K.H., Moors, M., Schmitz, M., Steger, G., Riesner, D. 2006. Transcription of potato spindle tuber viroid by RNA polymerase II starts in the left terminal loop. Virology 347:392-404

Krainer, A.R., Mayeda, A., Kozak, D., Binns, G. 1991. Functional expression of cloned human splicing factor SF2: homology to RNA-binding proteins, U1 70K, and *Drosophila* splicing regulators. Cell 66:383-394

Kuo, M.Y.-P., Sharmeen, L., Dinter-Gottlieb, G., Taylor, J. 1988. Characterization of self-cleaving RNA sequences on the genome and antigenome of human hepatitis *delta* virus. J. Virol. 62:4439-4444

Kuo, M.Y., Chao, M., Taylor, J. 1989. Initiation of replication of the human hepatitis *delta* virus genome from cloned DNA: role of *delta* antigen. J.Virol. 63:1945-1950

Lai, M.M. 1998. Cellular factors in the transcription and replication of viral RNA genomes: a parallel to DNA-dependent RNA transcription. Virology 244:1-12

Lai, M.M.C. 2005. RNA replication without RNA-dependent RNA polymerase: surprises from hepatitis *delta* virus. J. Virol. 79:7951-7958

Lakowicz, J.R. 2006. Principles of Fluorescence Spectroscopy, 3rd ed. Springer, New York, NY

Lau, D.T., Kleiner, D.E., Park, Y., DiBisceglie, A.M., Hoofnagle, J.H. 1999. Resolutions of chronic *delta* hepatitis after 12 years of interferon *alfa* therapy. Gastroenterology 117:1229-1233

Lazar, G., Schaal, T., Maniatis, T., Goodman, H.M. 1995. Identification of a plant serine-arginine-rich protein similar to the mammalian splicing factor SF2/ASF. Proc. Natl. Acad. Sci. U.S.A. 92:7672-7676

Lazinski, D.W., Taylor, J. M. 1993. Relating structure to function in the hepatitis *delta* virus antigen. J. Virol. 67:2672-2680

Lee, C.H., Chang, S.C., Chen, C.J., Chang, M.F. 1998. The nucleolin binding activity of hepatitis *delta* antigen is associated with nucleolus targeting. J. Biol. Chem. 273:7650-7656

Lee, C.H., Chang, S.C., Wu, C.H., Chang, M.F. 2001. A novel chromosome region maintenance 1-independent nuclear export signal of the large form of hepatitis *delta* antigen that is required for the viral assembly. J. Biol. Chem. 276:8142-8148

Lee, C.Z., Lin, J.H., Chao, M., McKnight, K., Lai, M.M. 1993. RNA-binding activity of hepatitis *delta* antigen involves two arginine-rich motifs and is required for hepatitis *delta* virus RNA replication. J. Virol. 67:2221-2227

Lee, C.Z., Chen, P.J., Lai, M.M.C., Chen, D.S. 1994. Isoprenylation of large hepatitis *delta* antigen is necessary but not sufficient for hepatitis *delta* assembly. Virology 199:169-175

Lee, C.Z., Chen, P.J., Chen, D.S. 1995. Large hepatitis *delta* antigen in packaging and replication inhibition: role of the carboxyl-terminal 19 amino acids and amino-terminal sequences. J. Virol. 69:5332-5336

Lee, C.Z., Sheu, J.C. 2008. Histone H1e interacts with small hepatitis *delta* antigen and affects hepatitis *delta* virus replication. Virology 375:197-204

Lee, E.J., Jo, M., Park, J., Zhang, W., Lee, J.H. 2006. Alternative splicing variants of IRF-1 lacking exons 7, 8, and 9 in cervical cancer. Biochem. Biophys. Res. Commun. 347:882-888

Lee, L.W., Chang, T.Y., Lo, H.W., Lo, S.J. 2011. Hepatitis D antigens cause growth retardation and brood-size reduction in *C. elegans*. Front. Biosci. (Elite Ed.) 3:380-390

Lee, Y. M., Lee, S.C. 1994. Transcriptional activation of the *alpha*-1 acid glycoprotein gene by YY1 is mediated by its functional interaction with a negative transcription factor. DNA Cell Biol. 13:1029-1036

Lehmann, E., Brueckner, F., Cramer, P. 2007. Molecular basis of RNA-dependent RNA polymerase II activity. Nature 450:445-449

Lemaire, R., Prasad, J., Kashima, T., Gustafson, J., Manley, J.L., Lafyatis, R. 2002. Stability of a PKCI-1-related mRNA is controlled by the splicing factor ASF/SF2: A novel function for SR proteins. Genes Dev. 16:594-607

Li, X., Manley, J.L. 2005. Inactivation of the SR protein splicing factor ASF/SF2 results in genomic instability. Cell 122:365-378

Li, Y.J., Stallcup, M.R., Lai, M.M. 2004. Hepatitis *delta* virus antigen is methylated at arginine residues and methylation regulates subcellular localization and RNA replication. J. Virol. 78:13325-13334

Li, Y.J., Macnaughton, T., Gao, L., Lai, M.M. 2006. RNA-templated replication of hepatitis *delta* virus: Genomic and antigenomic RNAs associate with different nuclear bodies. J. Virol. 80:6478-6486

Li, Y.P., Busch, R.K., Valdez, B.C., Busch, H. 1996. C23 interacts with B23, a putative nucleolar-localization-signal-binding protein. Eur. J. Biochem. 237:153-158

Li, Z., Pogany, J., Panavas, T., Xu, K., Esposito, A.M., Kinzy, T.G., Nagy, P.D. 2009. Translation elongation factor 1A is a component of the tombusvirus replicase complex and affects the stability of the p33 replication cofactor. Virology 385:245–260

Li, Z., Pogany, J., Tupman, S., Esposito, A.M., Kinzy, T.G., Nagy, P.D. 2010. Translation elongation factor 1A facilitates the assembly of the tombusvirus replicase and stimulates minus-strand synthesis. PLoS Pathog. 6:e1001175

Liao, F.T., Lee, Y.J., Ko, J.L., Tsai, C.C., Tseng, C.J., Sheu, G.T. 2009. Hepatitis *delta* virus epigenetically enhances clusterin expression via histone acetylation in human hepatocellular carcinoma cells. J. Gen. Virol. 90:1124-1134

Lima, S.M., Vaz, A.C., Souza, T.L., Peabody, D.S., Silva, J.L., Oliveira, A.C. 2006. Dissecting the role of protein-protein and protein-nucleic acid interactions in MS2 bacteriophage stability. FEBS J. 273:1463-1475

Lin, J.H., Chang, M.F., Baker, S.C., Govindarajan, S., Lai, M.M. 1990. Characterization of hepatitis *delta* antigen: specific binding to hepatitis *delta* virus RNA. J. Virol. 64:4051-4058

Lin, S., Fu, X.D. 2007. SR proteins and related factors in alternative splicing. Adv. Exp. Med. Biol. 623:107-122

Lin, S.S., Chang, S.C., Wang, Y.H., Sun, C.Y., Chang, M.F. 2000. Specific interaction between the hepatitis *delta* virus RNA and glyceraldehyde 3-phosphate dehydrogenase: an enhancement on ribozyme catalysis. Virology 271:46-57

Liu, X., Mertz, J.E. 1995. HnRNP L binds a *cis*-acting RNA sequence element that enables intron-dependent gene expression. Genes Dev. 9:1766-1780

Livak, K.J., Schmittgen, T.D. 2001. Analysis of relative gene expression data using real-time quantitative PCR and the $2^{-\Delta\Delta C}$T method. Methods 25:402-408

Long, M., de Souza, S.J., Gilbert, W. 1997. *Delta*-interacting protein A and the origin of hepatitis *delta* antigen. Science 276:824-825

Lopato, S., Mayeda, A., Krainer, A.R., Barta, A. 1996. Pre-mRNA splicing in plants: characterization of Ser/Arg splicing factors. Proc. Natl. Acad. Sci. U.S.A. 93:3074-3079

Lopato, S., Kalyna, M., Dorner, S., Kobayashi, R., Krainer, A.R., Barta, A. 1999. atSRp30, one of two SF2/ASF-like proteins from Arabidopsis thaliana, regulates splicing of specific plant genes. Genes Dev. 13:987-1001

Lundberg, K.S., Shoemaker, D.D., Adams, M.W., Short, J.M., Sorge, J.A., Mathur, E.J. 1991. High-fidelity amplification using a thermostable DNA polymerase isolated from *Pyrococcus furiosus*. Gene 108:1-6

Lütgehetmann, M., Mancke, L.V., Volz, T., Helbig, M., Allweiss, L., Bornscheuer, T., Pollok, J.M., Lohse, A.W., Petersen, J., Urban, S., Dandri, M. 2012. Humanized chimeric uPA mouse model for the study of hepatitis B and D virus interactions and preclinical drug evaluation. Hepatol. 55:685-694

Macnaughton, T.B., Gowans, E.J., Reinboth, B., Jilbert, A.R., Burrell, C.J. 1990. Stable expression of hepatitis *delta* virus antigen in a eukaryotic cell line. J. Gen. Virol. 71:1339-1345

Macnaughton, T.B., Gowans, E.J., McNamara, S.P., Burrell, C.J. 1991. Hepatitis *delta* antigen is necessary for access of hepatitis *delta* virus RNA to the cell transcriptional machinery but is not part of the transcriptional complex. Virology 184:387-390

Macnaughton, T.B., Shi, S.T., Modahl, L.E., Lai, M.M. 2002. Rolling circle replication of hepatitis *delta* virus RNA is carried out by two different cellular RNA polymerases. J. Virol. 76:3920-3927

Manche, L., Green, S.R., Schmedt, C., Mathews, M.B. 1992. Interactions between double-stranded RNA regulators and the protein kinase DAI. Mol. Cell. Biol. 12:5238-5248

Maris, M, Dominguez, C., Allain, F., H.,-T. 2005. The RNA recognition motif, a plastic RNA-binding platform to regulate post-transcriptional gene expression. FEBS J. 272:2118-2131

Martin, S.J., Reutelingsperger, C.P., McGahon, A.J., Rader, J.A., van Schie, R.C., LaFace, D.M., Green, D.R. 1995. Early redistribution of plasma membrane phosphatidylserine is

a general feature of apoptosis regardless of the initiating stimulus: inhibition by overexpression of Bcl-2 and Abl. J. Exp. Med. 182:1545-1556

Mathews, M.B. 1993. Viral evasion of cellular defense mechanisms: regulation of the protein kinase DAI by RNA effectors. Semin. Virol. 4:247–258

Mathur, M., Tucker, P.W., Samuels, H.H. 2001. PSF is a novel corepressor that mediates its effect through Sin3A and the DNA binding domain of nuclear hormone receptors. Mol. Cell. Biol. 21:2298-2311

McCracken, S., Fong, N., Yankulov, K., Ballantyne, S., Pan, G., Greenblatt, J., Patterson, S.D., Wickens, M., Bentley, D.L. 1997. The C-terminal domain of RNA polymerase II couples mRNA processing to transcription. Nature 385:357-361

Meister, G., Landthaler, M., Peters, L., Chen, P.Y., Urlaub, H., Lührmann, R., Tuschl, T. 2005. Identification of novel argonaute-associated proteins. Curr. Biol. 15:2149-2155

Melcher, T., Maas, S., Herb, A., Sprengel, R., Seeburg, P.H., Higuchi, M. 1996. A mammalian RNA editing enzyme. Nature 379:460-464

Meurs, E.F., Galabru, J., Barber, G.N., Katze, M.G., Hovanessian, A.G. 1993. Tumor suppressor function of the interferon-induced double-stranded RNA-activated protein kinase. Proc. Natl. Acad. Sci. U.S.A. 90:232-236

Meyer-Siegler, K., Mauro, D.J., Seal, G., Wurzer, J., deRiel, J.K., and Sirover, M.A. 1991. A human nuclear uracil DNA glycosylase is the 37-kDa subunit of glyceraldehyde-3-phosphate dehydrogenase. Proc. Nat. Acad. Sci. USA 88:8460-8464

Millhouse, S., Manley, J.L. 2005. The C-terminal domain of RNA polymerase II functions as a phosphorylation-dependent splicing activator in a heterologous protein. Mol. Cell. Biol. 25:533-544

Mitsuzawa, H., Kimura, M., Kanda E., Ishihama, A. 2005. Glyceraldehyde-3-phosphate dehydrogenase and actin associate with RNA polymerase II and interact with its Rpb7 subunit. FEBS Lett. 579:48-52

Modahl, L.E., Lai, M.M.C. 1998. Transcription of hepatitis *delta* antigen mRNA continues throughout hepatitis *delta* virus (HDV) replication: a new model of HDV RNA transcription and regulation. J. Virol. 72:5449-5456

Modahl, L.E., Macnaughton, T.B., Zhu, N., Johnson, D.L., Lai, M.M. 2000. RNA-dependent replication and transcription of hepatitis *delta* virus RNA involve distinct cellular RNA polymerases. Mol. Cell. Biol. 20:6030-6039

Moraleda, G., Taylor, J. 2001. Host RNA polymerase requirements for transcription of the human hepatitis *delta* virus genome. J. Virol. 75:10161-10169

Morgenegg, G., Winkler, G.C., Hubscher, U., Heizmann, C.W., Mous J., Kuenzle, C.C. 1986. Glyceraldehyde-3-phosphate dehydrogenase is a nonhistone protein and a possible activator of transcription in neurons. J. Neurochem. 47:54-62

Moroianu, J., Hijikata, M., Blobel, G., Radu, A. 1995. Mammalian karyopherin *alpha* 1 *beta* and *alpha* 2 *beta* heterodimers: *alpha* 1 or *alpha* 2 subunit binds nuclear localization signal and *beta* subunit interacts with peptide repeat-containing nucleoporins. Proc. Natl. Acad. Sci. U.S.A. 92:6532-6536

Mota, S., Mendes. M., Penque. D., Coelho, A.V., Cunha, C. 2008. Changes in the proteome of Huh7 cells induced by transient expression of hepatitis D virus RNA and antigens. J. Proteomics 71:71-79

Mota, S., Mendes, M., Freitas, N., Penque, D., Coelho, A.V., Cunha, C. 2009. Proteome analysis of a human liver carcinoma cell line stably expressing hepatitis *delta* virus ribonucleoproteins. J. Proteomics 72:616-627

Mu, J.J., Wu, H.L., Chiang, B.L., Chang, R.P., Chen, D.S., Chen, P.J. 1999. Characterization of the phosphorylated residues of hepatitis *delta* virus *delta* antigens. J. Virol. 73:10540-10545

Mu, J.J., Chen D.S., Chen P.J. 2001. The conserved serine 177 in the *delta* antigen of hepatitis *delta* virus is one putative phosphorylation site and is required for efficient viral RNA replication. J. Virol. 75:9087-9095

Mu, J.J., Tsay, Y.G., Juan, L.J., Fu, T.F., Huang, W.H., Chen, D.S., Chen, P.J. 2004. The small *delta* antigen of hepatitis *delta* virus is an acetylated protein and acetylation of lysine 72 may influence its cellular localization and viral RNA synthesis. Virology 319:60-70

Nagy, E., Rigby, W.F. 1995. Glyceraldehyde-3-phosphate dehydrogenase selectively binds AU-rich RNA in the NAD(+)-binding region (Rossmann fold). J. Biol. Chem. 270:2755-2763

Nagy, P., Schaff, Z., Lapis, K. 1991. Immunohistochemical detection of transforming growth factor-*beta* 1 in fibrotic liver diseases. Hepatology 14:269-273

Narita, T., Yamaguchi, Y., Yano, K., Sugimoto, S., Chanarat, S., Wada, T., Kim, D., Hasegawa, J., Omori, M., Inukai, N., Endoh, M., Yamada, T., Handa, H. 2003. Human transcription elongation factor NELF: identification of novel subunits and reconstitution of the functionally active complex. Mol. Cell. Biol. 23:1863-1873

Navarro, J.A., Flores, R. 2000. Characterization of the initiation sites of both polarity strands of a viroid RNA reveals a motif conserved in sequence and structure. EMBO J. 19:2662-2670

Netter, H.J., Kajino, K., Taylor, J. 1993. Experimental transmission of human hepatitis *delta* virus to the laboratory mouse. J. Virol. 67:3357-3362

Nie, X., Chang, J., Taylor, J.M. 2004. Alternative processing of hepatitis *delta* virus antigenomic RNA transcripts. J. Virol. 78:4517-4524

Nikolakaki, E., Drosou, V., Sanidas, I., Peidis, P., Papamarcaki, T., Iakoucheva, L.M., Giannakouros.,T. 2008. RNA association or phosphorylation of the RS domain prevents aggregation of RS domain-containing proteins. Biochim. Biophys. Acta 1780:214-225

Niranjanakumari, S., Lasda, E., Brazas, R., Garcia-Blanco, M.A. 2002. Reversible crosslinking combined with immunoprecipitation to study RNA–protein interactions *in vivo*. Methods 26:182-190

Ohashi, K., Marion, P.L., Nakai, H., Meuse, L., Cullen, J.M., Bordier, B.B., Schwall, R., Greenberg, H.B., Glenn, J.S., Kay, M.A. 2000. Sustained survival of human hepatocytes in mice: a model for *in vivo* infection with human hepatitis B and hepatitis *delta* viruses. Nat. Med. 6:327-331

Okuwaki, M. 2008. The structure and functions of NPM1/Nucleophsmin/B23, a multifunctional nucleolar acidic protein. J. Biochem. 143:441-448

Otto, J.C., Casey, P.J. 1996. The hepatitis *delta* virus large antigen is farnesylated both *in vitro* and in animal cells. J. Biol. Chem. 271:4569-4572

Ou, J.-H., Rutter, W.J. 1987. Regulation of secretion of the hepatitis B virus major surface antigen by the preS-1 protein. J. Virol. 61:782-786

Oubridge, C., Ito, N., Evans, P.R., Teo, C.-H., Nagai, K. 1994. Crystal structure at 1.92 Å resolution of the RNA-binding domain of the U1A spliceosomal protein complexed with an RNA hairpin. Nature 372:432-438

Park, C.Y., Oh, S.H., Kang, S.M., Lim, Y.S., Hwang, S.B. 2009. Hepatitis *delta* virus large antigen sensitizes to TNF-*alpha*-induced NF-*kappa*B signaling. Mol. Cells 28:49-55

Patterson, J.B., Samuel, C.E. 1995. Expression and regulation by interferon of a double-stranded-RNA-specific adenosine deaminase from human cells: evidence for two forms of the deaminase. Mol. Cell Biol. 15:5376-5388

Patton, J.G., Porro, E.B., Galceran, J., Tempst, P., Nadal-Ginard, B. 1993. Cloning and characterization of PSF, a novel pre-mRNA splicing factor. Genes Dev. 7:393-406

Pelchat, M., Perreault, J.P. 2004. Binding site of *Escherichia coli* RNA polymerase to an RNA promoter. Biochem. Biophys. Res. Commun. 319:636-642

Pelisch, F., Gerez, J., Druker, J., Schor, I.E., Muñoz, M.J., Risso, G., Petrillo, E., Westman, B.J., Lamond, A.I., Arzt, E., Srebrow, A. 2010. The serine/arginine-rich protein SF2/ASF regulates protein sumoylation. Proc. Nat. Acad. Sci. U.S.A. 107:16119-16124

Peng, R., Dye, B.T., Perez, I., Bernard, D.C., Thompson, A.B., Patton, J.G. 2002. PSF and $p54^{nrb}$ bind a conserved stem in U5 snRNA. RNA 8:1334-1347

Petrik, J., Parker, H., Alexander, G.J. 1999. Human hepatic glyceraldehyde-3-phosphate dehydrogenase binds to the poly(U) tract of the 3' non-coding region of hepatitis C virus genomic RNA. J. Gen. Virol. 80:3109-3113

Poisson, F., Roingeard, P., Baillou, A., Dubois, F., Bonelli, F., Calogero, R.A., Goudeau, A. 1993. Characterization of RNA-binding domains of hepatitis *delta* antigen. J. Gen. Virol. 74:2473-2478

Polo, J.M., Jeng, K.-S., Lim, B., Govindarajan, S., Hofman, F., Sangiorgi, F., Lai, M.M.C. 1995. Transgenic mice support replication of hepatitis *delta* virus RNA in multiple tissues, particularly in skeletal muscle. J. Virol. 69:4880-4887

Polson, A.G., Bass, B.L., Casey, J.L. 1996. RNA editing of hepatitis *delta* virus antigenome by dsRNA-adenosine deaminase. Nature 380:454-456

Ponting, C.P. 1997. Tudor domains in proteins that interact with RNA. Trends Biochem. Sci. 22:51-52

Ponzetto, A., Cote, P.J., Popper, H., Hoyer, B.H., London, W.T., Ford, E.C., Bonino, F., Purcell, R.H., Gerin, J.L. 1984. Transmission of the hepatitis B virus-associated *delta* agent to the eastern woodchuck. Proc. Natl. Acad. Sci. U.S.A. 81:2208-2212

Pospisil, H., Herrmann, A., Butherus, K.. Pirson, S.. Reich. J.G., Kemmner, W. 2006. Verification of predicted alternatively spliced Wnt genes reveals two new splice variants (CTNNB1 and LRP5) and altered Axin-1 expression during tumour progression. BMC Genomics 7:148

Predki, P.F., Nayak, L.M., Gottlieb, M.B.C., Regan, L. 1995. Dissecting RNA-protein interactions: RNA-RNA recognition by Rop. Cell 80:41-50

Radjef, N., Gordien, E., Ivaniushina, V., Gault, E., Anais, P., Drugan, T., Trinchet, J.C., Roulot, D., Tamby, M., Milinkovitch, M.C., Deny, P. 2004. Molecular phylogenetic analyses indicate a wide and ancient radiation of African hepatitis *delta* virus, suggesting a deltavirus genus of at least seven major clades. J. Virol. 78:2537-2544

Randall, G., Panis, M., Cooper, J.D., Tellinghuisen, T.L., Sukhodolets, K.E., Pfeffer, S., Landthaler, M., Landgraf, P., Kan, S., Lindenbach, B.D., Chien, M., Weir, D.B., Russo, J.J., Ju, J., Brownstein, M.J., Sheridan, R., Sander, C., Zavolan, M., Tuschl, T., Rice, C.M. 2007. Cellular cofactors affecting hepatitis C virus infection and replication. Proc. Nat. Acad. Sci. U.S.A. 104:12884-12889

Reid, C.E., Lazinski, D.W. 2000. A host-specific function is required for ligation of a wide variety of ribozyme-processed RNAs. Proc. Nat. Acad. Sci. U.S.A. 97:424-429

Rizzetto, M., Canese, M.G., Arico, J., Crivelli, O., Bonino, F., Trepo, C.G., Verme, G. 1977. Immunofluorescence detection of a new antigen–antibody system associated to the hepatitis B virus in the liver and in the serum of HBsAg carriers. Gut 18:997-1003

Rizzetto, M., Canese, M.G., Gerin, J.L., London, W.T., Sly, D.L., Purcell, R.H. 1980. Transmission of the hepatitis B virus-associated *delta* antigen to chimpanzees. J. Infect. Dis. 141:590-602

Rizzetto, M., Verme, G., Recchia, S., Bonino, F., Farci, P., Arico, S., Calzia, R., Picciotto, A., Colombo, M., Popper, H. 1983. Chronic hepatitis in carriers of hepatitis B surface antigen, with intrahepatic expression of the *delta* antigen. An active and progressive disease unresponsive to immunosuppressive treatment. Ann. Intern. Med. 98:437-441

Rizzetto, M., Hadziyannis, S., Hansson, B.G., Toukan, A., Gust, I. 1992. Hepatitis *delta* virus infection in the world, epidemiological patterns and clinical expression. Gastroenterol. Int. 5:18-32

Robertson, H.D., Manche, L., Matthews, M.B. 1996. Paradoxical interactions between human *delta* hepatitis agent RNA and the cellular protein kinase PKR. J. Virol. 70:5611-5617

Romeo, R., Del Ninno, E., Rumi, M., Russo, A., Sangiovanni, A., de Franchis, R., Ronchi, G., Colombo, M. 2009. A 28-year study of the course of hepatitis *delta* infection, a risk factor for cirrhosis and hepatocellular carcinoma. Gastroenterology 136:1629-1638

Rosa-Calatrava, M., Puvion-Dutilleul, F., Lutz, P., Dreyer, D., de Thé, H., Chatton, B., Kedinger, C. 2003. Adenovirus protein IX sequesters host-cell promyelocytic leukaemia protein and contributes to efficient viral proliferation. EMBO Rep. 4:969-975

Rust, M.J., Lakadamyali, M., Zhang, F., Zhuang X. 2004. Assembly of endocytic machinery around individual influenza viruses during viral entry. Nat. Struct. Mol. Biol. 11:567-573

Ryu, W.S., Bayer, M., Taylor, J. 1992. Assembly of hepatitis *delta* virus particles. J. Virol. 66:2310-2315

Ryu, W.S., Netter, H.J., Bayer, M., Taylor, J. 1993. Ribonucleoprotein complexes of hepatitis *delta* virus. J. Virol. 67:3281-3287

Salehi-Ashtiani, K., Luptak, A., Litovchick, A., Szostak, J.W. 2006. A genomewide search for ribozymes reveals an HDV-like sequence in the human CPEB3 gene. Science 313:1788-1792

Sanford, J.R., Gray, N.K., Beckmann, K., Cáceres, J.F. 2004. A novel role for shuttling SR proteins in mRNA translation. Genes Dev. 18:755-768

Sanford, J.R., Coutinho, P., Hackett, J.A., Wang, X., Ranahan, W., Caceres, J.F. 2008. Identification of nuclear and cytoplasmic mRNA targets for the shuttling protein SF2/ASF. PLoS One 3:e3369

Sanford, J.R., Wang, X., Mort, M., Vanduyn, N., Cooper, D.N., Mooney, S.D., Edenberg, H.J., Liu, Y. 2009. Splicing factor SFRS1 recognizes a functionally diverse landscape of RNA transcripts. Genome Res. 19:381-394

Sato, S., Cornillez-Ty, C., Lazinski, D.W. 2004. By inhibiting replication, the large hepatitis *delta* antigen can indirectly regulate amber/W editing and its own expression. J. Virol. 78:8120-8134

Schindler, I.M., Mühlbach, H.P. 1992. Involvement of nuclear DNA-dependent RNA polymerases in potato spindle tuber viroid replication: a reevaluation. Plant Sci. 84:221-229

Schultz, D.E., Hardin, C.C., Lemon, S.M. 1996. Specific interaction of glyceraldehyde 3-phosphate dehydrogenase with the 5′-nontranslated RNA of hepatitis A virus. J. Biol. Chem. 271:14134-14142

Sharmeen, L., Kuo, M.Y.-P., Dinter-Gottlieb, G., Taylor, J. 1988. Antigenomic RNA of human hepatitis *delta* virus can undergo self-cleavage. J. Virol. 62:2674-2679

Sharmeen, L., Kuo, M.Y.-P., Taylor, J. 1989. Self-ligating RNA sequences on the antigenome of human hepatitis *delta* virus. J. Virol. 63:1428-1430

Shaulian, E. 2010. AP-1—The Jun proteins: Oncogenes or tumor suppressors in disguise? Cell. Signal. 22:894-899

Shav-Tal, Y., Zipori, D. 2002. PSF and $p54^{nrb}$/NonO--multi-functional nuclear proteins. FEBS Lett. 531:109-114

Shi, S.T., Lai, M.M.C. 2005. Viral and cellular proteins involved in coronavirus replication. Curr. Top. Microbiol. Immunol. 287:95-131

Showalter, S.A., Hall, K.B. 2004. Altering the RNA-binding mode of the U1A RBD1 protein. J. Mol. Biol. 335:465-480

Silverman, N., Maniatis, T. 2001. NF-*kappa*B signaling pathways in mammalian and insect innate immunity. Genes Dev. 15:2321-2342

Sinclair, A.H., Berta, P., Palmer, M.S., Hawkins, J.R., Griffiths, B.L., Smith, M.J., Foster, J.W., Frischauf, A.M., Lovell-Badge, R., Goodfellow, P.N. 1990 A gene from the human sex determining region encodes a protein with homology to a conserved DNA-binding motif. Nature 346:240-244

Singh, R., Green, M. 1993. Sequence-specific binding of transfer RNA by glyceraldehyde-3-phosphate dehydrogenase. Science 259:365-368

Sirover, M.A. 1999. New insights into an old protein: the functional diversity of mammalian glyceraldehyde-3-phosphate dehydrogenase. Biochim. Biophys. Acta 1432:159-184

Sletta, H., Tøndervik, A., Hakvåg, S., Vee Aune, T.E, Nedal, A., Aune, R., Evensen, G., Valla, S., Ellingsen, T.E., Brautaset, T. 2007. The presence of N-terminal secretion signal sequences leads to strong stimulation of the total expression levels of three tested medically important proteins during high-cell-density cultivations of *Escherichia coli*. Appl. Environ. Microbiol. 73:906-912

Smedile, A., Ciancio, A., Rizzetto, M. 2002. Hepatitis D. Hepatitis D virus. In: Richman, D.D., Whitley, R. J., Hayden, F. G., editors. Clinical Virology. Washington DC: ASM Press; pp. 1227-1240

Smith, P.J., Zhang, C., Wang, J., Chew, S.L., Zhang, M.Q., Krainer, A.R. 2006. An increased specificity score matrix for the prediction of SF2/ASF-specific exonic splicing enhancers. Hum. Mol. Genet. 15:2490-2508

Song, X., Wang, B., Bromberg, M., Hu, Z., Konigsberg, W., Garen, A. 2002. Retroviral-mediated transmission of a mouse VL30 RNA to human melanoma cells promotes metastasis in an immunodeficient mouse model. Proc. Natl. Acad. Sci. U. S. A. 99:6269-6273

Song, X., Sui, A., Garen, A. 2004. Binding of mouse VL30 retrotransposon RNA to PSF protein induces genes repressed by PSF: effects on steroidogenesis and oncogenesis. Proc. Natl. Acad. Sci. U. S. A.101:621-626

Song, X., Sun, Y., Garen, A. 2005. Roles of PSF protein and VL30 RNA in reversible gene regulation. Proc. Natl. Acad. Sci. U. S. A. 102:12189-12193

Soulière, M.F., Perreault, J.P., Bisaillon, M. 2008. Magnesium-binding studies reveal fundamental differences between closely related RNA triphosphatases. Nuc. Acids. Res. 36:451-461

Straub, T., Grue, P., Uhse, A., Lisby, M., Knudsen, B.R., Tange, T.O., Westergaard, O., Boege, F. 1998. The RNA-splicing factor PSF/p54 controls DNA-topoisomerase I activity by a direct interaction. J Biol. Chem 273:26261-26264

Su, C.W., Huang, Y.H., Huo, T.I., Shih, H.H., Sheen, I.J., Chen, S.W., Lee, P.C., Lee, S.D., Wu, J.C. 2006. Genotypes and viremia of hepatitis B and D viruses are associated with outcomes of chronic hepatitis D patients. Gastroenterology 130:1625-1635

Sureau, C. 2006. The role of the HBV envelope proteins in the HDV replication cycle. Curr. Top. Microbiol. Immunol. 307:113-131

Sureau, C., Jacob, J.R., Eichberg, J.W., Lanford, R.E. 1991. Tissue culture system for infection with human hepatitis *delta* virus. J. Virol. 65:3443-3450

Sureau, C., Guerra, B., Lanford, R.E. 1993. Role of the large hepatitis B virus envelope protein in infectivity of the hepatitis *delta* virion. J. Virol. 67:366-372

Szebeni, A., Herrera, J.E., Olson, M.O. 1995. Interaction of nucleolar protein B23 with peptides related to nuclear localization signals. Biochemistry 34:8037-8042

Szebeni, A., Mehrotra, B., Baumann, A., Adam, S.A., Wingfield, P.T., Olson, M.O. 1997. Nucleolar protein B23 stimulates nuclear import of the HIV-1 Rev protein and NLS-conjugated albumin. Biochemistry 36:3941-3949

Tabler, M., Tsagris, M. 2004. Viroids : petite RNA pathogens with distinguished talents. Trends Plant Sci. 9:339-348

Tacke, R., Manley, J.L. 1995. The human splicing factors ASF/SF2 and SC35 possess distinct, functionally significant RNA binding specificities. EMBO J. 14:3540-3551

Tan, K.P., Shih, K.N., Lo, S.J. 2004. Ser-123 of the large antigen of hepatitis *delta* virus modulates its cellular localization to the nucleolus, SC-35 speckles or the cytoplasm. J. Gen. Virol. 85:1685-1694

Tang, Q., Bell, P., Tegtmeyer, P., Maul, G.G. 2000. Replication but not transcription of simian virus 40 DNA is dependent on nuclear domain 10. J. Virol. 74:9694-9700

Taylor, J.M. 1999. Replication of human hepatitis *delta* virus: influence of studies on subviral plant pathogens. Adv. Virus Res. 54:45-60

Taylor, J.M. 2006. Hepatitis *delta* virus. Virology 344:71-76

Taylor, J.M. 2009. Chapter 3: Replication of the hepatitis *delta* virus RNA genome. Adv. Virus Res. 74:103-121

Taylor, J., Mason, W., Summers, J., Goldberg, J., Aldrich, C., Coates, L., Gerin, J., Gowans, E. 1987. Replication of human hepatitis *delta* virus in primary cultures of woodchuck hepatocytes. J. Virol. 61:2891-2895

Taylor, J., Pelchat, M. 2010. Origin of hepatitis *delta* virus. Future Microbiol. 5:393-402

Thivierge, K., Cotton, S., Dufresne, P.J., Mathieu, I., Beauchemin, C., Ide, C., Fortin, M.G., Laliberté, J.F. 2008. Eukaryotic elongation factor 1A interacts with turnip mosaic virus RNA-dependent RNA polymerase and VPg-Pro in virus-induced vesicles. Virol. 377:216-225

Thompson, J.D., Higgins, D.G., Gibson, T.J. 1994. CLUSTAL W: improving the sensitivity of progressive multiple sequence alignment through sequence weighting, position-specific gap penalties and weight matrix choice. Nucleic Acids Res. 22:4673-4680

Tintaru, A.M., Hautbergue, G.M., Hounslow, A.M., Hung, M.-L., Lian, L.-Y., Craven, C.J., Wilson, S.A. 2007. Structural and functional analysis of RNA and TAP binding to SF2/ASF. EMBO Reports 8: 756-762

Tristan, C., Shahani, N., Sedlak, T.W., Sawa, A. 2011. The diverse functions of GAPDH: views from different subcellular compartments. Cell Signal 23:317-323

Trougakos, I.P., Gonos, E.S. 2006. Regulation of clusterin/apolipoprotein J, a functional homologue to the small heat shock proteins, by oxidative stress in ageing and age-related diseases. Free Radic. Res. 40:1324-1334

Tseng, C.H., Jeng, K.S., Lai, M.M. 2008. Transcription of subgenomic mRNA of hepatitis *delta* virus requires a modified hepatitis *delta* antigen that is distinct from antigenomic RNA synthesis. J. Virol. 82:9409-9416

Tseng, C.H., Cheng, T.S., Shu, C.Y., Jeng, K.S., Lai, M.M. 2010. Modification of small hepatitis *delta* virus antigen by SUMO protein. J. Virol. 84:918-927

Tuteja, R. Tuteja, N. 1998. Nucleolin: a multifunctional major nucleolar phosphoprotein. Crit. Rev. Biochem. Mol. Biol. 33:407-436

Ueda, H., Iyo, H., Doi, M., Inoue, M., Ishida, T. 1991. Cooperative stacking and hydrogen bond pairing interactions of fragment peptide in cap binding protein with mRNA cap structure. Biochim Biophys Acta. 1075:181-186

Urban, R.J., Bodenburg, Y., Kurosky, A., Wood, T.G., Gasic, S. 2000. Polypyrimidine tract-binding protein-associated splicing factor is a negative regulator of transcriptional activity of the porcine p450scc insulin-like growth factor response element. Mol. Endocrinol. 14:774-782

Usheva, A., Shenk, T. 1996. YY1 transcriptional initiator: protein interactions and association with a DNA site containing unpaired strands. Proc. Nat. Acad. Sci. U.S.A. 93:13571-13576

Van Damme N, Guatelli J. 2008. HIV-1 Vpu inhibits accumulation of the envelope glycoprotein within clathrin-coated, Gag-containing endosomes. Cell. Microbiol. 10:1040-1057

Veretnik, S. Gribskov, M. 1999. RNA binding domain of HDV antigen is homologous to the HMG box of SRY. Arch. Virol. 144:1139-1158

Vioque, A., Altman, S. 1986. Affinity chromatography with an immobilized RNA enzyme. Proc. Natl. Acad. Sci. U.S.A. 83:5904-5908

Vogt, P.K. 2001. Jun, the oncoprotein. Oncogene 20:2365-2377

Wada, T., Takagi, T., Yamaguchi, Y., Watanabe, D., Handa, H. 1998. Evidence that P-TEFb alleviates the negative effect of DSIF on RNA polymerase II-dependent transcription *in vitro*. EMBO J. 17:7395-7403

Wadkins, T.S., Perrotta, A.T., Ferré-D'Amaré, A.R., Doudna, J.A., Been, M.D. 1999. A nested double pseudoknot is required for self-cleavage activity of both the genomic and antigenomic hepatitis *delta* virus ribozymes. RNA 5:720-727

Wang, C.C., Chang, T.C., Lin, C.W., Tsui, H.L., Chu, P.B., Chen, B.S., Huang, Z.S., Wu, H.N. 2003. Nucleic acid binding properties of the nucleic acid chaperone domain of hepatitis *delta* antigen. Nucleic Acids Res. 31:6481-6492

Wang, D., Pearlberg, J., Liu, Y.T., Ganem, D. 2001. Deleterious effects of hepatitis *delta* virus replication on host cell proliferation. J. Virol. 75:3600-3604

Wang, H.W., Chen, P.J., Lee, C.Z., Wu, H.L., Chen, D.S. 1994. Packaging of hepatitis *delta* virus RNA via the RNA-binding domain of hepatitis *delta* antigens: different roles for the small and large *delta* antigens. J. Virol. 68:6363-6371

Wang, K.S., Choo, Q.L., Weiner, A.J., Ou, J.H., Najarian, R.C., Thayer, R.M., Mullenbach, G.T., Denniston, K.J., Gerin, J.L., Houghton, M. 1986. Structure, sequence and expression of the hepatitis *delta* (δ) viral genome. Nature 323:508-514

Wang, R.Y., Nagy, P.D. 2008. Tomato bushy stunt virus co-opts the RNA-binding function of a host metabolic enzyme for viral genomic RNA synthesis. Cell Host Microbe 3:178-187

Wang, Y.C., Huang, C.R., Chao, M., Lo, S.J. 2009. The C-terminal sequence of the large hepatitis *delta* antigen is variable but retains the ability to bind clathrin. Virol. J. 6:31

Wang, Y.H., Chang, S.C., Huang, C., Li, Y.P., Lee, C.H., Chang, M.F. 2005. Novel nuclear export signal-interacting protein, NESI, critical for the assembly of hepatitis *delta* virus. J. Virol. 79:8113-8120

Warrilow, D., Symons, R.H. 1999. Citrus exocortis viroid RNA is associated with the largest subunit of RNA polymerase II in tomato *in vivo*. Arch. Virol. 144:2367-2375

Webb, C.H., Riccitelli, N.J., Ruminski, D.J., Lupták, A. 2009. Widespread occurance of self-cleaving ribozymes. Science 326:953

Webb, C.H., Lupták, A. 2011. HDV-like self-cleaving ribozymes. RNA Biol. 8

Wei, Y., Ganem, D. 1998. Activation of heterologous gene expression by the large isoform of hepatitis *delta* antigen. J. Virol. 72:2089-2096

Williams, V., Brichler, S., Radjef, N., Lebon, P., Goffard, A., Hober, D., Fagard, R., Kremsdorf, D., Deny, P., Gordien, E. 2009. Hepatitis *delta* virus proteins repress hepatitis B virus enhancers and activate the *alpha*/*beta* interferon-inducible MxA gene. J. Gen. Virol. 90:2759-2767

Wong, S.K., Lazinski, D.W. 2002. Replicating hepatitis *delta* virus RNA is edited in the nucleus by the small form of ADAR1. Proc. Natl. Acad. Sci. U.S.A. 99:15118-15123

Wu, H.N., Wang, Y.J., Hung, C.F., Lee, H.J., Lai, M.M. 1992. Sequence and structure of the catalytic RNA of hepatitis *delta* virus genomic RNA. J. Mol. Biol. 223:233-245

Wu, J.C., Chen, P.J., Kuo, M.Y., Lee, S.D., Chen, D.S., Ting, L.P. 1991. Production of hepatitis *delta* virus and suppression of helper hepatitis B virus in a human hepatoma cell line. J. Virol. 65:1099-1104

Wu, T.T., Netter, H.J., Lazinski, D.W., Taylor, J.M. 1997. Effects of nucleotide changes on the ability of hepatitis *delta* virus to transcribe, process, and accumulate unit-length, circular RNA. J. Virol. 71:5408-5414

Xia, Y.P., Lai, M.M. 1992. Oligomerization of hepatitis *delta* antigen is required for both the trans-activating and trans-dominant inhibitory activities of the *delta* antigen. J. Virol. 66:6641-6648

Xia, Y.P., Yeh, C.T., Ou, J.H., Lai, M.M. 1992. Characterization of nuclear targeting signal of hepatitis *delta* antigen: nuclear transport as a protein complex. J. Virol. 66:914-921

Yamaguchi, Y., Takagi, T., Wada, T., Yano, K., Furuya, A., Sugimoto, S., Hasegawa, J., Handa, H. 1999. NELF, a multisubunit complex containing RD, cooperates with DSIF to repress RNA polymerase II elongation. Cell 97:41-51

Yamaguchi, Y., Filipovska, J., Yano, K., Furuya, A., Inukai, N., Narita, T., Wada, T., Sugimoto, S., Konarska, M.M., Handa, H. 2001. Stimulation of RNA polymerase II elongation by hepatitis *delta* antigen. Science 293:124-127

Yamaguchi, Y., Mura, T., Chanarat, S., Okamoto, S., and Handa, H. 2007. Hepatitis *delta* antigen binds to the clamp of RNA polymerase II and affects transcriptional fidelity. Genes Cells 12:863-875

Yamaji, Y., Sakurai, K., Hamada, K., Komatsu, K., Ozeki, J., Yoshida, A., Yoshii, A., Shimizu, T., Namba, S., Hibi, T. 2010. Significance of eukaryotic translation elongation factor 1A in tobacco mosaic virus infection. Arch. Virol. 155:263-268

Yang, S.H., Liu, M.L., Tien, C.F., Chou, S.J., Chang, R.Y. 2009. Glyceraldehyde-3-phosphate dehydrogenase (GAPDH) interaction with 3' ends of Japanese encephalitis virus RNA and colocalization with the viral NS5 protein. J. Biomed. Sci. 16:40

Yeh, T.S., Lo, S.J., Chen, P.J., Lee, Y.H. 1996. Casein kinase II and protein kinase C modulate hepatitis *delta* virus RNA replication but not empty viral particle assembly. J. Virol. 70:6190-6198

Yeh, T.S., Lee, Y.H. 1998. Assembly of hepatitis *delta* virus particles: package of multimeric hepatitis *delta* virus genomic RNA and role of phosphorylation. Virology 249:12-20

Yue, B.-G., Ajuh, P., Akusjärvi, G., Lamond, A.I., Kreivi, J.-P. 2000. Functional coexpression of serine protein kinase SRPK1 and its substrate ASF/SF2 in *Escherichia coli*. Nucleic Acids Res. 28:e14

Yuryev, A., Patturajan, M., Litingtung, Y., Joshi, R.V., Gentile, C., Gebara, M., Corden, J.L. 1996. The C-terminal domain of the largest subunit of RNA polymerase II interacts with a novel set of serine/arginine-rich proteins. Proc. Natl. Acad. Sci. U. S. A. 93:6975-6980

Zahler, A.M., Lane, W.S., Stolk, J.A., Roth, M.B. 1992. SR proteins: a conserved family of pre-mRNA splicing factors. Genes Dev. 6:837-847

Zahler, A.M., Neugebauer, K.M., Lane, W.S., Roth, M.B. 1993. Distinct functions of SR proteins in alternative pre-mRNA splicing. Science 260:219-222

Zhang, Z., Carmichael, G.G. 2001. The fate of dsRNA in the nucleus: a p54(nrb)-containing complex mediates the nuclear retention of promiscuously A-to-I edited RNAs. Cell 106:465-475

Zhang, W.W., Zhang, L.X., Busch, R.K., Farres, J., Busch, H. 1993. Purification and characterization of a DNA-binding heterodimer of 52 and 100 kDa from HeLa cells. Biochem. J. 290:267-272

Zheng, L., Roeder, R.G., Luo, Y. 2003. S phase activation of the histone H2B promoter by OCA-S, a coactivator complex that contains GAPDH as a key component. Cell 114:255-266

Zhou, T., Rosen, B.P. 1997. Tryptophan fluorescence reports nucleotide-induced conformational changes in a domain of the ArsA ATPase. J. Biol. Chem. 272:19731-19737

Zhou, T., Liu, S., Rosen, B.P. 1995. Interaction of substrate and effector binding sites in the ArsA ATPase. Biochemistry 34:13622-13626

Zuccola, H.J., Rozzelle, J.E., Lemon, S.M., Erickson, B.W., Hogle, J.M. 1998. Structural basis of the oligomerization of hepatitis *delta* antigen. Structure 6:821-830

Zuo, P., Manley, J.L. 1993. Functional domains of the human splicing factor ASF/SF2. EMBO J. 12:4727-4737

Contributions of Collaborators

Purification of the splicing factor hnRNP-L (Figure 3.2) was performed by Ms. Emilie Lemay. *In vitro* co-immunoprecipitations of R199G with $p54^{nrb}$, eEF1A1, and GAPDH (Figure 3.4) were performed by Mr. Paul Miron, under the direct supervision of Dorota Sikora. Co-immunoprecipitations of HDV RNA from HeLa cells (Figure 3.5) were performed by Dr. Valerie Greco-Stewart. Binding of ASF/SF2 to the R177GΔASF mutant (Figure 4.6) was performed by Mr. Ali Tanara. MiniHDV reverse transcription-PCR reactions and cloning of miniHDV cDNA products were performed by Ms. Ji Yin (Figures 5.4 and 5.5) under the direct guidance of Dorota Sikora.

Appendices

Appendix I: Primer sequences

Primers used to generate DNA templates for the synthesis of viroid and HDV RNA fragments (T7 promoter sequences are underlined):

RNA species	**Primer pair**
R199G	5’-GGAATTCTAATACGACTCACTATAGGGACTGCTCGAGGATC TCTTCTCTCC-3’ 5’-CACTCCCCTCTCGGTGCTG-3’
Y-R199G	5’-GGAATTCTAATACGACTCACTATAGGGCATTCGATCTACAC CTGACACTGCTCGAGGATCTCTTCTCTCC-3’ 5’-CACTCCCCTCTCGGTGCTG-3’
R177G	5’-GGAATTCTAATACGACTCACTATAGGGATCTCTTCTCTCCCT CCGCGGTTC-3’ 5’-GGTGCTGATCCTCCCCCCGCG-3’
R161G	5’-GGAATTCTAATACGACTCACTATAGGGTTCTCTCCCTCCGCG GTTCTTCCT-3’ 5’-ATCCTCCCCCCGCGTCTCCTCGCT-3’
R156G	5’-GGAATTCTAATACGACTCACTATAGGGCTCCCTCCGCGGTTC TTCCTCGAC-3’ 5’-CTCCCCCCGCGTCTCCTCGCTCGG-3’
R47G	5’-GGAATTCTAATACGACTCACTATAGGG-3’ 5’-AGTCCAGCAGTCTCCTCTTTACAGAAAAGAGTAAGAGTACT GAGGACTCCCTATAGTGAGTCGTATTAGAATTCC-3’
PSTVd(+)	5’-GGAATTCTAATACGACTCACTATAGGGAACTAAACTCGTGG TTCCTGTGGTTC-3’ 5’-GGAACCAACTGCGGTTCCAAGGGCTAAACACCC-3’
PSTVd(-)	5’-GGAATTCTAATACGACTCACTATAGGGAACCAACTGCGGTT CCAAGGGCTAAACACCC-3’ 5’-GGAACTAAACTCGTGGTTCCTGTGGTTC-3’
P11.60	5’-GGAATTCTAATACGACTCACTATAGGG-3’ 5’-GGGCCGCTGAAATGCGGCGAAACTTTTGATGATATGAGTTT CGTCTCATTTCAGAGACCCTATAGTGAGTCGTATTA-3’

Appendix II: ***Curriculum vitae***

Dorota Sikora

EDUCATION

2004-2012 **Ph.D. Biochemistry**, University of Ottawa, Ottawa, ON

Thesis Title: Hepatitis *delta* virus: Identification of host factors involved in the viral life cycle, and the investigation of the evolutionary relationship between HDV and plant viroids.

Supervisor: Dr. Martin Pelchat

2003-2004 **B.Sc.H. Biology/Biotech. option**, University of Ottawa, Ottawa, ON

Undergraduate thesis title: The identification and characterization of a DivIVA binding protein in *Enterococcus faecalis.*

Supervisor: Dr. Jo-Anne R. Dillon

1998-2002 **B.Sc.H. Biology**, Queen's University, Kingston, ON

WORK EXPERIENCE

2011 **Teaching Assistant**/Corrector for second year undergraduate zoology laboratory. Department of Biology, University of Ottawa, Ottawa, ON

2010 **Teaching Assistant**/Corrector for third year undergraduate metabolism course. Department of Biochemistry, Microbiology and Immunology, University of Ottawa, Ottawa, ON

2009 **Teaching Assistant**/Demonstrator for second year undergraduate genetics laboratory. Department of Biology, University of Ottawa, Ottawa, ON

2008-2009 **Teaching Assistant** for third year undergraduate molecular biology course. Department of Biochemistry, Microbiology and Immunology, University of Ottawa, Ottawa, ON

2007-2008 **Teaching Assistant**/Corrector for second year undergraduate genetics laboratory. Department of Biology, University of Ottawa, Ottawa, ON

2002 **Research Assistant** (summer placement), Laboratory of Dr. Perin Sankar. Department of Biochemistry, Queen's University, Kingston, ON

PUBLISHED ABSTRACTS

Issa, M., **Sikora, D.**, Bojić, T., and M. Pelchat. (2010). Construction of a minimal replicon derived from the hepatitis *delta* virus. Ribo-Club 11th Opening Session, Orford, Quebec, Canada

Sikora, D., Greco-Stewart, V., Miron, P. and M. Pelchat. (2009) The hepatitis *delta* virus RNA genome interacts with eEF1A1, $p54^{nrb}$, hnRNP-L, GAPDH and ASF/SF2. Ribo-Club 10th Opening Session, Orford, Quebec, Canada

Dimitrijevic, T., **Sikora, D.**, Schissel, E., Issa, M. and M Pelchat. Evolutionary relationship between hepatitis *delta* virus and viroids. (2009) International Meeting on Molecular Biology of Hepatitis B Viruses, Tours, France

Sikora, D., Greco-Stewart, V., Miron, P. and M. Pelchat. (2008) Interactions of the hepatitis *delta* virus RNA with various host proteins and potential roles of these interactions in viral pathogenesis. Ribo-Club 9th Opening Session, Orford, Quebec, Canada

Sikora, D., Greco-Stewart, V., Miron, P. and M. Pelchat. (2008) Identification of eEF1A1, $p54^{nrb}$, hnRNP-L, GAPDH and ASF/SF2 as novel interacting partners for the hepatitis *delta* virus RNA genome. 13^{th} annual meeting of the RNA Society, Berlin, Germany

Sikora, D. and M. Pelchat. (2006) Identification of an ASF/SF2 binding site on the hepatitis *delta* virus RNA. Ribo-Club 7th Opening Session, Orford, Quebec, Canada

Sikora, D. and M. Pelchat. (2006) Identification of a hepatitis *delta* virus binding protein. 11^{th} annual meeting of the RNA Society, Seattle, Washington, USA

Sikora, D. and M. Pelchat. (2005) The human SR splicing factor ASF/SF2 interacts with genomic and antigenomic HDV RNA. Ribo-Club 6th Opening Session, Orford, Quebec, Canada

Sikora, D. and M. Pelchat. (2005) Interaction of the genomic hepatitis *delta* virus RNA promoter with the human splicing factor ASF/SF2. 10^{th} annual meeting of the RNA Society, Banff, Alberta, Canada

PUBLICATIONS

Pelchat, M., **Sikora, D.**, Dubé, A. and J.-P. Perreault. Viroids and related RNA species, book chapter in Fundamental Virology, "Textbook" edited by N.H. Achelson (John Wiley & Sons), 2010

Sikora, D., Greco-Stewart, V., Miron, P. and M. Pelchat. (2009) The hepatitis *delta* virus RNA genome interacts with eEF1A1, $p54^{nrb}$, hnRNP-L, GAPDH and ASF/SF2. Virology 390:71-78

GRANTS RECEIVED

Travel Grant, Graduate Studies Committee of the Biochemistry Program, University of Ottawa, Ontario, May 2008

Travel Grant, Faculty of Graduate and Postdoctoral Studies, University of Ottawa, Ontario, May 2008

Travel Grant, Graduate Studies Committee of the Biochemistry Program, University of Ottawa, Ontario, May 2005

Travel Grant, Faculty of Graduate and Postdoctoral Studies, University of Ottawa, Ontario, July 2005

Student Summer Research Grant, Canadian Infectious Disease Society, Ottawa, Ontario, May 2000

PRESENTATIONS AS GUEST SPEAKER

Sikora, D. and M. Pelchat. (2010) Interaction of host factors with the hepatitis *delta* virus RNA. University of Ottawa RNA Club, Ottawa, Ontario

Sikora, D. and M. Pelchat. (2007) Interaction of host mRNA processing proteins with the hepatitis *delta* virus RNA. University of Ottawa RNA Club, Ottawa, Ontario

Sikora, D. and M. Pelchat. (2005) Host's involvement in the life cycle of the hepatitis *delta* virus. University of Ottawa RNA Club, Ottawa, Ontario

Rembisz, D., Hsueh, O., and P. Sankar. (2001) Identification of verotoxin-producing *Escherichia coli* in drinking water. Faculty of Health Sciences, Queen's University, Kingston, Ontario

SKILLS

Laboratory skills: cell culture, nucleic acid and protein extraction and purification, PCR and quantitative RT-PCR, molecular cloning, *in vitro* transcription, electrophoretic mobility shift assay, Northern/Southern/Western blotting, protein purification (FPLC), protein SDS-PAGE, radioisotope labelling, immunoprecipitation, fluorescence spectroscopy, yeast two-hybrid analysis.

Additional skills: basic computer skills including Microsoft Office applications, Corel Draw, web-based bioinformatics tools (BLAST, ClustalW, mFold); fluent in English, German and Polish.